ACID-FUNCTIONALIZED NANOPARTICLES FOR BIOMASS HYDROLYSIS

by

LEIDY EUGENIA PEÑA DUQUE

B.S., National University of Colombia, 2004
M.S., Kansas State University, 2009

AN ABSTRACT OF A DISSERTATION

submitted in partial fulfillment of the requirements for the degree

DOCTOR OF PHILOSOPHY

Department of Biological & Agricultural Engineering
College of Engineering

KANSAS STATE UNIVERSITY
Manhattan, Kansas

2013

Abstract

Cellulosic ethanol is a renewable source of energy. Lignocellulosic biomass is a complex material composed mainly of cellulose, hemicellulose, and lignin. Biomass pretreatment is a required step to make sugar polymers liable to hydrolysis. Mineral acids are commonly used for biomass pretreatment. Using acid catalysts that can be recovered and reused could make the process economically more attractive. The overall goal of this dissertation is the development of a recyclable nanocatalyst for the hydrolysis of biomass sugars.

Cobalt iron oxide nanoparticles ($CoFe_2O_4$) were synthesized to provide a magnetic core that could be separated from reaction using a magnetic field and modified to carry acid functional groups. X-ray diffraction (XRD) confirmed the crystal structure was that of cobalt spinel ferrite. $CoFe_2O_4$ were covered with silica which served as linker for the acid functions.

Silica-coated nanoparticles were functionalized with three different acid functions: perfluoropropyl-sulfonic acid, carboxylic acid, and propyl-sulfonic acid. Transmission electron microscope (TEM) images were analyzed to obtain particle size distributions of the nanoparticles. Total carbon, nitrogen, and sulfur were quantified using an elemental analyzer. Fourier transform infra-red spectra confirmed the presence of sulfonic and carboxylic acid functions and ion-exchange titrations accounted for the total amount of catalytic acid sites per nanoparticle mass.

These nanoparticles were evaluated for their performance to hydrolyze the β-1,4 glycosidic bond of the cellobiose molecule. Propyl-sulfonic (PS) and perfluoropropyl-sulfonic (PFS) acid functionalized nanoparticles catalyzed the hydrolysis of cellobiose significantly better than the control. PS and PFS were also evaluated for their capacity to solubilize wheat straw hemicelluloses and performed better than the control. Although PFS nanoparticles were stronger acid catalysts, the acid functions leached out of the nanoparticle during the catalytic reactions.

PS nanoparticles were further evaluated for the pretreatment of corn stover in order to increase digestibility of the biomass. The pretreatment was carried out at three different catalyst load and temperature levels. At 180°C, the total glucose yield was linearly correlated to the catalyst load. A maximum glucose yield of 90% and 58% of the hemicellulose sugars were obtained at this temperature.

ACID-FUNCTIONALIZED NANOPARTICLES FOR BIOMASS HYDROLYSIS

by

LEIDY EUGENIA PEÑA DUQUE

B.S., National University of Colombia, 2004
M.S., Kansas State University, 2009

A DISSERTATION

submitted in partial fulfillment of the requirements for the degree

DOCTOR OF PHILOSOPHY

Department of Biological & Agricultural Engineering
College of Engineering

KANSAS STATE UNIVERSITY
Manhattan, Kansas

2013

Approved by:

Major Professor
Donghai Wang

Abstract

Cellulosic ethanol is a renewable source of energy. Lignocellulosic biomass is a complex material composed mainly of cellulose, hemicellulose, and lignin. Biomass pretreatment is a required step to make sugar polymers liable to hydrolysis. Mineral acids are commonly used for biomass pretreatment. Using acid catalysts that can be recovered and reused could make the process economically more attractive. The overall goal of this dissertation is the development of a recyclable nanocatalyst for the hydrolysis of biomass sugars.

Cobalt iron oxide nanoparticles ($CoFe_2O_4$) were synthesized to provide a magnetic core that could be separated from reaction using a magnetic field and modified to carry acid functional groups. X-ray diffraction (XRD) confirmed the crystal structure was that of cobalt spinel ferrite. $CoFe_2O_4$ were covered with silica which served as linker for the acid functions.

Silica-coated nanoparticles were functionalized with three different acid functions: perfluoropropyl-sulfonic acid, carboxylic acid, and propyl-sulfonic acid. Transmission electron microscope (TEM) images were analyzed to obtain particle size distributions of the nanoparticles. Total carbon, nitrogen, and sulfur were quantified using an elemental analyzer. Fourier transform infra-red spectra confirmed the presence of sulfonic and carboxylic acid functions and ion-exchange titrations accounted for the total amount of catalytic acid sites per nanoparticle mass.

These nanoparticles were evaluated for their performance to hydrolyze the β-1,4 glycosidic bond of the cellobiose molecule. Propyl-sulfonic (PS) and perfluoropropyl-sulfonic (PFS) acid functionalized nanoparticles catalyzed the hydrolysis of cellobiose significantly better than the control. PS and PFS were also evaluated for their capacity to solubilize wheat straw hemicelluloses and performed better than the control. Although PFS nanoparticles were stronger acid catalysts, the acid functions leached out of the nanoparticle during the catalytic reactions.

PS nanoparticles were further evaluated for the pretreatment of corn stover in order to increase digestibility of the biomass. The pretreatment was carried out at three different catalyst load and temperature levels. At 180°C, the total glucose yield was linearly correlated to the catalyst load. A maximum glucose yield of 90% and 58% of the hemicellulose sugars were obtained at this temperature.

Table of Contents

List of Figures

List of Tables

Acknowledgements

I would like to thank my advisor, Dr. Donghai Wang, for giving me the opportunity to work under his guidance, advice, and financial support. After six years in graduate school, I have become a researcher, and I owe it to Dr. Wang.

I would like to thank Dr. Keith Hohn as member of my supervisory committee, for his support and ideas pertaining to my research.

I also thank the other members of my supervisory committee, Dr. Xiuzhi Susan Sun and Dr. Jun Li, for their time in serving on the supervisory committee and providing valuable suggestions. I also appreciate Dr. J.M. Shawn Hutchinson for willing to serve as my outside chair of my supervisory committee.

I thank to Dr. Daniel L. Boyle for his assistance with imaging magnetic nanoparticles. I could not have accomplished this work without his diligent help.

I would like to thank the IGERT program and its chair, Dr. Mary Rezac, for the financial support I received during two years.

I thank all the members in the bioprocessing group, Dr. Xiaorong Wu, Dr. Renyong Zhao, Dr. Karnnalin Theerarattananoon, Dr. Feng Xu, Dr. Ningbo Li, Mr. Ke Zhang, Ms.Yaritza Sanchez Gil, Liman Liu, and Mr. Nana Baah Appiah-Nkansah, for making this process an enjoyable experience.

Profound thanks to Dr. Naiqian Zhang, Ms. Barb Moore, Mr. Randy Erickson, Mr. Darrel Oard, and other faculty and staff in the Department of Biological and Agricultural Engineering for their help.

I thank Kansas State University for providing a high level education, with outstanding faculty, excellent facilities, and supportive staff. Kansas State University and the city Manhattan have been a home away from home throughout my six years in graduate school.

Last, but not least, I deeply express appreciation and gratitude to my parents Olivier Dario Peña Arboleda and Maria Amparo Duque Gil, to my sister Yenny Alejandra Peña Duque, who were always my drive and motivation, and to my husband Alexi Thompson for his unconditional love and support.

Dedication

To my parents Amparo and Olivier.

Chapter 1 - Introduction

Abstract

At present, sugary and starchy crops are the primary source of glucose for ethanol production. A dramatic increase in ethanol production using current grain-starch-based technology may be limited by demand for food and feed staples. Cellulose is the most abundant polysaccharide on the earth, and it can be used for ethanol production after hydrolysis of the polymer to monomer sugars. Pretreatment of lignocellulosic biomass is necessary in order to increase the susceptibility of biomass to enzymatic action. The most common pretreatment methods employ mineral acids and high temperatures to remove the lignin component. At these thermochemical conditions, a majority of the sugars from hemicelluloses are degraded to products that can cause inhibition of the alcoholic fermentation. Moreover, substantial capital investment is required because corrosion resistant materials must be utilized.

Neutralization, detoxification, and waste disposal are other associated costs of the acid pretreatment of lignocellulosic biomass. Acid functionalized magnetic nanoparticles are solid catalysts that can catalyze hydrolysis reactions and be separated from products by using a strong magnetic field. The goal of this research is to develop acid-functionalized nanoparticles with high catalytic performance on biomass pretreatment and biomass hydrolysis. Acid-functionalized nanoparticles could have similar catalytic effect as mineral acids during biomass pretreatment, with the added advantage that these nanoparticles are recoverable and reusable. Recyclability of the pretreatment catalysts would improve the profitability of the cellulosic biofuel industry; instead of losing the catalyst in an acid stream that would require neutralization, the catalyst can be feed back into the process.

1.1 Introduction

In developed nations such as the United States, the national economy depends heavily on the availability of fossil fuels such as coal, oil, and natural gas. Uncertainties relative to the oil supply and environmental problems associated with fossil fuel utilization have motivated interest in renewable energy sources such as fuel ethanol. Bio-ethanol is a renewable fuel produced from the alcoholic fermentation of monosaccharides. Renewable fuels are increasingly considered as substitutes for petroleum-based fuels. In 2007, the U.S. government under the Energy Independence and Security Act expanded the Renewable Fuel Standard (RFS). RFS2 requires the nation to annually produce 36 billion gallons of renewable fuels by 2022 (Allred et al 2008). In 2011, approximately 13.9 billion gallons of fuel ethanol were produced in the United States (U.S. Energy Information Administration 2012). In 2012, ethanol production decreased to 13.3 billion gallons of fuel ethanol. This reduction was driven by peak corn prices due to an extensive drought in 2012 (U.S. Department of Energy 2012; U.S. Department of Energy 2012). At present, ethanol is produced primarily from corn (97%). Corn production reached 13 billion bushels in 2010 (Capehart et al 2012), the utilization of which yields approximately 36 billion gallons of biofuel (2.77 gal/bushel). However, this amount of fuel is only approximately 16% of total motor gasoline demand in the U.S. in 2010 (Newell 2010). Furthermore, a dramatic increase in ethanol production using current grain-starch-based technology may be limited by demand for food and feed staples. In comparison, cellulosic biofuels do not have the food vs. fuel limitation of grain-starch-based biofuel production, thus making them ideal for the production of renewable fuels.

Ethanol production from cellulosic biomass encounters significant technical challenges. Efficient production of cellulosic ethanol depends on several factors, such as the physical and chemical properties of the biomass, pretreatment methods, the enzyme system, fermentative microorganisms, and processing conditions. Cellulose, the most abundant polysaccharide on Earth, can be used for commercial ethanol production once the cellulose fibrils are enzymatically hydrolyzed to glucose monomers (Okamura 1991). *C*ellulose, in its native form, is not readily available for enzymatic hydrolysis. Lignocellulosic biomass is a complex mixture of cellulose, hemicellulose, and lignin. Consequently, a physical or chemical pretreatment is required before biomass saccharification. Acidic or basic solutions, in conjunction with physical treatments, have

been used to hydrolyze hemicelluloses and break down lignin sheaths in order to improve the subsequent enzymatic hydrolysis of the cellulose polymer (Herrera et al 2004; Jacobsen and Wyman 2002; Liu and Wyman 2005; Teymouri et al 2004). High sugar yields have been reached with sulfuric acid treatment (Corredor et al 2008; Lee and Kim 2002; U.S. Department of Energy 2006; Viola et al 2007); however, even low concentrations of sulfuric acid can degrade cellulose and hemicellulose sugars to hydroxymethylfurfural and furfural as well as other undesirable compounds (Bobleter 1994; Mosier et al 2002). The use of sulfuric acid also requires a larger investment because corrosion resistant materials must be employed. Further costs are incurred for separation and neutralization of acidic streams.

In addition, a variety of degradation products derived from the pretreatment of cellulosic biomass could inhibit normal growth and ethanol production of fermentative microorganisms (Nilsson et al 2005; Oliva et al 2006). Detoxification, neutralization, and separation steps must precede enzymatic hydrolysis. Acid catalysts have successfully been used for a number of catalytic organic reactions (Alvaro et al 2005; Alvaro 2005; Bootsma and Shanks 2007; Lien and Zhang 2007), and nanoporous solids with acid sites have shown high catalytic activity in gas and liquid phase reactions (Harmer et al 2007). Efficient catalysis of cellulose hydrolysis was observed using amorphous carbon with surface sulfonic acid, carboxylic acid, and hydroxyl groups (Suganuma et al 2008). Significant glucose yields were reported for selective cellulose hydrolysis using acid zeolites and sulfonated activated-carbon (Onda et al 2008). Hydrolysis of hemicellulose using zeolites yielded up to 55% of xylose and arabinose (Dhepe and Sahu 2010). Catalytic performance of sulfonic acid-modified mesoporous silica was also evaluated for the hydrolysis of sucrose and starch (Dhepe et al 2005). Additionally, high cellobiose conversion was obtained using sulfonic and carboxylic acid-functionalized mesoporous silica (Bootsma and Shanks 2007). Catalysis using mesoporous silicas engenders mass transfer limitations that could be avoided using nanoparticles. Because of their tunable properties, functionalized nanoparticles have become an important research subject (Corma and Garcia 2006). Nanoparticles with magnetic properties can be recovered by applying a magnetic field (Yoon et al 2003), and acid-functionalized nanoparticles are potential catalysts for pretreatment and hydrolysis of lignocellulosic biomass. Using magnetic acid-functionalized nanoparticles could combine the catalyst accessibility of homogeneous acid catalysts with the recoverability and reusability of heterogeneous catalysts.

1.2 Materials and Methods

1.2.1 Materials

Ammonium hydroxide, isopropanol, and toluene (A.C.S. reagents) were purchased from Fisher Scientific (Pittsburgh, Pa., USA). Cobalt(II) chloride hexahydrate (99%), D-(+)-cellobiose (98%), iron(II) chloride tetrahydrate (99.99%), 3-mercaptopropyltrimethoxysilane (MPTMS) (95%), 4-(triethoxysilyl)-butyronitrile (CPTES) (98%), methylamine (40% w/w, 98.5%), sodium dodecyl sulfate (98.5%), and tetraethylorthosilicate (TEOS) (99.999%) were purchased from Sigma-Aldrich (St. Louis, MO, USA). Ethanol (95%) was purchased from Decon Laboratories (King of Prussia, Pa., USA). Hexafluoro(3-methyl-1-2-oxathiethane)-2,2-dioxide (HFP sultone) (95%) was purchased from SynQuest Labs (Alachua, Fla., USA). Wheat biomass was harvested from the Kansas State University Agronomy Farm (Manhattan, Kan.) in November, 2008. Corn stover was harvested by the Kansas State University Agronomy Farm in October 2011. Corn stover was ground in a cutting mill (SM2000, Retsch, Inc., Newtown, Pa.) to pass a 1 mm mesh.

1.2.2 Synthesis of a Magnetic Core

Various methods to prepare cobalt iron oxides have been described in the literature. Nlebedim et al. used the ceramic method (Nlebedim 2013). An alkalide reduction method was also utilized by Mooney, K. et al., in which Co^{+2} and Fe^{+3} ions were reduced to $CoFe_2$ and later oxidized to $CoFe_2O_4$ in an aqueous solution at room temperature (Mooney et al 2004). Co-precipitation of Co^{+2} and Fe^{+2} in basic solutions was used by El-OKr, M.M. (El-Okr et al 2011). Reverse micellar method was also used by placing the salts in a water-in-oil emulsion stabilized with surfactants (Lee et al 2005). For this dissertation, magnetic nanoparticles (MNPs) of $CoFe_2O_4$ were synthesized following a microemlusion method (Gill et al 2007; Phan and Jones 2006; Rondinone et al 1999). A scheme of the procedure followed to synthesize $CoFe_2O_4$ nanoparticles can be seen in Figure 1-1. An aqueous solution (500 ml) was prepared containing 7 mmol of Cobalt (II) chloride hexahydrate, 14 mmol of iron (II) chloride, and 40 mmol of sodium dodecylsulfate (SDS). The solution was stirred at room temperature with a mechanical stirrer for 30 min and heated to 60 °C. Then, a warm methylamine solution (12% w/w) was added and the mixture was stirred for 3 h. The nanoparticles were separated magnetically and washed using

distilled water and ethanol. The nanoparticles were dispersed in 100 ml of ethanol and stored at room temperature before coating with silica.

Figure 1-1 Synthesis of cobalt iron oxide nanoparticles

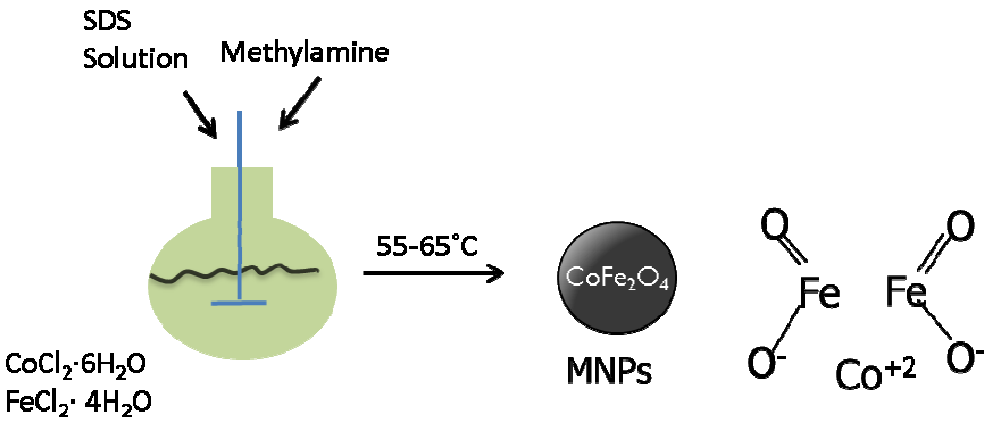

1.2.3 Silica coating of $CoFe_2O_4$

Silica materials have often been used as catalyst support because they offer unique tunable characteristics, and physical and chemical properties such as pore size structure and surface functional groups can be modified according to the needs of a particular application (Bernal et al 2012; Climent et al 2013; Morales et al 2008). Synthesis procedures can be adapted to obtain particular features that promote targeted reactions (Corma and Garcia 2006; Hair 1975; Wight and Davis 2002). Because of their versatility, silica materials can even be used for biological reactions as enzyme support (Bautista et al 2010). Silicas are often prepared by hydrolysis of tetraorthosilicate (TEOS) in aqueous solutions. Ethyl silicate is hydrolyzed to monomeric silicic acid which later condenses into polysilicic acids and then gels. The reaction is carried out in either basic or acid media at mild temperatures 30-60°C (Figure 1-2).

Figure 1-2 Hydrolysis of ethyl silicate and its condensation to form a silicate

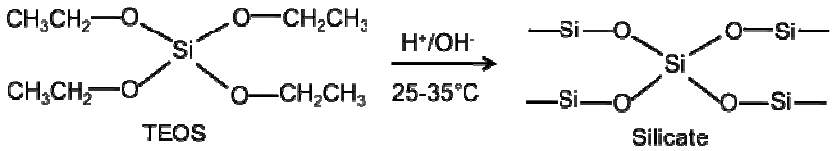

Despite large surface areas offered by porous silica, their domain of action is narrowed to reactions in the liquid phase. Porous silicas are usually aged at temperatures between 60-150°C for 10-24 h; sometimes they are also calcined to remove surfactants used to produce porous structures because these surfactants get trapped in the pores. Magnetic nanoparticles (MNPs) were coated with silica using similar procedures to the synthesis of silica materials (Haddad et al 2004; Yi et al 2005; Zhang et al 2008). A scheme of the coating procedure can be seen in Figure 1-3. In a typical experiment, ethanol dispersion of nanoparticles from the previous synthesis was sonicated and stirred for 30 min, and then 15 ml of the solution were added to a solution containing 500 ml isopropanol, 50 ml water, and 50 ml concentrated ammonium hydroxide. This solution was sonicated under mechanical stirring for 1 h. After drop wise addition of a solution of 1 ml of tetraethylorthosilicate (TEOS) in 40 ml of isopropanol, the mixture was sonicated under mechanical stirring for another 2 h. Then, the nanoparticles were magnetically separated and washed with distilled water. Finally, SiMNPs were dried at various temperatures (45-103 °C) according to acid functionalization requirements.

Figure 1-3 Silica coating of cobalt iron oxide nanoparticles

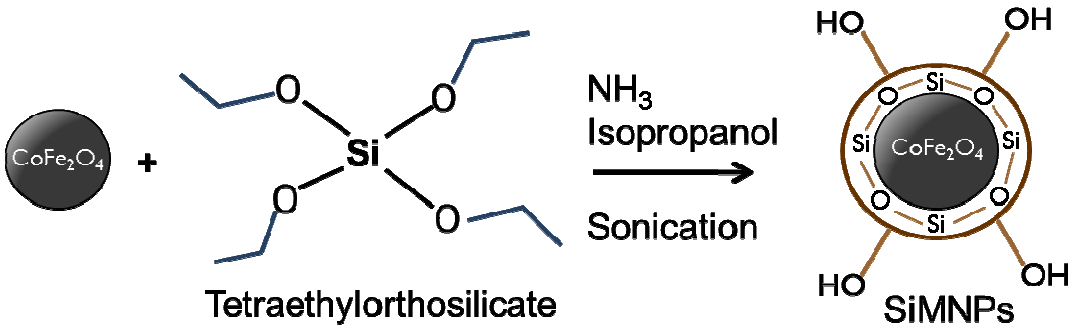

1.2.4 Surface grafting of acid groups

Conventionally, catalysts have been categorized as homogeneous or heterogeneous. Homogeneous catalysts are catalysts which are in the same phase as reactants and/or products. Because reactants and catalysts are closer to each other, homogeneous catalysts are advantageous because they do not introduce mass transfer problems like their heterogeneous counterparts. Becasue homogeneous catalysts are completely miscible in the reaction mixture; they demand more specialized methods of separation once the reaction is completed. Homogeneous acid catalysts have been used successfully for a diverse array of catalytic organic reactions. On the other hand, heterogeneous catalysts are advantageous because the catalytic site can be recovered from the reaction media and reused (Alvaro et al 2005; Corma and Garcia 2006). Nanoporous solids containing acid sites, such as silica materials, have shown high catalytic activity in gas and liquid phase reactions (Gao 2007). Solid acids have successfully been proven to catalyze numerous reactions such as alkylation (Ronchin et al 2012), isomerization (Prakash et al 1999), acylation (Olah et al 1999), dehydration of alcohols to ethers (Olah et al 1997), oligomerization (Bucsi and Olah 1992), and monoglycerides synthesis (Bossaert et al 1999). Efficient catalysis of cellulose hydrolysis was also observed using amorphous carbon with surface sulfonic acid, carboxylic acid, and hydroxyl groups (Suganuma et al 2008). Significant yields of glucose were reported for selective hydrolysis of cellulose using acid zeolites and sulfonated activated-carbon (Onda et al 2008). Hydrolysis of hemicellulose using zeolites yielded up to 55% of xylose and arabinose (Dhepe and Sahu 2010). Catalytic performance of sulfonic acid-modified mesoporous silica was also evaluated for the hydrolysis of sucrose and starch (Dhepe et al 2005). High cellobiose conversion was obtained using sulfonic and carboxylic acid-functionalized mesoporous silica (Bootsma and Shanks 2007). In order to avoid mass transfer limitations, these catalysts must have large surface areas available for reaction, thus leading to the use of nanoparticles as substitute to porous solid supports in this project. Grafting of acids groups has been conducted through the silanization of hydroxylated surfaces. Trialcoxysilanes are hydrolyzed in the presence of water in acid or alkaline media to form silanols. One silanol group reacts with surface hydroxyl groups, consequently losing water in the process (Plueddemann 1982) (Figure 1-4).

Figure 1-4 Silanization of hydroxylated surfaces

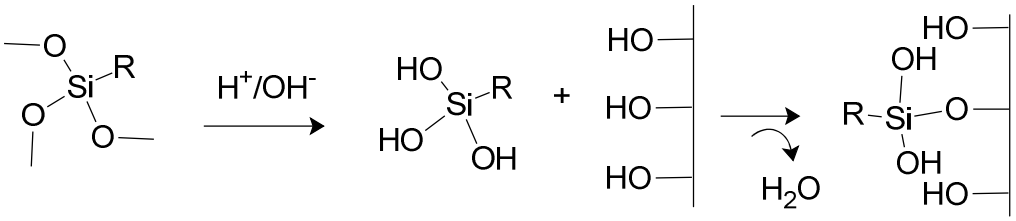

Silanols are unstable and can also react with each other to form siloxans chains (Figure 1-5). Silane concentration, water concentration, pH and time must be carefully controlled so the trialxoxysilanol molecules react with the surface first instead of with each other.

Figure 1-5 Silanols condensation to siloxans

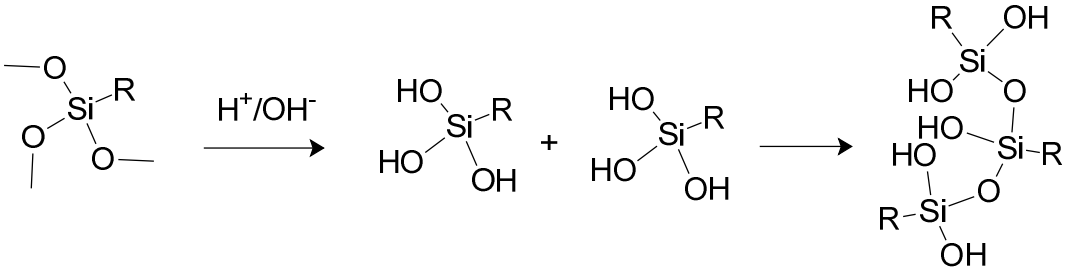

In this dissertation, three precursors of acid functionalities were used to modify the surface of SiMNPs: two silanes and one sultone. The silanes served as precursors of carboxylic and sulfonic acids, and the sultone was used to graft perfluorosulfonic acids.

1.2.4.1 Preparation of supported butylcarboxylic acid (BCOOH)

Synthesis of BCOOH nanoparticles was carried out following silica modification methods reported in the literature (Bootsma and Shanks 2007). A scheme of this procedure is shown in Figure 1-6. SiMNPs (1 g) and CPTES were added to a diluted HCl solution. This mixture was sonicated and then mechanically stirred overnight under heat. The nanoparticles were magnetically separated from the reaction solution and washed with distilled water. The cyano groups were oxidized to carboxylic acid groups with a H_2SO_4 solution. BCOOH nanoparticles were washed with distilled water until the wash water was neutral. Finally, the BCOOH nanoparticles were dried at 103°C.

Figure 1-6 Grafting butylcarboxilic acid groups on silica surfaces

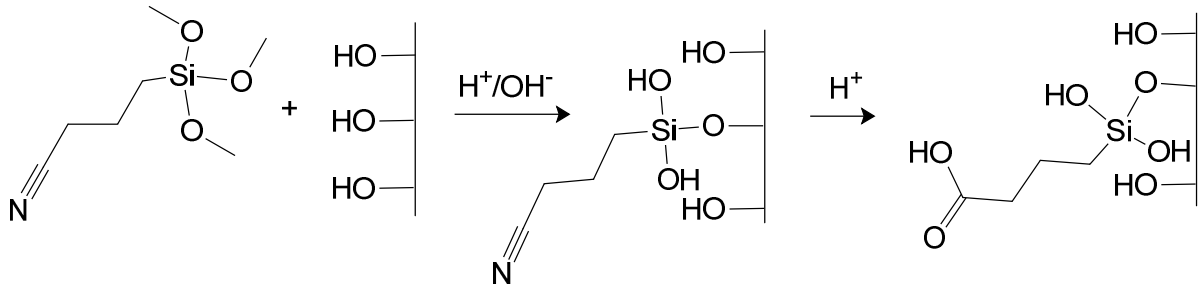

1.2.4.2 Preparation of supported alkylsulfonic acid (AS)

Synthesis of PS nanoparticles was performed following silica modification methods reported in the literature (Cano Serrano et al 2003; Diaz et al 2000; Gill et al 2007). A scheme of this synthesis procedure is shown in Figure 1-7. In a typical experiment, SiMNPs were added to a solution of MPTMS and solvent. The mixture was sonicated and then stirred under heat overnight. SiMNPs with attached thiol groups (SiMNP-C_3H_6SH) were recovered magnetically and washed with distilled water. The thiol groups in the recovered SiMNP-C_3H_6SH were oxidized to sulfonic acid groups with a 25% hydrogen peroxide solution. The product of the oxidation was recovered magnetically and washed with distilled water. The particles were reacidified with a diluted solution of H_2SO_4, washed with distilled water, and dried at 103°C.

Figure 1-7 Grafting propylsulfonic acid groups on silica surfaces

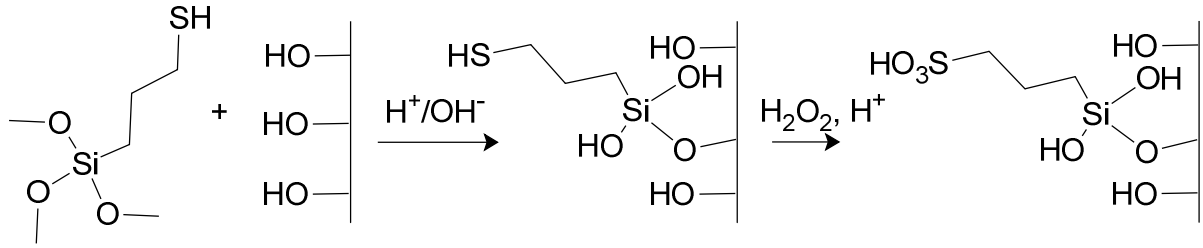

1.2.4.3 Preparation of supported perfluoropropylsulfonic acid (PFS)

Grafting perfluoropropylsulfonic acid groups has been reported in the literature (Alvaro et al 2005; Harmer et al 1996; Harmer et al 1997). A scheme of the procedure is shown in Figure

1-8. In this dissertation a similar procedure was used. Dried SiMNPs and toluene were placed in a three-neck, round-bottom reaction flask and subjected to sonication. After sonication of the nanoparticles, HFP sultone was added to the flask in a fume hood. The mixture was mechanically stirred and heated at 80°C for 4 h. The PFS product was magnetically separated, washed with anhydrous toluene, and washed with hexane. Finally, the PFS nanoparticles were dried at 103°C.

Figure 1-8 Grafting perfluoropropylsulfonic acid groups on silica surfaces

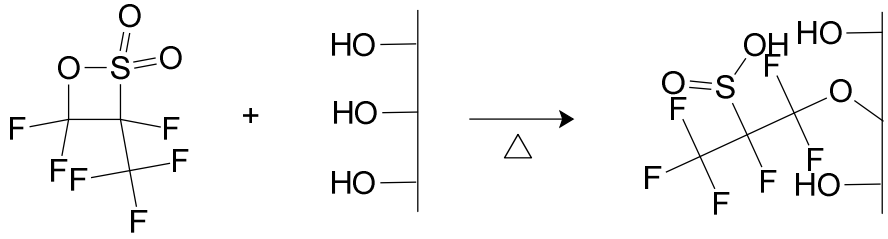

1.2.5 Cellobiose hydrolysis

Cellobiose hydrolysis was used as the model reaction to evaluate the catalytic performance of BCOOH, PS, and PFS nanoparticles in breaking β-(1→4) glycosidic bonds (Figure 1-9). Cellobiose is the repeating unit of cellulose. The β-(1→4) bond that links two glucose molecules makes the cellulose polymer highly crystalline, water insoluble, and highly resistant to depolymerization (Bayer et al 1998; Brown 2003; Chanzy 1990; Fleming et al 2001; O'Sullivan 1997; Preston 1986; Preston 1951; Saxena and Brown 2005). Understanding the mechanisms for cellobiose hydrolysis is useful to device more efficient cellulose depolymerization methods. In this dissertation, cellobiose was hydrolyzed with acid functionalized nanoparticles at 160°C and 175°C. Hydrothermolysis of cellobiose was carried out at the same temperatures and served as control for the experiments. After pretreatment, the nanoparticles were washed with water, separated with a magnet, and dried at 103°C for subsequent reactions. The recyclability of the PFS and AS catalysts was evaluated by running the reaction on each catalyst (BCOOH, AS, and PFS nanoparticles) three times. The organic content before and after reaction was determined to estimate how many functional groups were lost

during reaction. The amount of glucose degraded to hydroxymethylfurfural (HMF) and levulinic acid was also accounted to identify the amount of glucose lost during hydrolysis.

Figure 1-9 Acid hydrolysis of cellobiose to glucose

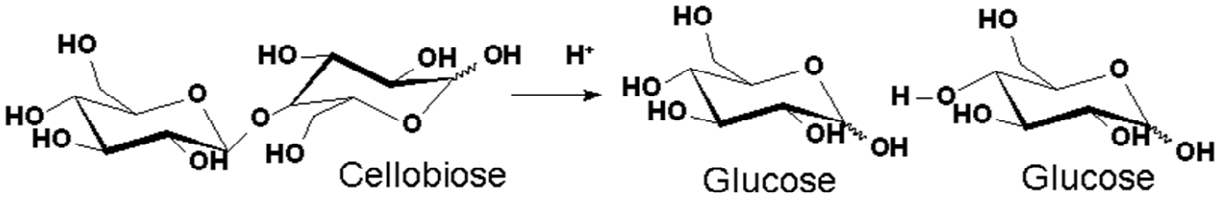

1.2.6 Biomass pretreatment

Production of ethanol from renewable biomass is done through metabolic conversion of monomeric sugars by yeast. Because lignocellulosic biomass in its native form is highly resistant to enzymatic digestion, it must undergo a physical and/or chemical pretreatment. Pretreatment makes lignocellulosic biomass more susceptible to enzyme action because pretreatment removes lignin and hemicelluloses and exposes the cellulose fibrils (McMillan 1994). High digestibility has been correlated to low cellulose cristallinity values, low lignin content, and/ or low acetyl content (Hendriks and Zeeman 2009; Yang and Wyman 2004). Various methods, physical and chemical or a combination, have been evaluated for pretreatment of lignocellulosic biomass (Hendriks and Zeeman 2009; Mosier et al 2005; Zhang et al 2009). Steam explosion (Corredor et al 2008; Varga et al 2004; Viola et al 2007), liquid hot water (Allen et al 2001; Liu and Wyman 2005), dilute acid and alkaline pretreatments such as ammonia fiber explosion (AFEX), and ammonia recycle percolation (ARP) are among the most common methods to pretreat lignocellulosic biomass reported in the literature (Dale and Lau 2009; Sousa et al 2009; Teymouri et al 2005). Alkaline pretreatment works well primarily for hardwood biomasses. Acid treatments increase biomass digestibility for a large variety of biomasses, but hemicellulose recovery is low because some sugars are lost to degradation products (Bobleter 1994; Dien et al 2006; Liu and Wyman 2004; Lloyd and Wyman 2005; Marzialetti et al 2008; McMillan 1994; Sievers et al 2009; Sousa et al 2009; Torget and Hsu 1994; Wyman et al 2005).

Acid-based pretreatments

Numerous studies have used mineral acids as the preferred catalyst for pretreatment of lignocellulosic biomass (Dien et al 2006; Liu and Wyman 2004; Lloyd and Wyman 2005;

Marzialetti et al 2008; Sievers et al 2009; Torget and Hsu 1994). Acid hydrolysis is typically combined with thermal and physical treatments, and the principle of acid treatments is the acid catalysis of hemicelluloses and lignin-carbohydrate linkages (Liu and Wyman 2004). For softwoods, 60% of the hemicellulose from loblolly pine was solubilized to monosaccharides when 1% sulfuric acid solutions were used for 60 min at 150°C (Marzialetti et al 2008). For hardwood pretreatment, xylan solubilization reached 96% from yellow poplar sawdust when a 0.8% (w/v) sulfuric acid solution at 175°C during 10 min treatment was used (Allen et al 2001). Hybrid poplar was pretreated with 0.73% (w/w) sulfuric acid and two temperature stages, 140°C and 170°C, in order to solubilize the fast and slow hydrolyzing fractions of xylan (Torget and Hsu 1994). Alfalfa, reed canarygrass, and switchgrass were pretreated with 0-2.5% (w/v) sulfuric acid solutions at 121-150°C for 20-60 min (Dien et al 2006), and agricultural residues, such as corn stover, were pretreated at 180°C with 0.05-0.1% (w/w) sulfuric acid solutions (Liu and Wyman 2004). In order to reach 80% wheat straw digestibility in 1h at 140°C, 0.5% sulfuric acid solutions are commonly used (Grohmann et al 1984).

The primary goal of pretreatment is exposition of the cellulose fibrils in order to increase the available area for enzymatic action. Some common temperatures and acid concentrations used on pretreatment of corn stover are shown in Table 1-1 Pretreatment conditions for corn stover. The lower the acid concentration, the stronger the thermal treatment undergone by the sample must be. High temperatures require high energy inputs. High energy requirements reduce the economic feasibility of the process. Lower temperatures require the use of higher acid concentrations, but acid solutions should be avoided because of neutralization and corrosion issues associated with their use. A recoverable and reusable catalyst that allows the use of low temperatures is desirable for biomass pretreatment. In this project, an investigation on the possible application of solid acids to the pretreatment of lignocellulosic biomass was carried out.

Table 1-1 Pretreatment conditions for corn stover

Temperature	Sulfuric acid concentration wt. %	Time/rate (min)	Xylan solubilization	Reference
140 °C	0.98	40	32.4%	(Lloyd and Wyman 2005)
160 °C	0.5	40	93.1%	(Shen and Wyman 2011)
180 °C	0.1	10 ml/min	95-97%	(Liu and Wyman 2004)
200 °C	0.0	15	53.0%	(Stuhler 2002)

In this work, wheat straw and corn stover were pretreated using acid-functionalized nanoparticles. The biomass was pretreated at temperatures between 140-200°C, and acid concentration in the solutions was equivalent to 30 mmol H^+/L. The time used for pretreatment was 60 min for all experiments. A scheme of the process can be observed in Figure 1-10.

Figure 1-10 Pretreatment of biomass using acid-functionalized nanoparticles

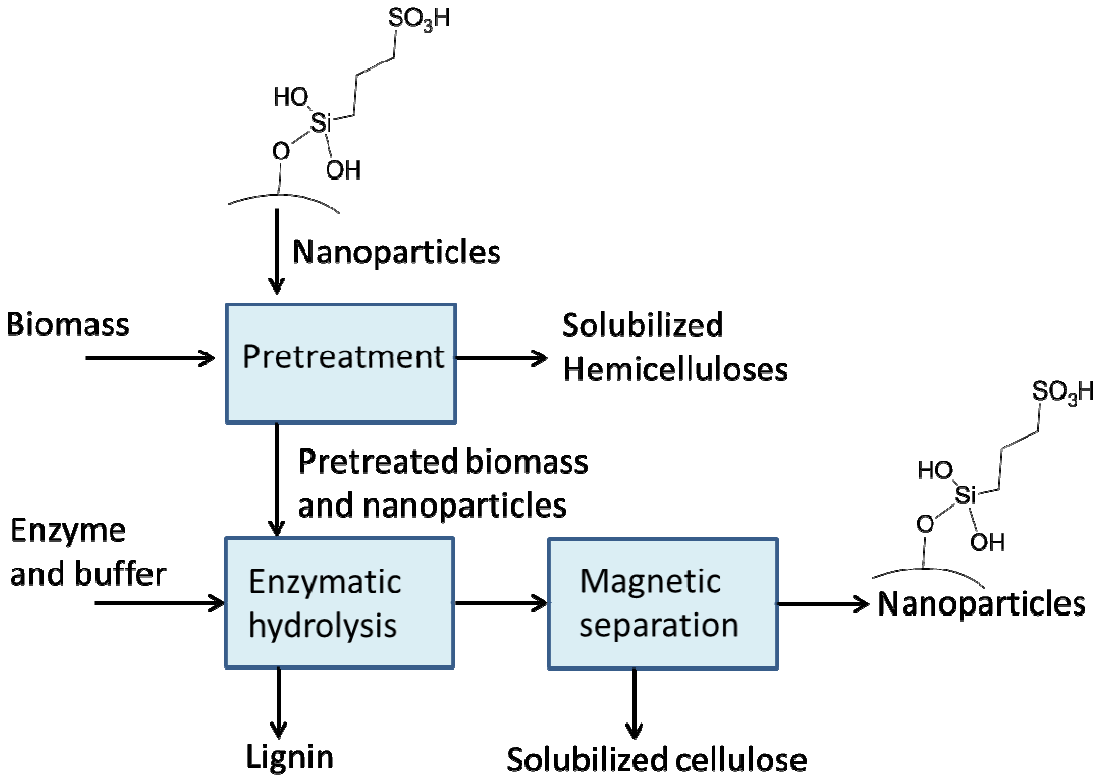

Chapter 2 - Cellobiose Hydrolysis Using Acid-Functionalized Nanoparticles[1]

Abstract

Mineral acids have been used effectively for the pretreatment of cellulosic biomass to improve sugar recovery and promote its conversion to ethanol; however, substantial capital investment is required to enable separation of the acid, and corrosion-resistant materials are necessary. Disposal and neutralization costs are also concerns because they can decrease the economic feasibility of the process. In this work, three acid-functionalized nanoparticles were synthesized for pretreatment and hydrolysis of lignocellulosic biomass. Silica-protected cobalt spinel ferrite nanoparticles were functionalized with perfluoropropylsulfonic acid (PFS), propylsulfonic acid (PS), and butylcarboxylic acid (BCOOH) groups. These nanoparticles were magnetically separated from the reaction media and reused. TEM images showed that the average diameter was 2 nm for both PFS and BCOOH nanoparticles and 7 nm for PS nanoparticles. FTIR confirmed the presence of sulfonic and carboxylic acid functional groups. Ion exchange titration measurements yielded 0.9, 1.7, and 0.2 mmol H^+/g of catalyst for PFS, PS, and BCOOH nanoparticles, respectively. Elemental analysis results indicated that PFS and PS nanoparticles had 3.1% and 4.9% sulfur, respectively. Cellobiose hydrolysis was used as a model reaction to evaluate the performance of acid-functionalized magnetic nanoparticles for breaking β-(1→4) glycosidic bonds. Cellobiose conversion of 78% was achieved when using PS nanoparticles as the catalyst at 175°C for 1 h, which was significantly higher than the conversion for the control experiment (52%) (P-value: 0.0051). PS nanoparticles retained more than 60% of their sulfonic acids groups after the first run, and 65% and 60% conversion were obtained for the second and third runs, respectively.

[1] Results have been published as a peer-reviewed paper. Peña, L., Ikenberry, M., Ware, B., Hohn, K. L., Boyle, D., and Wang, D. 2011. Cellobiose hydrolysis using acid-functionalized nanoparticles. Biotechnology and bioprocess engineering. 16:1214-1222

2.1 Introduction

The world's economies, especially the U.S. economy, are dependent on fossil fuels (coal, oil, and natural gas), which are finite energy sources. Renewable fuels are increasingly being considered as replacements for petroleum-based fuels due to the natural resource limitations, environmental problems, and national security issues associated with petroleum. The U.S. government recently called for the nation to produce 36 billion gallons of renewable fuels annually by 2022 (Allred et al 2008). In 2009, about 10.8 billion gallons of fuel ethanol were produced in the U.S. (U.S. Energy Information Administration). At present, ethanol is produced primarily from corn (97%); however, using the entire 2009 corn crop for ethanol production would yield about 36 billion gallons of ethanol, or only about 17% of the nation's needs. Furthermore, a dramatic increase in ethanol production using current grain-starch-based technology may be restrained by demand for food and feed staples. Cellulosic biofuels do not have the same limitations of grain-starch-based biofuel production.

Biofuel production from cellulosic biomass faces significant technical challenges. Success largely depends on the physical and chemical properties of the biomass, pretreatment methods, effective enzyme systems, efficient fermentation microorganisms, and optimization of processing conditions. Lignocellulosic materials are a complex mixture of cellulose, hemicellulose, and lignin. The cellulose component of these materials is not readily available for enzymatic hydrolysis, so a physical and chemical pretreatment is required before proceeding to hydrolysis: Acidic or basic solutions in conjunction with physical treatments have been used to hydrolyze hemicelluloses and break down the lignin seals to improve the subsequent enzymatic hydrolysis of the cellulose polymer (Herrera et al 2004; Jacobsen and Wyman 2002; Liu and Wyman 2005; Teymouri et al 2004). High yields have been reached with treatments that employ sulfuric acid solutions (Corredor et al 2008; Lee and Kim 2002; U.S. Department of Energy 2006; Viola et al 2007); however, even low concentrations of sulfuric acid can degrade glucose to hydroxymethylfurfural and other undesirable compounds (Mosier et al 2002). Using sulfuric acid also requires a greater investment; because of its corrosive nature, more expensive equipment is required and further costs for its separation and neutralization are incurred. In addition, a variety of degradation products derived from the pretreatment of cellulosic biomass could inhibit the normal growth and ethanol fermentation using *Saccharomyces cerevisiae*

(Nilsson et al 2005; Oliva et al 2006). Detoxification, neutralization, and separation steps must precede enzymatic hydrolysis.

Acid catalysts have been used successfully for a diverse array of catalytic organic reactions (Alvaro 2005; Bootsma and Shanks 2007; Lien and Zhang 2007). Nanoporous solids with acid sites have shown high catalytic activity in gas and liquid phase reactions (Harmer et al 2007). Efficient catalysis of cellulose hydrolysis was observed using amorphous carbon with surface sulfonic acid, carboxylic acid, and hydroxyl groups (Suganuma et al 2008). Significant yields of glucose were reported for selective hydrolysis of cellulose using acid zeolites and sulfonated activated-carbon (Onda et al 2008). Hydrolysis of hemicellulose using zeolites yielded up to 55% of xylose and arabinose (Dhepe and Sahu 2010). Catalytic performance of sulfonic acid-modified mesoporous silica was also evaluated for the hydrolysis of sucrose and starch (Dhepe et al 2005). High cellobiose conversion was obtained using sulfonic and carboxylic acid-functionalized mesoporous silica (Bootsma and Shanks 2007). Because of their tunable properties, functionalized nanoparticles have become an important research subject (Corma and Garcia 2006). Nanoparticles that have magnetic properties can be recovered by applying a magnetic field (Yoon et al 2003), and acid-functionalized nanoparticles may have potential as catalysts for pretreatment and hydrolysis of lignocellulosic biomass. Using magnetic acid-functionalized nanoparticles could combine the benefits of an acidic catalyst with the advantages of being recoverable and reusable.

Cellobiose hydrolysis has been previously used as the model reaction for conversion of cellulose to its glucose monomers (Bootsma and Shanks 2007; Shimizu et al 2009). The objective of this study was to measure the catalytic cellobiose conversion using silica-coated cobalt spinel ferrite magnetic nanoparticles functionalized with one of three different acid functional groups: butylcarboxylic acid (BCOOH), propylsulfonic acid (PS), and perfluoropropylsulfonic acid (PFS).

2.2 Materials and Methods

2.2.1 Materials

Ammonium hydroxide, isopropanol, and toluene (A.C.S. reagents) were purchased from Fisher Scientific (Pittsburgh, Pa., USA). Cobalt(II) chloride hexahydrate (99%), diethylamine (99.5%), D-(+)-cellobiose (98%), iron(II) chloride tetrahydrate (99.99%), 3-

mercaptopropyltrimethoxysilane (MPTMS) (95%), 4-(triethoxysilyl)-butyronitrile (CPTES) (98%), methylamine (40% w/w, 98.5%), sodium dodecyl sulfate (98.5%), and tetraethylorthosilicate (TEOS) (99.999%) were purchased from Sigma-Aldrich (St. Louis, Mo., USA). Ethanol (95%) was purchased from Decon Laboratories (King of Prussia, Pa., USA). Hexafluoro(3-methyl-1-2-oxathiethane)-2,2-dioxide (HFP sultone) (95%) was purchased from SynQuest Labs (Alachua, Fla., USA).

2.2.2 Synthesis and functionalization of nanoparticles

Cobalt spinel ferrite ($CoFe_2O_4$) nanoparticles were synthesized using the microemulsion method described in the literature (Gill et al 2007; Phan and Jones 2006; Rondinone et al 1999). Silica coating, AS functionalization, and PFS functionalization procedures were carried out following methods slightly modified from previous literature (Gill et al 2007). Preparation of BCOOH-functionalized nanoparticles was based on the methods used for carboxylic acid modification of amorphous silicas (Bootsma and Shanks 2007).

2.2.2.1 Preparation of magnetic nanoparticles (MNPs)

In a typical experiment, 4 mmol of cobalt (II) chloride hexahydrate and 8 mmol of iron (II) chloride were mixed to form an aqueous solution (500 ml). Forty-five mmol sodium dodecyl sulfate (SDS) were dissolved in distilled water to make 500 ml of solution. This solution was added to the cobalt and iron solution and the mixture was stirred at room temperature with a mechanical stirrer for 30 min before heating to 60°C. Another solution (1L) was prepared with 300 ml of methylamine (40% w/w) and distilled water. Then this solution was also heated to 60°C. Both solutions were finally mixed and stirred for 3 h. The nanoparticles were separated magnetically, washed three times with distilled water, washed once with ethanol, and suspended in 100 ml of ethanol. About 1g of MNPs was dried at room temperature under vacuum for XRD and FTIR analysis.

2.2.2.2 Silica coating of the magnetic nanoparticles (SiMNPs)

The ethanol dispersion of MNPs was sonicated and stirred for 30 min, after which 12 ml of the solution were added to 530 ml of isopropanol and 40 ml of water. This solution was also sonicated under mechanical stirring for 1 h. Then 50 ml of concentrated ammonium hydroxide were added to the mixture. A solution of 1ml of tetraethylorthosilicate (TEOS) in 40 ml of

isopropanol was added dropwise to the former solution. The mixture was sonicated under mechanical stirring for 3 h total. The nanoparticles were magnetically separated and washed with large amounts of distilled water, then dried in a forced-air oven at 103°C for 24 h.

2.2.2.3 Acid functionalization of the silica-coated magnetic nanoparticles

Preparation of supported propylsulfonic acid (PS): A solution with 4 ml of MPTMS, 50 ml of ethanol, and 50 ml of water was prepared, and then 1 g of SiMNP was added. The mixture was sonicated for 60 min and stirred at 80°C overnight. SiMNPs with thiol groups attached (SiMNP-SH) were recovered magnetically and washed three times with 50 ml of distilled water. A solution of 30 ml of 50% hydrogen peroxide, 30 ml of distilled water, and 30 ml of methanol was added to the recovered SiMNP-SH. The mixture was left two days at room temperature to oxidize the thiol groups to sulfonic acid groups. The product of the oxidation step was recovered magnetically and washed three times with 100 ml of distilled water. The particles were reacidified with 50 ml of 2 M H2SO4, washed three times with distilled water, and dried in a forced-air oven at 103°C for 24 h. PS nanoparticles were stored in a desiccator at room temperature.

Preparation of supported perfluoropropylsulfonic acid (PFS): One gram of SiMNPs dried at 103°C overnight was placed in a three-neck, round-bottom reaction flask. Approximately 150 ml of anhydrous toluene were poured into the flask. After 1 h of sonication, 3 ml of FHP sultone were added to the flask in a fume hood. The mixture was mechanically stirred overnight at 80°C. The PFS product was magnetically separated, washed with anhydrous toluene, and washed twice with hexane. The nanoparticles were dried at 103°C overnight and stored in a desiccator at room temperature.

Preparation of supported butylcarboxylic acid (BCOOH): Synthesis of BCOOH nanoparticles was carried out in 200 ml of 0.5 N HCl. One gram of SiMNPs and 4 ml of CPTES were placed in this solution and sonicated for 1 h; this mixture was then mechanically stirred overnight at 80°C. The nanoparticles were magnetically separated from the reaction solution and washed with distilled water. The nanoparticles were left in a 2 M H_2SO_4 solution overnight to oxidize the cyano groups to carboxylic acid groups. Finally, the carboxylic acid-functionalized nanoparticles were washed with abundant amounts of distilled water, dried at 103°C and stored in a desiccator at room temperature.

2.2.3 Characterization

Transmission electron microscope (TEM) images were used to estimate the size distribution of the nanoparticles. A model CM100 (FEI Company, Hillsboro, Ore., USA) equipped with an AMT digital image capturing system was operated at 100 kV. Before analysis, the PS and PFS nanoparticles were dispersed in water and sonicated for one hour. The dispersed nanoparticles were absorbed for approximately 30 s at room temperature onto Formvar/carbon-coated, 200-mesh copper grids (Electron Microscopy Sciences, Fort Washington, Pa., USA), then viewed by TEM.

Fourier transform infrared (FTIR) spectra were used to investigate the functional groups covalently attached on the surface of the synthesized nanoparticles. Reagent KBr and samples were dried for 24 h at 103°C and then prepared by mixing 2 mg of sample with 200 mg of spectroscopy-grade KBr. The measurement was carried out for wavenumbers 400–4000 cm-1, with the detector reading at 4 cm-1 resolution and 32 scans per sample using a Thermo Nicolet NEXUSTM 870 infrared spectrometer (Spectra-Tech: Model No. 0031-901) with a ZnSe window. The OMNIC software program by Nicolet was used to determine the peak positions and intensities.

X-ray diffraction (XRD) spectra were collected for MNPs and acid functionalized nanoparticles samples. The spectra were acquired on a Rigaku MiniflexII desktop x-ray diffractometer using CuKα radiation. The data were collected from 10 to 70° (2θ) with 0.02 degree resolution.

2.2.4 Hydrolysis of Cellobiose

Cellobiose hydrolysis was used as the model reaction to evaluate the catalytic performance of BCOOH, PS, and PFS nanoparticles in breaking the β-(1→4) glycosidic bonds. Figure 2-1 Diagram acid hydrolysis of cellobioseshows a possible mechanism for the hydrolysis of cellobiose using PS nanoparticles. Hydrothermolysis of cellobiose was carried out at the same conditions and served as the control for the experiments. The reaction was run with 1% cellobiose and 0.2% catalyst by weight in a 600 ml pressure reactor (Model 4544; Parr Instrument Co., Moline, Ill.) for 60 min at both 160°C and 175°C. All experiments were run at least twice. After each run, the nanoparticles were washed with abundant water, separated with a magnet, and dried at 103°C for subsequent reactions. The recyclability of the PFS and PS

catalysts was evaluated by running the reaction on each catalyst (BCOOH, PS, and PFS nanoparticles) three times; all reaction parameters were held constant except for only using the 175°C reaction temperature during the second and third runs.

Figure 2-1 Diagram acid hydrolysis of cellobiose

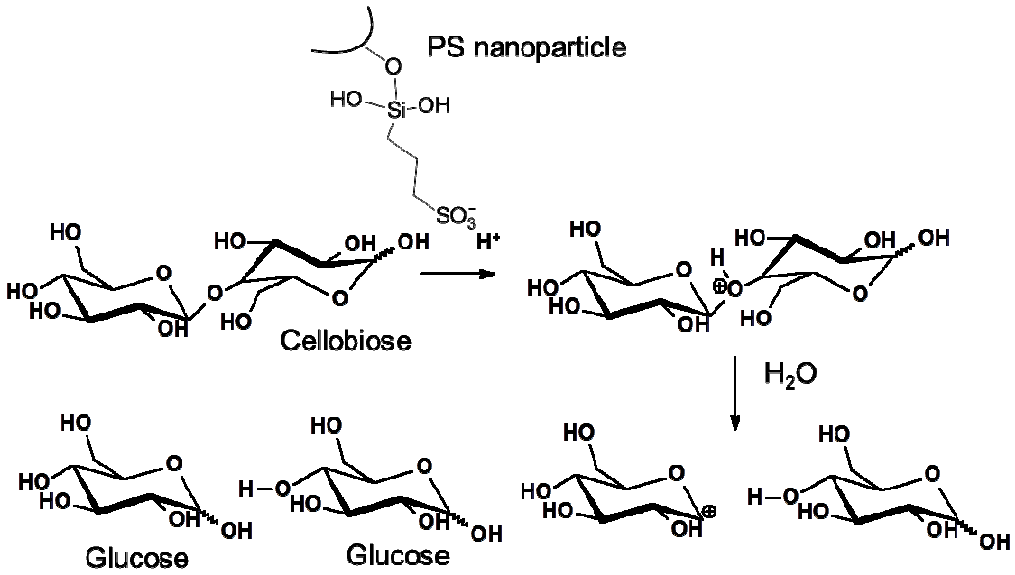

2.2.5 Analytical methods

Hydronium ion concentration per unit mass of catalyst was determined with the ion-exchange titration method (Melero et al 2002). To withdraw the hydronium ions from the catalyst, 0.05 g of catalyst was added to 20 ml of a salt solution, either sodium chloride (NaCl, 2 *M*) or tetramethylammonium chloride (TMACl, 2 *M*). The suspensions were sonicated, left overnight at static conditions and room temperature, and then titrated to neutrality with a 0.01*M* NaOH solution. Samples were analyzed after each synthesis batch in duplicate. Samples of sugar solutions from hydrolysis reactions were analyzed by HPLC using a RCM-Ca monosaccharide column (300 x 7.8mm; Phemomenex®, Torrance, Cal., USA) and refractive index detector. Samples were neutralized with $CaCO_3$ and run at 80°C at 0.6 ml/min with double-distilled water. The conversion of cellobiose was calculated as the ratio of cellobiose present in the reaction media after and before hydrolysis. To calculate glucose yield, the initial mass of glucose was obtained by multiplying the cellobiose mass by 1.053, which is the hydration factor (Sluiter et al

2008a). The products of the decomposition of glucose were measured using an ROA-organic acid column (300 x 7.8 mm; Phemomenex®, Torrance) and UV detector. Samples were run at 65°C at 0.6 ml/min with 5 mM H_2SO_4 for 55 min. The sulfur content was used as an indicator of the number of sulfonic acid groups grafted to the nanoparticles. Sulfur content values were measured in an elemental analyzer (PerkinElmer Model 2400 SeriesII). Each sample was tested for sulfur content at least twice.

2.3 Results and Discussion

2.3.1 Characterization of the acid functionalized nanoparticles

TEM images of $CoFe_2O_4$ nanoparticles are shown in Figure 2-2A. The silica coating process is quite sensitive to the TEOS concentration in the solution. When added at high rates, silica-coated particles up to 500 nm in diameter were obtained. To get silica coatings in the nanometer scale, drop-wise TEOS addition is required. The mean size of the nanoparticles was estimated using the software ImageJ, available from the National Institutes of Health. Figure 2-2B shows the TEM images of the PFS nanoparticles. Some magnetic core nanoparticles were coated and joined together during the functionalization process, as can be seen in Figure 2-2B, where some particles have more than one inner black dot. However, a sample of 400 PFS-functionalized particles remains in the nanoscale and has a mean diameter of 2.0 nm with a standard deviation of 0.5 nm. Approximately 600 AS-functionalized particles were counted. The diameter of the nanoparticles was 3.1 to 19.3 nm, with an average of 6.9 nm and standard deviation of 2.7 nm. Figure 2-2C shows well-dispersed PS-functionalized nanoparticles. For BCOOH-functionalized nanoparticles, we found a mean diameter of 2.0 nm with a standard deviation of 0.8 nm from a count of 529 particles. Aggregation of the nanoparticles was observed after samples were dried at both low (45°C) and high temperatures (103°). We think that the surface chemistry of the nanoparticle has a bigger effect in the dispersion of the nanoparticles. Therefore, either solvents with higher hydrophobicity or more polar functional groups are required to maintain individual particles.

Figure 2-2 TEM images, the arrows indicate: A. $CoFe_2O_4$ nanoparticles. B. PFS-functionalized nanoparticles. C. PS-functionalized nanoparticles

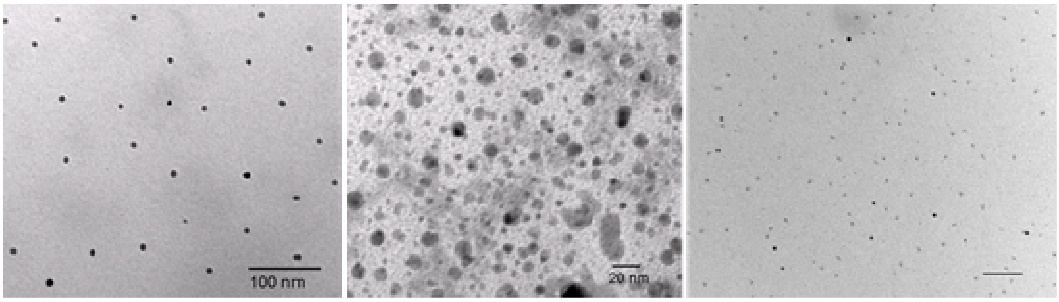

FTIR spectra for the acid-functionalized nanoparticles are shown below in Figure 2-3. The peak at 3390 cm^{-1} in all spectra could be attributed to the O-H stretching vibrations of physisorbed water and possibly surface hydroxyl groups; the peak near 1620 cm^{-1} has been attributed to an O-H deformation vibration and the peak around 1017 cm^{-1}, found in both the PS and PFS spectra, have been associated to Si-O stretching (Phan and Jones 2006). Similarly, the peaks at 810 and 980 cm^{-1} could be attributed to the stretching vibrations of Si-O-Si and Si-O-H groups (Zhao et al 2000). The peak at 1420 cm^{-1} has been assigned to undissociated $–SO_3H$ groups (Alvaro et al 2005). The vibration bands at 1040 cm^{-1} were reported for the stretching of the SO_3 and 1377 cm^{-1} for the O=S=O stretching in the SO_3H group (Blanco-Brieva et al 2008; Suganuma et al 2008). Although the peak from 1100-1200 cm^{-1} is assigned to the C-F bond, it is overlapped by the peak of the Si-O bond (Kim et al 2003; Scaranto et al 2008). The bands between 1020 and 1220 cm^{-1} were reported as the peaks associated to the CF, CF_2, and CF_3 bonds (Biloiu et al 2004). In the FTIR spectra for the butylcarboxylic acid nanoparticles (not shown here), we could see the peaks at 2931 and 2879 cm^{-1}, which have been attributed to $-CH_2$ stretching vibrations (Colilla et al 2010; Kim et al 2010); 1721 cm^{-1} has been associated with carboxylic acid functional moieties (Buruiana et al 2009; Colilla et al 2010; Suganuma et al 2008). The peak at 1326 cm^{-1} corresponds to the nitrile group (Colilla et al 2010), the presence of which indicates that not all cyano groups were oxidized.

Figure 2-3 FTIR spectra for SiMNPs, PFS-functionalized nanoparticles, and PS-functionalized nanoparticles

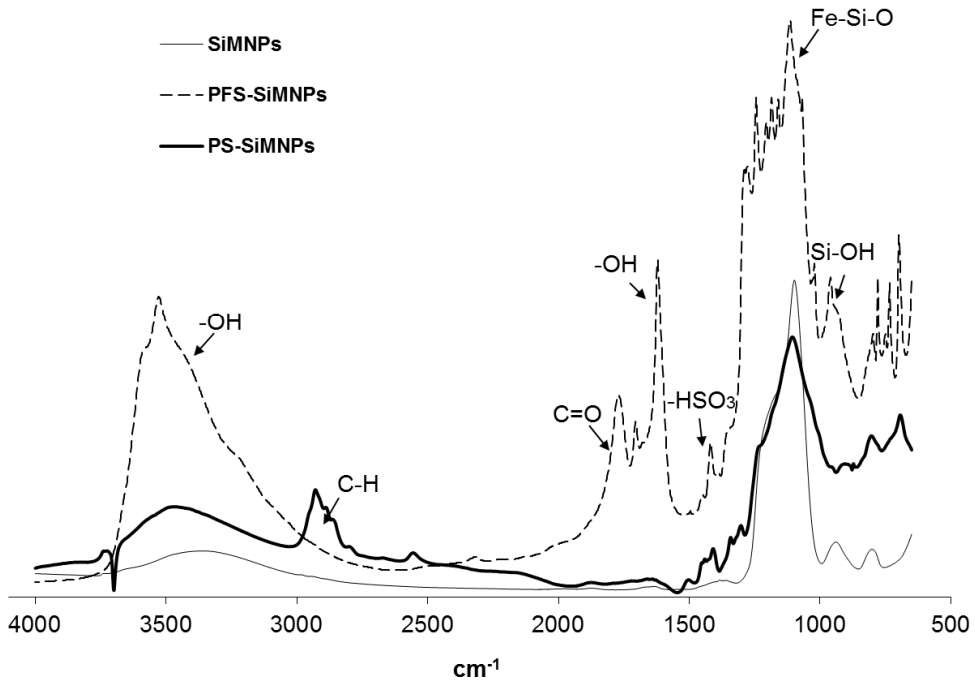

XRD spectra for PS and $CoFe_2O_4$ are shown in Figure 2-4. The spectrum for $CoFe_2O_4$ agrees with previous results (Naseri et al 2010; Senapati et al 2011). All the representative signals for $CoFe_2O_4$ are observed in the XRD spectra of MNPs. Similarly, the XRD pattern for PS nanoparticles shows all the respective signals for the $CoFe_2O_4$ crystals; this spectrum has an additional peak between 20 and 30° (2θ) which is associated to amorphous silica. About 1g of MNPs was dried at room temperature under vacuum; PS nanoparticles. Scherrer's formula was used to calculate the particle size of the nanoparticles. PS and MNPs size was calculated as 19.0 and 17.6 nm, respectively. These averages are larger than those obtained with TEM. The larger sizes calculated from XRD patterns could be explained by possible aggregation of the nanoparticles during the drying step.

Figure 2-4 XRD spectra of MNPs (bottom) and PS nanoparticles

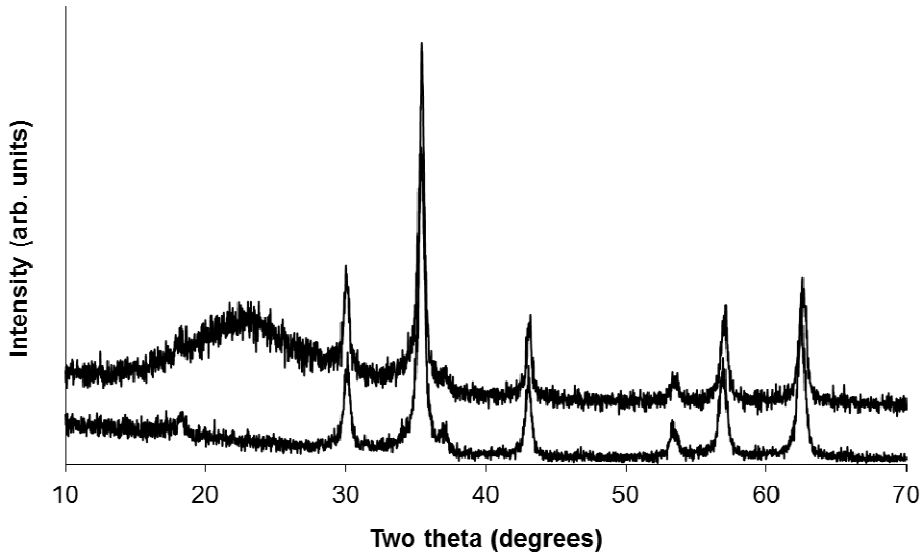

2.3.2 Acid and organic incorporation

The number of acid sites was quantified through ion exchange capacity titration and elemental analysis. The small particle size of the acid-functionalized nanoparticles provided large surface areas and allowed a significant number of acid sites. The measured concentrations of hydronium ions obtained when using NaCl and TMA salts are summarized in Table 2-1 Acid capacity and elemental analysis. The results obtained with both salts are not significantly different, as was expected. Acid-functionalized nanoparticles catalysis did not show a preference for ions of different sizes; meanwhile, a difference can be observed when using porous materials (Melero et al 2002). PFS nanoparticles gave a higher hydronium ion load (1.7 mmol H^+/g) than the PS and BCOOH nanoparticles at 0.9 and 0.2 mmol H^+/g, respectively. The acid capacity values of PFS and AS agree with the values previously reported in the literature (Dube et al 2009a; Dube et al 2009b; Hamoudi et al 2004; Melero et al 2002; Morales et al 2008; Van Rhijn et al 1998). PS nanoparticles had larger sulfur content (4.9%) than PFS nanoparticles (3.1%). High sulfur content and low acid loading may be an indication that not all thiol groups were oxidized to sulfonic acid groups. BCOOH nanoparticles had 3.0% N content, which indicates that not all nitrile groups were oxidized to a carboxylic acid group. Stronger oxidation

conditions, such as ozone treatment, could be used to maximize the acid capacity of PS and BCOOH nanoparticles.

Table 2-1 Acid capacity and elemental analysis

	Acid capacity titration (mmol H^+/g)		% C	% H	% N	% S
	Na^+	TMA^+				
PFS	1.68+0.22	1.82+0.05	12.42+0.73	2.40+0.24	0.38+0.05	3.12+0.11
PS	0.88+0.21	0.93+0.14	6.11+0.09	1.90+0.08	0.20+0.05	4.89+0.15
BCOOH	0.18+0.05	0.18+0.05	19.49+1.98	3.22+0.22	2.98+1.44	0.51+0.15

PFS=perfluoropropyl-sulfonic acid nanoparticles, PS=propyl-sulfonic acid nanoparticles, BCOOH=butylcarboxylic acid.

All data in this table are listed as mean ±95% CI.

2.3.3 Cellobiose hydrolysis

Cellobiose, a disaccharide of glucose units, has the same linkage β-(1→4) bonds as the glucose units in cellulose. At 175°C reaction temperature, 78% cellobiose conversion was obtained when PS nanoparticles were used as the catalyst (P-value: 0.0051); PFS nanoparticles, in another hand, gave 75% conversion of cellobiose (Figure 2-5 Hydrolysis of cellobiose using 1% wt. cellobiose, 0.2% wt. catalyst for 1 h) (P-value: 0.0062). The conversion of cellobiose for both acid-functionalized nanoparticles was higher than that of the control (51%). Shimizu *et al.* (2009) reported cellobiose conversions between 53% and 83% using heteropolyacids at 120°C for 24 h (Shimizu et al 2009). Bootsma and Shanks (2007) reported 90% cellobiose conversion using acid-functionalized mesoporous silicas (Bootsma and Shanks 2007). Their experiments were carried out at similar conditions of acid load and temperature, but the authors did not report control experiments.

Figure 2-5 Hydrolysis of cellobiose using 1% wt. cellobiose, 0.2% wt. catalyst for 1 h

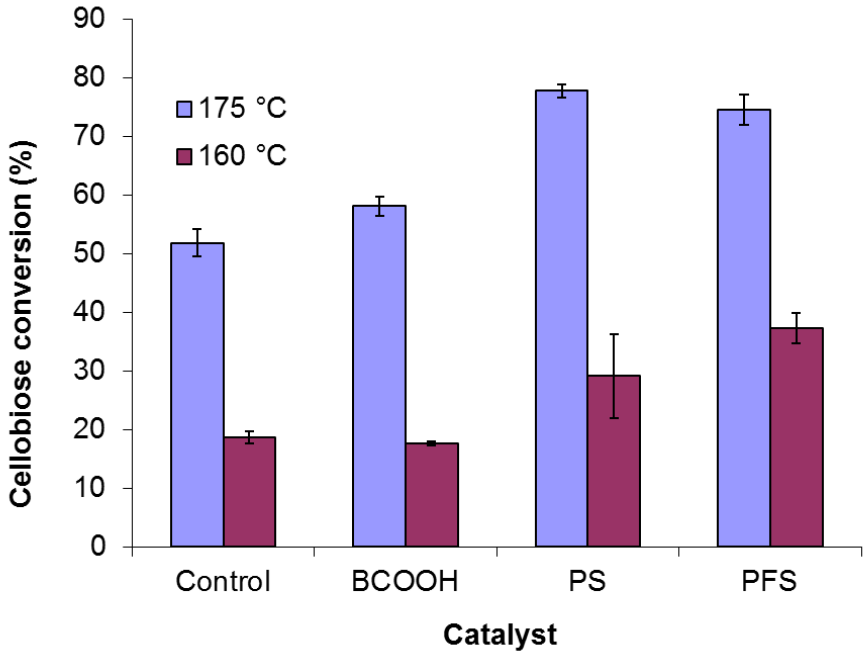

The hydrolysis of cellobiose has been used as the model reaction for cellulose degradation to glucose in several studies (Bootsma and Shanks 2007), (Mosier et al 2002). The same mechanism of acid hydrolysis has been proposed for cellulose and cellobiose because both sugars have similar activation energies. Concentrations levels of 0.02% for the hydronium ion gave a maximum cellulose conversion of 20% at 240°C (Bobleter 1994). In this work, cellobiose conversions above 70% were obtained when the reaction temperature and the hydronium ion concentration were only 175°C and 0.02%, respectively. Mosier *et al.* (2002) found that the hydrolysis of cellobiose depends exclusively on the hydronium ion concentration, regardless of the acid source (Mosier et al 2002). Therefore, PFS nanoparticles, which have an H^+ load almost twice as much as PS nanoparticles have, should give a better conversion than the latter. However, the cellobiose conversion was almost the same for both catalysts. Perfluoropropylsulfonic acids supported on mesoporous silicas have shown high catalytic activity in polar solvents; however, in the presence of water the acid strength of the acid is

leveled off by the solvent (Corma et al 2004). Aggregation of PFS nanoparticles could have decreased the available area for catalytic hydrolysis also. Likewise, PS nanoparticles are difficult to disperse in aqueous solutions which could be explained by the poor water affinity of PS and PFS functionalized materials (Beamson and Alexander 2004; Van Rhijn et al 1998). Higher cellobiose conversion could be attained with this catalyst if a better dispersion is achieved.

Although the conversion of cellobiose is close to 80% with PS nanoparticles at 175°C, the highest glucose yield obtained was only 49.5% during the first run (Figure 2-6), indicating that some glucose was degraded to other products. At high temperature, glucose can undergo mutarotation, isomerization, and dehydration reactions. Bonn, G. and Bobleter O. (1983) reported the presence of fructose, dihydroxyacetone, glycolaldehyde, methylglyoxal, HMF, and furfural in the decomposition productos of the hydrothermolysis of glucose at 240°C (Bobleter 1994; Bonn and Bobleter 1983). Moderate amounts of fructose, formic acid, HMF, and furfural were found in the hydrolysis solution (Figure 2-6). Degradation of sugars limits the temperature of operation (Bootsma and Shanks 2007; Xiang et al 2004). At low temperatures such as 160°C, the conversion of cellobiose is very close to that of the control for all the catalysts used in this work. .Because high temperatures and acidic conditions degrade sugar monomers; the catalyst should reduce the activation energy of the hydrolysis so the reaction can be carried out at lower temperatures. To be more effective at low temperature, higher specificities of the catalysts towards β-(1→4) bonds are required. Tuning the surface functional groups could provide selectivity of the catalyst for β-(1→4) glycosidic bonds.

Figure 2-6 Glucose yield and decomposition products of the hydrolysis of 1% wt. cellobiose with 0.2% catalyst for 1 h at 175°C

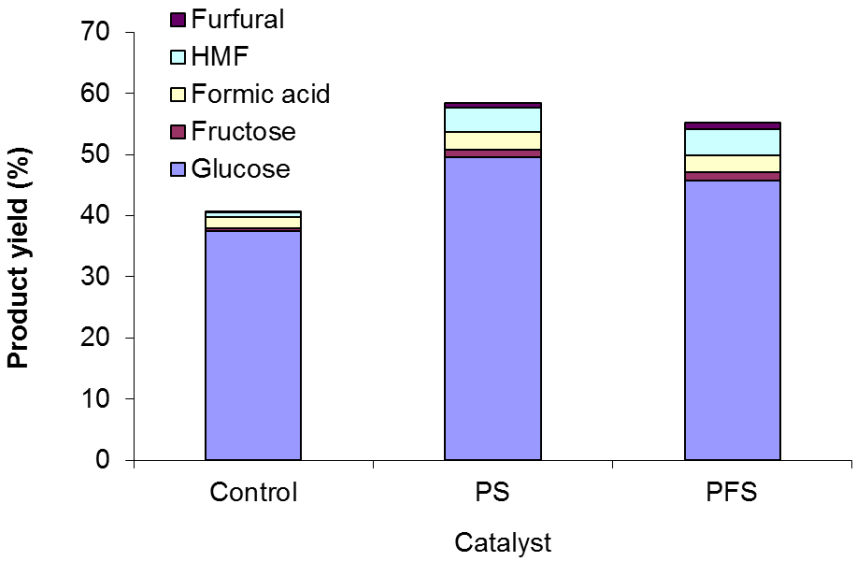

PS nanoparticles gave cellobiose conversions of 64% and 60% after the second and third runs, respectively; in another hand, cellobiose conversion by PFS dropped to 44% and 47%, on the second and third runs, respectively (Figure 2-7 Recycling experiments of cellobiose hydrolysis using 1% wt. cellobiose, 0.2% wt. recycled catalyst for 1 h at 175°C).

Figure 2-7 Recycling experiments of cellobiose hydrolysis using 1% wt. cellobiose, 0.2% wt. recycled catalyst for 1 h at 175°C

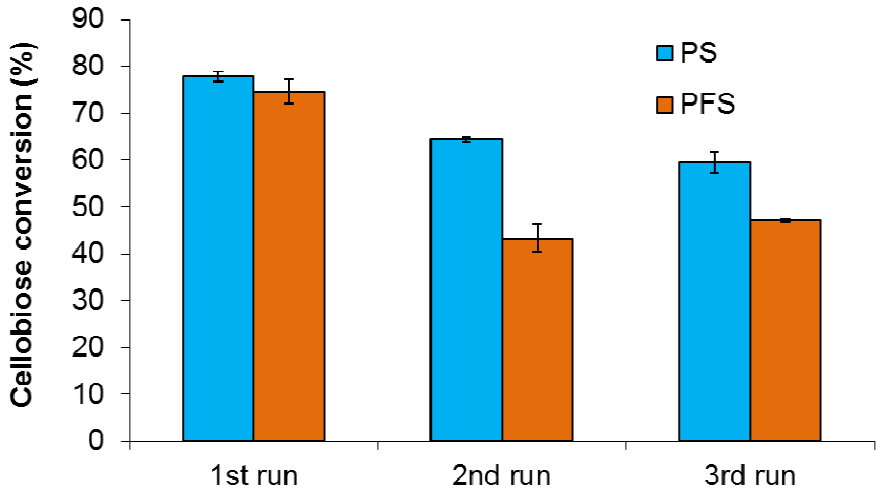

The cellobiose conversion using the recycled PFS nanoparticles decreased about 30% with respect to the PFS nanoparticles used after synthesis, whereas the cellobiose conversion of PS nanoparticles decreased about 15% after the first run. The lower cellobiose conversion for the second and third runs may be explained by the loss of sulfonic acid groups that is confirmed by the sulfur content drop of these catalysts after reaction (Figure 2-8). PFS nanoparticles lost their acid groups to a larger extent than PS nanoparticles did. Fluoroalkyl-sulfonic acids have superacidic character but they are also water sensitive (Dube et al 2009a; Dube et al 2009b; Harmer et al 2007; Woolf 1954). The anchorage of PFS acids on SiMNPs was not enough to improve its stability. A similar situation has been observed before with mesoporous silicas where the -Si-O-CF_2-bond was hydrolyzed during reaction (Alvaro et al 2005). Even though the H^+ load of PS is lower than that of PFS, this catalyst had a higher conversion yield and recyclability; therefore, PS is a better candidate for biomass hydrolysis.

Figure 2-8 Percentage of sulfur content retained on PFS and PS acid-functionalized nanoparticles after hydrolysis of cellobiose at 175°C

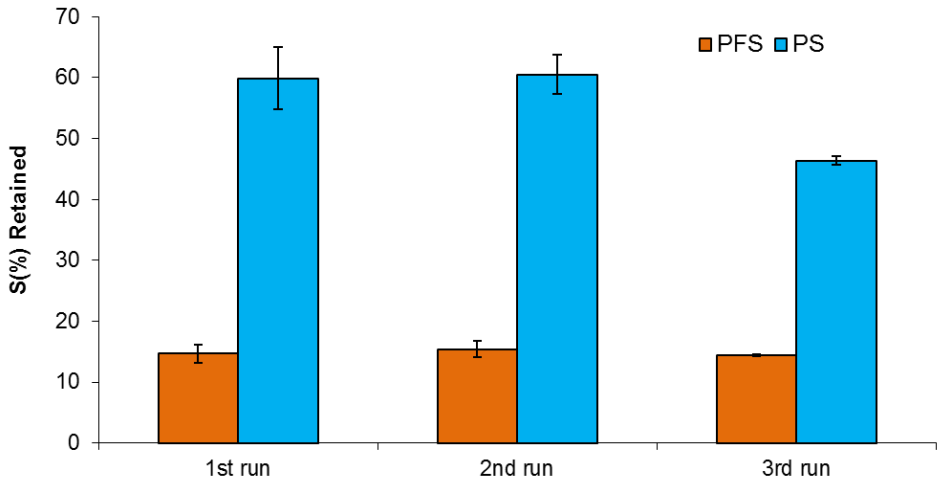

2.4. Conclusions

Silica-coated maganetic nanoparticles (SiMNPs) were functionalized with prefluoroalkylsulfonic (PFS), alkylsulfonic (PS), and butylcarboxylic (BCOOH) acid functions. Feret diameters were calculated from TEM images as 2.0, 6.9, and 2.0 nm, respectively. Total organic content was 32.5%, 12.6%, and 25.9% for PFS, PS, and BCOOH, respectively, determined as loss weight from 200 to 600°C. The sulfur content of PFS and PS was measured as 3.1% and 4.9%, respectively. The carbon content of PFS, PS, and BCOOH was 12.4%, 6.1%, and 19.5%, respectively. The FTIR spectra for all nanoparticles had a broad Si-O band. A band at 1929 cm-1 associated with C-H was observed in the PFS and BCOOH spectra. Peaks associated to undissociated sulfonic acid (1420 cm^{-1}) and to O=S=O groups (1377 cm^{-1}) were observed in PFS and PS spectra. A band at 1738 cm-1 corresponding to the carbonyl group was observed in the BCOOH spectrum.

Hydrolysis of cellobiose using PS and PFS acid functionalized nanoparticles (0.2 g catalyst/g cellobiose) yielded 77.8% (P-value: 0.0051) and 74.6% (P-value: 0.0062) cellobiose conversion at 175°C for 1 h, respectively. Glucose yields hydrolyzed by PS and PFS nanoparticles were 49.5% and 45.8%, respectively. Low glucose yields were due to thermal degradation of the sugar. PS nanoparticles retained approximately 60% of its propyl-sulfonic

acid functional groups and 75% of its original catalytic activity, giving which resulted in 47% cellobiose conversions after a third cycle. PFS nanoparticles lost most catalytic activity, since the cellobiose conversion was 47% after the third cycle. Hydrolysis using BCOOH nanoparticles gave yielded 58.1% cellobiose conversion, and the conversion rate of control was 51.9% (P-value: 0.2306).

Chapter 3 - Acid-Functionalized Nanoparticles for Pretreatment of Wheat Straw[2]

Abstract

Perfluoropropylsufonic (PFS) and propylsufonic (PS) acid-functionalized magnetic nanoparticles were synthesized and characterized, then evaluated for their ability to hydrolyze hemicelluloses. The magnetic core was made of cobalt spinel ferrite and was coated with silica to protect it from oxidation. The silanol groups allowed surface chemical modification of the nanoparticles with the PFS and PS acid functionalities. Thermogravimetric analysis gave a total organic load of 12.6 % and 32.5% (w/w) for PS and PFS nanoparticles, respectively. The surface sulfur content was calculated from XPS analysis as 1.37% and 1.93% for PFS and PS nanoparticles, respectively. Wheat straw samples were treated with the acid-functionalized nanoparticles at two different conditions: 80 °C for 24 h and 160 °C for 2 h. These experiments aimed to hydrolyze wheat straw hemicelluloses to soluble oligosaccharides. PFS nanoparticles solubilized significantly higher amounts of hemicelluloses (24.0 ± 1.1%) than their alkyl-sulfonic counterparts (9.1 ± 1.7%) at 80 °C, whereas the hydrothermolysis control solubilized 7.7 ± 0.8% of the original hemicelluloses in the sample. At 160 °C, PFS and PS nanoparticles gave significantly higher amounts of oligosaccharides (46.3 ± 0.4% and 45 ± 1.2%, P-values: 0.02, and 0.01, respectively) than the control (35.0 ± 1.8%). The hemicelluloses conversion at 160 °C reached 66.3 ± 0.9% using PFS nanoparticles and 61.0 ± 1.2% using PS nanoparticles compared with the control experiment, which solubilized 50.9 ± 1.7% of hemicelluloses in the biomass.

3.1 Introduction

Uncertainties in the oil supply and environmental problems associated with fossil fuels have motivated the search for other energy sources. Ethanol is a renewable energy source that can be used as transportation fuel. Global ethanol production increased 400% in the last decade.

[2] Results have been published as a peer-reviewed paper. Peña, L., Ikenberry, M., Hohn, K. L., and Wang, D. 2012. Acid-Functionalized Nanoparticles for Pretreatment of Wheat Straw. Journal of Biomaterials and Nanobiotechnology. 3:342-352

In 2009, 19 billion gallons of ethanol were produced worldwide (Renewable Fuels Association 2010). In 2007, The US government called for an increase in domestic biofuel production of up to 36 billion gallons by 2030 (Senate and House of Representatives of the United States of America in Congress 2007). Production of ethanol as transportation fuel reached more than 13 billion gallons in 2010 in the US (Office of the Biomass Program 2010). Currently, bio-ethanol is obtained from the alcoholic fermentation of monosaccharides derived from sugar-based and starchy crops (Renewable Fuels Association 2010). These materials are also staple foods, so using them as fuel could strain the food supply. Alternatively, forest- and agricultural-derived biomass can be used for ethanol production after hydrolysis of their constitutive sugar polymers into monomers.

Lignocellulosic biomass comprises 38-50% cellulose, 23-32% hemicellulose, 15-22% lignin, and other minor components (Iborra et al 2006; Wyman and Goodman 1993). Cellulose fibers are polymers of β-1,4-linked glucopyranose units whose linear chains are glued with hemicelluloses and covered with a lignin sheath (Bobleter 1994; McMillan 1994; Preston 1951). Hemicellulose is a heteropolymer of five- and six-carbon sugars that can be simultaneously fermented by modified strains (Rodrussamee et al 2011). Arabinoxylans are the most common hemicelluloses of the cell wall of cereal grains. The backbones of arabinoxylans are made of β-1,4-D-xylopyranosyl units substituted with α-D-arabinofuranosyl units linked to the oxygen in the second or third position. Endosperm cell walls of wheat also have hemicelluloses rich in hexose units such as 1,4- and 1,3-linked β-D-glucan (Bacic and Stone 1980; Girio et al 2010; Olsson et al 2006). Xyloglucans are other hemicelluloses containing six carbon sugars; these hemicelluloses have β-1,4-linked D-glucopyranosyl backbones substituted with D-xylopyranose residues at the O-6 position. Xylose residues in xyloglucans can be further substituted with galactose or arabinose. These hemicelluloses can be found in the primary cell wall of plants; because of their chemical composition, xyloglucans can form strong associations with the cellulose fibrils (de Vries and Visser 2001; Girio et al 2010; Menon et al 2010; Vincken et al 1997). Significant efforts have been made to obtain genetically engineered strains that can simultaneously metabolize hexose and pentose sugars into ethanol (Girio et al 2010; Matsushika et al 2009; Olsson et al 2006; Song and Wei 2010). The utilization of sugars from both hemicelluloses and celluloses could improve the economic feasibility of the production of cellulosic ethanol (Zhang et al 2011).

Pretreatment of lignocellulosic biomass is necessary to increase its susceptibility to enzymatic action. The most common pretreatment methods employ mineral acids and high temperatures to remove the lignin component (Corredor et al 2008; Lee and Kim 2002; U.S. Department of Energy 2006; Viola et al 2007). Under these conditions, most of the sugars from hemicelluloses are degraded and can't be used for alcoholic fermentation (Bobleter 1994; Cejpek et al 2008; Delgenes 1996; Mosier et al 2002; Oliva et al 2006); moreover, substantial capital investment is required because corrosion-resistant materials need to be used. Neutralization, detoxification, and waste disposal are additional costs. Solid acids provide the catalytic properties of homogeneous acids with the advantage that they can be recovered from the reaction media by physical separation (Corma and Garcia 2006; Harmer et al 2000; Yurdakoc et al 1999). In previous studies, acid-functionalized mesoporous silicas have been employed for the conversion of starch and cellobiose to glucose (Bootsma and Shanks 2007; Dhepe et al 2005). Zeolites, Amberlyst-15, heteropolyacids, and sulfonated activated-carbon have been used for hydrolysis of cellulose into its glucose monomers (Onda et al 2008; Shimizu et al 2009). Similar types of solid acids were used in the hydrolysis of hemicellulose and the recovery of xylose and arabinose sugars (Dhepe and Sahu 2010). Dispersions of functionalized nanoparticles have similar catalylitic performance as their homogeneous counterparts (Bell 2003; Polshettiwar and Varma 2010). Because the size of these acid-functionalized particles is in the nanoscale, they could provide effective catalysis over a solid substrate such as biomass, and because they are magnetic, the nanoparticles can be recovered from the reaction media using a strong magnetic field (Gill et al 2007; Stevens et al 2005; Zhang et al 2008). The present work uses perfluoro-alkylsulfonic and alkyl-sulfonic acid-functionalized nanoparticles (PFS and PS) to catalyze the hydrolysis of hemicelluloses into oligosaccharides at two different temperatures.

3.2. Materials and Methods

3.2.1 Materials

Cobalt (II) chloride hexahydrate (99%), D-(+)-Cellobiose (98%), diethylamine (99.5%), iron (II) chloride tetrahydrate (99.99%), 3-mercaptopropyltrimethoxysilane (MPTMS) (95%), Nafion® SAC-13 (98%), methylamine (40%w/w, 98.5%), sodium dodecyl sulfate (98.5%), and tetraethylorthosilicate (TEOS) (99.999%) were purchased from Sigma-Aldrich Co. (St. Louis, Mo.). Ammonium hydroxide, toluene, and isopropanol (A.C.S. reagent) were purchased from

Fisher Scientific (Pittsburgh, Pa.). Ethanol (95%) was purchased from Decon Laboratories (King of Prussia, Pa.). Hexafluoro(3-methyl-1-2-oxathiethane)-2,2-dioxide (HFP sultone) (95%) was purchased from SynQuest Labs (Alachua, Fla.). Wheat biomass was harvested from the Kansas State University Agronomy Farm (Manhattan, Kan.) in November, 2008.

3.2.2 Preparation of silica-coated magnetic nanoparticles (SiMNPs)

SiMNPs were synthesized according to methods previously described in the literature (Gill et al 2007; Phan and Jones 2006; Rondinone et al 1999). First, the magnetic core, which is composed of cobalt spinel ferrite ($CoFe_2O_4$), was synthesized with the microemulsion method. Figure 3-1, step 1, shows the procedure for preparation of SiMNPs. In a typical experiment, 500 ml of an aqueous solution was prepared containing 4 mmol of Cobalt (II) chloride hexahydrate, 5 mmol of iron (II) chloride, and 45 mmol of sodium dodecylsulfate (SDS). The solution was stirred at room temperature with a mechanical stirrer for 30 min and heated to 60 °C. Then, a warm methylamine solution (12% w/w) was added, and the mixture was stirred for 3 h. The nanoparticles were separated magnetically and washed 3 times using distilled water and twice with ethanol. The nanoparticles were dispersed in 100 ml of ethanol and stored at room temperature before coating with silica. The ethanol dispersion of nanoparticles was sonicated and stirred for 30 min, then 15 ml of the solution was added to a solution containing 500 ml isopropanol, 50 ml water, and 50 ml concentrated ammonium hydroxide. This solution was also sonicated under mechanical stirring for 1 h. A solution of 1 ml of tetraethylorthosilicate (TEOS) in 40 ml of isopropanol was added dropwise to the former solution. The mixture was sonicated under mechanical stirring for another 2 h. The nanoparticles were magnetically separated and washed with distilled water. Then the nanoparticles were dried in a vacuum oven at 45 °C for 48 h.

3.2.3 Acid functionalization of the SiMNPs

Acid functionalization of SiMNPs was carried out following procedures reported in the literature (Gill et al 2007). Figure 3-1, steps 2 and 3 show the procedure for acid functionalization of SiMNPs. For the preparation of supported perfluoropropylsufonic (PFS) acid-functionalized nanoparticles, dried SiMNPs (250 mg) were placed in a pressure bottle. Approximately 1 ml of HFP sultone and 20 ml of anhydrous toluene were poured into the bottle in a nitrogen glove bag. The pressure bottle was sealed and sonicated for 30 min. The mixture

was stirred at 80 °C for 4 h in a water bath. The product (PFS nanoparticles) was magnetically separated and washed three times with 20 ml of anhydrous toluene. The nanoparticles were dried at 45 °C overnight in a vacuum oven. Figure 3-1, step 3, shows the procedure for preparation of supported propylsufonic acid-functionalized (PS) nanoparticles. A solution containing 1 ml of MPTMS, 10 ml of ethanol, and 10 ml of distilled water was prepared, and then 1 g of SiMNPs was added. The mixture was sonicated for 60 min and refluxed overnight. The product was recovered magnetically and washed four times with 10 ml of water. To oxidize the mercapto groups in the nanoparticles, a blend of 10 ml of 30% hydrogen peroxide, 10 ml of water, and 10 ml of methanol was added to the nanoparticles. This mixture was kept under static conditions and at room temperature for three days. The product from the oxidation step was recovered magnetically and washed three times with 20 ml water. The particles were reacidified with 20 ml of 2 M H_2SO_4, washed three times with distilled water, and dried at 45 °C for 48 h.

Figure 3-1 Synthesis of SiMNPs and acid functionalization with alkyl and perfluoropropyl sulfonic acid groups

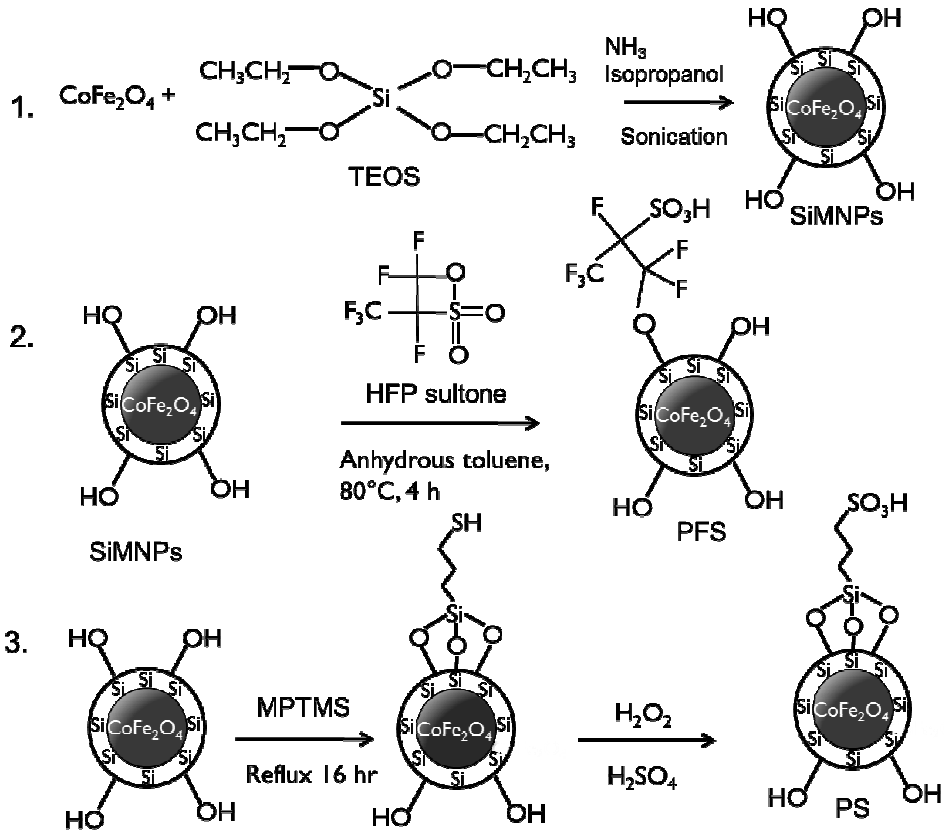

3.2.4 Characterization of acid-functionalized nanoparticles

Transmission electron microscope (TEM) images were used to estimate the size and size distribution of the nanoparticles. A model CM100 TEM (FEI Company, Hillsboro, Ore.) equipped with an AMT digital image capturing system was operated at 100 kV. The images were taken under both dispersed and dried conditions. For dispersed solutions, the nanoparticles were absorbed for approximately 30 s at room temperature onto Formvar/carbon-coated, 200-mesh copper grids (Electron Microscopy Sciences, Fort Washington, Pa.), then viewed by TEM. Particle analysis of aggregates was done on an LTS-150 particle size analyzer and LECOTRAC analysis software. The mean size of the nanoparticles was estimated using the software ImageJ, available from the National Institutes of Health.

Fourier transform infrared (FTIR) spectra were used to investigate the chemical bonds presented on the nanoparticles. Spectroscopy-grade KBr and samples were dried at 45 °C for 48 h, and then prepared by mixing 2 mg of sample with 200 mg of KBr. The measurement was carried out in the wavelength numbers 400–4000 cm^{-1}, with detectors at 4 cm^{-1} resolution and 32 scans per sample using a Thermo Nicolet NEXUSTM 870 infrared spectrometer with a ZnSe window. An OMNIC software program (Thermo Electron Corporation, Madison, Wis.) was used to determine the peak positions and intensities.

X-ray photoelectron spectroscopy (XPS) was used to analyze the surface functional groups covalently attached to SiMNP. The data were obtained with a PerkinElmer PHI 5400 (Waltham, Mass.) electron spectrometer using acrochromatic AlKα radiation (1486.6 eV). Spectra were obtained under vacuum pressure around 2.0×10^{-8} Torr. XPS binding energies were measured with a precision of 0.1 eV. The analyzer pass energy was 17.9 eV, with a contact time of 50 ms., and the nanoparticles were sputtered for 2 min before analysis.

Thermogravimetric analysis (TGA) was used to count the organic load over the nanoparticles after immobilization. The TGA was carried out in a PerkinElmer Pyris1 TGA (Waltham, Mass.). About 5 mg of each sample was placed in the pan and heated from 30 °C to 700 °C at a rate of 20 °C/min under a nitrogen atmosphere.

3.2.5 Biomass pretreatment

The capacity of PFS and PS nanoparticles to hydrolyze hemicellulose was evaluated at two temperatures, 80 °C and 160 °C. For the experiments at 80 °C, 2.5% (w/w) wheat straw and

1.5% (w/w) catalyst were used. The total weight of the slurry was 26 g. The hydrolysis was carried out in pressure bottles for 24 h. All bottles were sealed to avoid mass loss. For the experiments at 160 °C, 2.5 % (w/w) wheat straw samples were pretreated with 0.25% (w/w) PS or PFS nanoparticles for 2 h. In this case, the hydrolysis was carried out in a 600 ml pressure reactor (Model 4544; Parr Instrument Co., Moline, Ill.). An experimental control was also run at both temperatures with the biomass sample under the same conditions but without catalyst. After pretreatment, the solid fraction was separated from the slurry using a 200-mesh sieve. The nanoparticles were magnetically separated from the liquid fraction, which was analyzed for sugar content.

3.2.6 Analytical methods

Structural carbohydrates and lignin content of wheat straw were analyzed following the NREL LAP procedure TP-510-42618 (Sluiter et al 2008b) (Table 3-1 Whole wheat straw composition). After the biomass pretreatment with PS, PFS, and without catalyst (control), the total amount of carbohydrates in the liquid fraction was determined following the NREL LAP procedure TP-510-42623 (Sluiter et al 2008a). This method hydrolyzes the oligosaccharides in the liquid fraction into their monomer constituents. Sulfuric acid (72% w/w) was used to bring the acid concentration of the liquid fraction to 4% (w/w). The samples were placed in pressure bottles and sealed. The bottles were autoclaved at 121 °C for 1 h, and then the samples were neutralized with $CaCO_3$, filtered, and analyzed by HPLC. The sugars were quantified using RCM-Ca+2 and RPM-Pb+2 monosaccharide columns (300 x 7.8mm; Phenomenex, Torrance, CA) and a refractive index detector. Samples were run at 80 °C and 0.6 ml/min with double-distilled water. Recovered hemicellulose was counted as the amount of D-(+)-xylose, and D-(+)-arabinose derived from the initial hemicellulose fraction in the biomass samples before pretreatment. Hemicellulose recovery (%) was calculated as the ratio of total hemicellulose sugars detected in the liquid fraction after pretreatment to the initial amount of hemicelluloses in the biomass before pretreatment.

Table 3-1 Whole wheat straw composition

Biomass constituents	Wheat straw
95% ethanol extractives	16.4±2.5
Acid-insoluble ash (%)	3.6±1.0
Acid-soluble lignin (%)	0.8±0.1
Acid-insoluble lignin (%)	15.3±0.6
Total lignin (%)	16.1±0.6
Xylan (%)	17.2±2.1
Glucan (%)	33.5±3.1
Arabinan (%)	1.7±0.4

3.3 Results and Discussion

3.3.1 Characterization of acid-functionalized nanoparticles

The TEM images were taken under both dispersed and dried conditions. Images A and B in Figure 3-2 were taken over $CoFe_2O_4$ particles dispersed in ethanol. Ethanol-dispersed nanoparticles were sonicated for 60 min before TEM analysis. Dispersed $CoFe_2O_4$ nanoparticles can be seen in Figure 3-2A. $CoFe_2O_4$ aggregates were also observed in ethanol solution (Figure 3-2B). Monodispersed nanoparticles had an average diameter of 7.6 nm with a standard deviation of 2.7 nm based on a total of 120 particles. The size of the aggregates measured the particle analyzer was equal to 2.3 µm with a standard deviation of 0.3 µm.

The silica-coating process is sensitive to the TEOS addition rate. When the TEOS was added at high rates, the mean size and standard deviation of the silica-coated nanoparticles were 653 nm and 56 nm, respectively, based on total of 226 nanoparticles (Figure 3-2C). A TEM image of SiMNPs obtained after dropwise addition of the TEOS is shown in Figure 3-2D. The mean size of SiMNPs was 3.5 nm with a standard deviation of 1.6 nm based on 629 nanoparticles. The mean size of SiMNPs aggregates was 2.2 µm with a standard deviation of 0.3 µm. Acid functionalization changed the dispersability of the nanoparticles because larger aggregates were found after this step. The material functionalized with PFS acid groups showed a bimodal distribution; the smaller distribution could be attributed to silica-coated iron oxide that escaped the functionalization. The smaller material had a mean of 2.3 µm (±0.1 µm), which is

the same as that obtained for silica-coated iron oxide aggregates. The functionalization with PFS had promoted the formation of larger aggregates with a mean size of 74.0 µm (±4.1 µm). PS nanoparticles had a bimodal distribution. The distribution with larger aggregates had a mean diameter of 13.1 µm (±2.5), and the distribution with smaller aggregates had a mean diameter of 0.8 µm (±0.1 µm).

Figure 3-2 TEM images of A) cobalt iron oxide ($CoFe_2O_4$) nanoparticles, B) $CoFe_2O_4$ aggregates of nanoparticles, C) SiMNPs synthesized at high addition rates of TEOS, and D) SiMNPs synthesized at low addition rates of TEOS

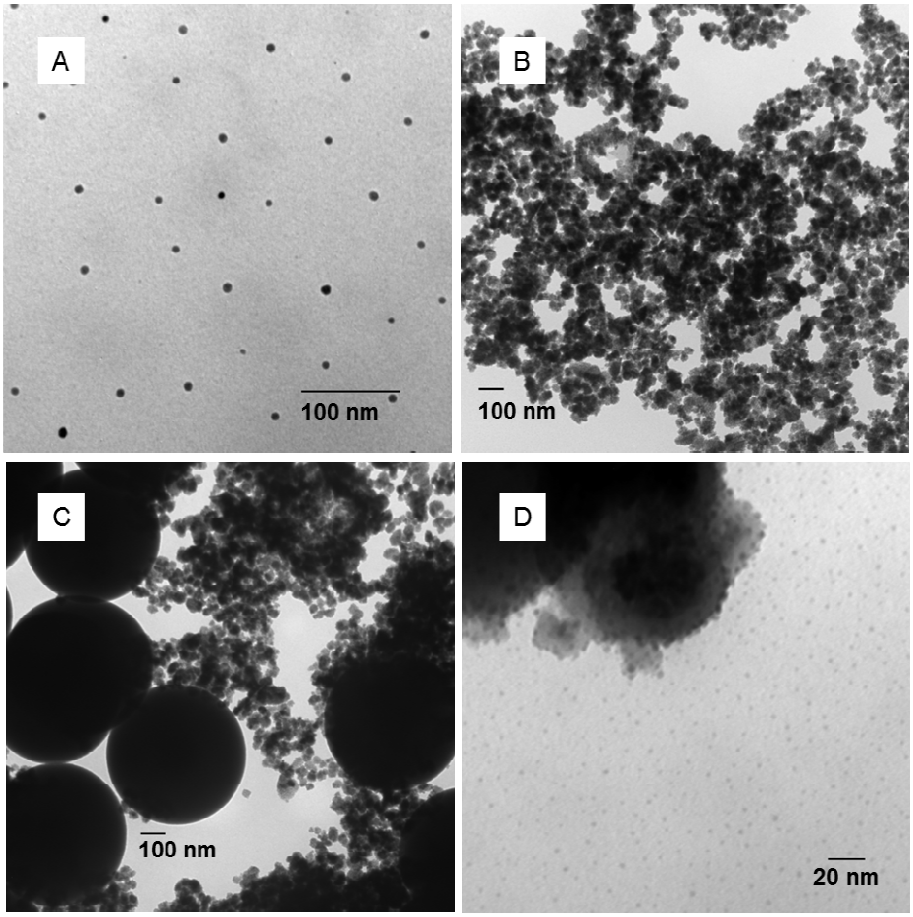

FTIR spectra for acid-functionalized nanoparticles are shown in Figure 3-3. The broad band in the wavelength 500-600 cm^{-1} appears in all the spectra. This band has been associated to Fe-O bonds (Naseri et al 2010; Silva et al 2004). The bands at 820 and 960 cm^{-1} in SiMNPs, PS, and PFS spectra have been attributed to the stretching vibrations of Si-O-Si and Si-O-H groups

(Zhao et al 2000). Similarly, a broad band at 1120 cm^{-1} from the Si-O bond appears in all these spectra (Colilla et al 2010). The peak at 1370 cm^{-1} has been assigned to the O=S=O stretching vibrations (Alvaro et al 2005; Blanco-Brieva et al 2008; Buzzoni et al 1995; Suganuma et al 2008). The peaks at 1425 cm^{-1} in the spectra of PS and PFS nanoparticles have been attributed to undissociated SO_3H groups (Alvaro et al 2005; Buzzoni et al 1995). The peaks at 1080, 1150, and 1190 cm^{-1} in the spectrum of PFS nanoparticles have been assigned to the C-F bond (Biloiu et al 2004; Kim et al 2003; Scaranto et al 2008). The results from FTIR analysis showed that all of the nanoparticles had the functional groups we expected.

Figure 3-3 FTIR spectra of $CoFe_2O_4$, SiMNPs, PS-SiMNPs, and PFS-SiMNPs

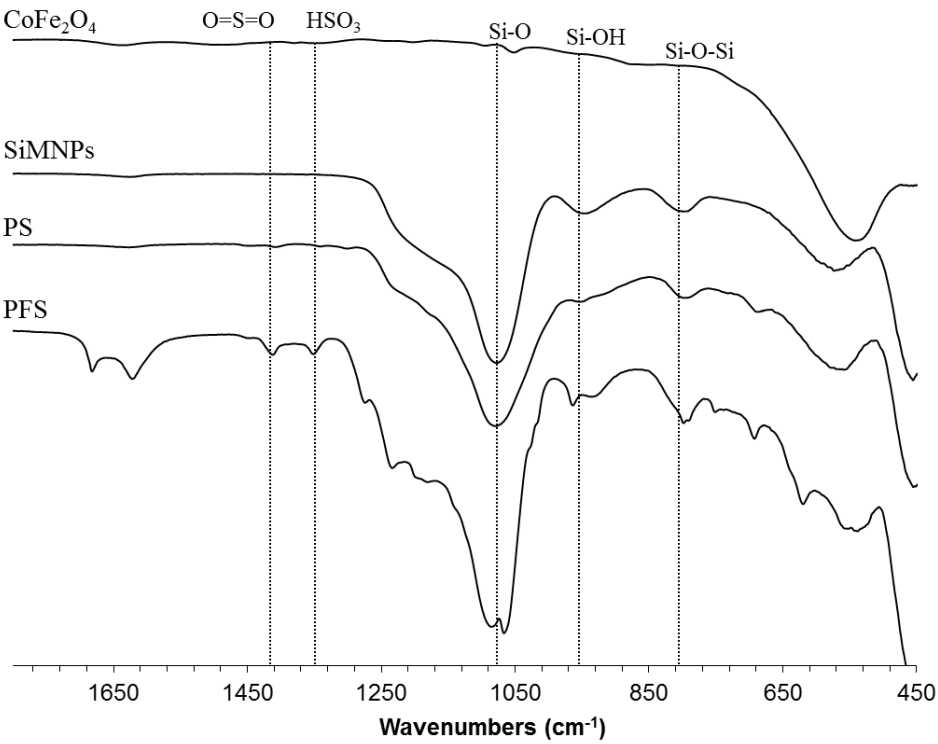

XPS profiles for PFS and PS functionalized nanoparticles were used to analyze their atomic concentration (Figure 3-4). A peak at 104-108 eV was observed for both acid-functionalized nanoparticles. This peak is associated with silicon bonds from the silica layer that covers the $CoFe_2O_4$ nanoparticles (Blanco-Brieva et al 2008; Zavadil et al 1989). The peaks associated with carbon, silicon, and sulfur were observed in the PS spectrum. The surface composition of both PFS and PS nanoparticles is shown in Table 3-2. For PS, the C/Si theoretical

value was calculated from the molecular formula of the propylsulfonic acid attached to the silica surface as 3. The C/Si ratio of 3.4 from the XPS experiment agrees with the theoretical value. The C/S ratio of 26.6 was much larger than the theoretical value, which is also 3. The large amount of carbon with respect to sulfur suggests that the loss of the sulfonic acid groups might have occurred during the synthesis procedure. The peaks that correspond to F, O, C, S, and Si were found in the XPS profiles for PFS nanoparticles. As in the PS case, the C/S ratio of 10.4 was greater than the theoretical value of 3.0. The large amount of carbon also suggests the loss of the sulfonic acid group during the synthesis process; however, the ratio of fluorine to carbon (0.8) was lower than expected (3.0), which indicates that the acid sulfonic group leached out along with other fluorine atoms of the HFP sultone sulfone moities.

Figure 3-4 XPS profiles of PFS and PS nanoparticles

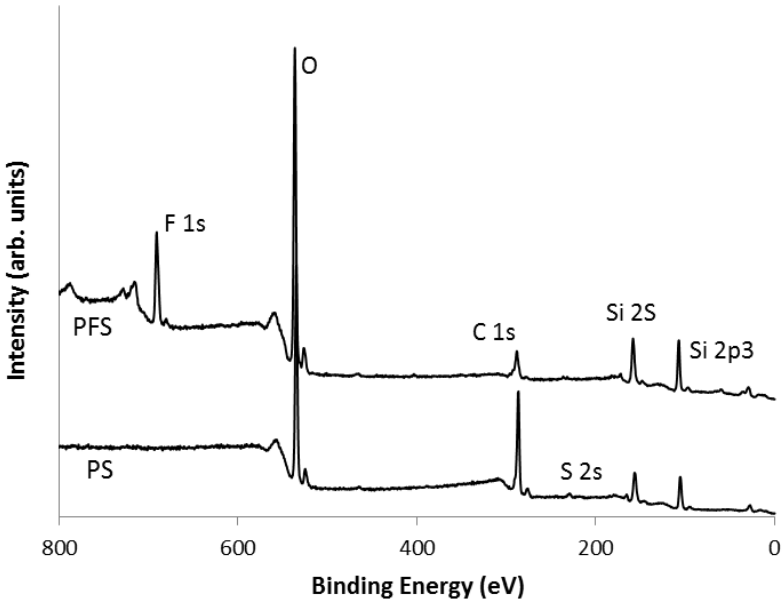

Table 3-2 Atomic concentration and organic load of the acid-functionalized nanoparticles

	Atomic concentration[a] (%)					Organic load[b] (%)	mmol H+/g[c]
	F	*O*	*C*	*S*	*Si*		
PFS	11.52	47.94	14.2	1.37	24.36	30.4	0.13
PS	-	31.61	51.28	1.93	15.19	12.6	0.07

a From XPS analysis.

b From TGA analysis.

c Calculated.

The thermal decomposition scans of the nanoparticles before and after acid functionalization were used to evaluate the thermal stability of the nanoparticles and their total organic loading (Figure 3-5). The DTA curves show that the drying step occurred before the samples reached 150 °C. SiMNPs had absorbed more water than the acid-functionalized nanoparticles. The moisture content of SiMNPs, PS, and PFS nanoparticles was 3.9, 2.6, and 2.6% (db), respectively. The incorporation of alkyl-sulfonic and perfluoropropylsulfonic acids groups increased the hydrophobicity of the nanoparticles. Similar results were found during functionalization of silica with perfluoropropylsulfonic acid (Blanco-Brieva et al 2008). An increase in the hydrophobic properties of the nanoparticles can affect their dispersability in the biomass slurry and could promote aggregation of nanoparticles, thus reducing the available area for the reaction. The TGA profile of SiMNPs showed a total weight loss of 4.2% during heating from 150 to 800 °C. The weight loss between 150 and 400 °C was 1.7% and it has been attributed to bound water. The weight loss at temperatures higher than 400°C was measured as 2.5% and it has been explained as the weight lost due to a ferrite crystallization process (Senapati et al 2011; Silva et al 2004). PFS and PS nanoparticles showed similar thermal stabilities; when heated to 450 °C, PFS nanoparticles lost 22% of their weight, or about 60% of their original organic content; PS lost 10% of their weight, or about 55% of their original organic content. The first derivative profile for PFS nanoparticles shows four peaks at 225, 292, 417, and 492 °C, which indicates that the perfluoropropylsulfonic acid group splits into smaller moieties. The sulfonic acid groups and the -CF2-chains decompose at different temperatures (Blanco-Brieva et al 2008). The first derivative profile for PS nanoparticles shows a main peak at 437 °C that corresponds to the alkyl-sulfonic acid. The left shoulder on this peak could be attributed to mercaptopropyl groups that were not completely oxidized to the sulfonic acid (Hamoudi et al 2004). The total organic content was counted as the total mass lost between 150 °C and 600 °C; these values can be seen in Table 2 along with the number of acid sites on the nanoparticles. The hydronium ion concentration per mass of catalyst was calculated from the values of total organic content on the nanoparticles and the surface sulfur concentration.

Figure 3-5 TG/DTA profiles of SiMNP, PFS, and PS functionalized nanoparticles

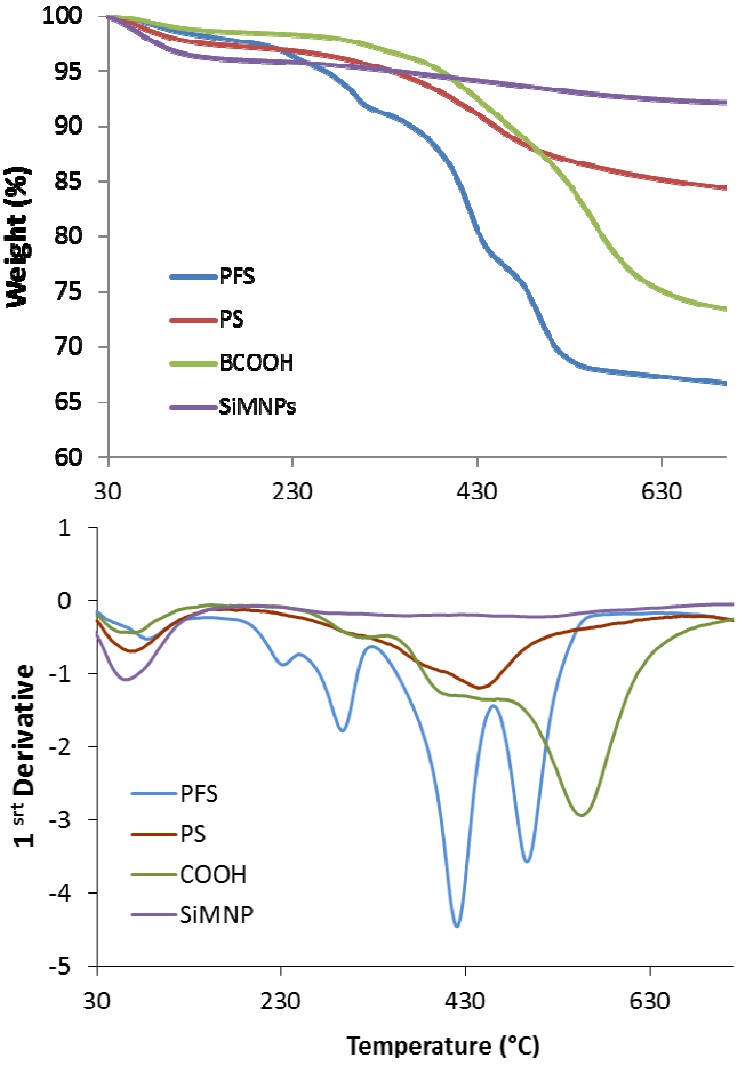

3.3.2 Biomass pretreatment

Table 3-1 shows the biomass composition on a dry mass basis, and the total hemicellulose sugars recovered at 80 °C and 160 °C from wheat straw are shown in Figure 3-6. The left columns correspond to results of the experiments carried out at 80 °C for 24 h with a catalyst load of 1.5% and biomass load of 2.5%. Results of the experiments carried out at 160 °C for 2 h with a catalyst load of 0.25% and biomass load of 2.5% are shown in the right columns. The error bars represent the standard errors of two replicate experiments. At temperatures as low

as 80 °C, solubilization of hemicellulose rather than cellulose hydrolysis is expected (McMillan 1994). The amount of sugars solubilized (24.0 ± 1.1%) at 80 °C in the presence of PFS nanoparticles was greater than the sugars released from the control (7.7 ± 0.8%); but the amount of hemicelluloses recovered with PS (9.1 ± 1.7%) was not significantly different from the control. Based on the values obtained for organic content and sulfur atomic concentration, we calculated that 2 mmol H^+/L were used for the experiment that used PFS; this is equivalent to using 0.02% (w/w) sulfuric acid solutions. In a similar way, we calculated that the load of PS nanoparticles could provide 1.02 mmol H^+/L, which would be equivalent to using 0.01% (w/w) sulfuric acid solutions. Because we used low temperature and acidity levels, 20% hemicellulose recovery can be considered moderate. Complete (100%) hemicellulose solubilization requires temperatures higher than 160 °C using 1% sulfuric acid (McMillan 1994). Previous work reported that complete xylan solubilization was reached at 130 °C using 3% (w/w) sulfuric acid solutions for 4 h (Carvalheiro et al 2004). Higher temperatures have been used (180-220 °C) for hemicellulose hydrolysis with acid concentrations between 0 to 0.1% sulfuric acid (w/w) (Allen et al 2001; Jacobsen and Wyman 2002; Wyman et al 2005).

Figure 3-6 Total wheat straw hemicelluloses recovered after pretreatment with PFS and PS acid-functionalized nanoparticles

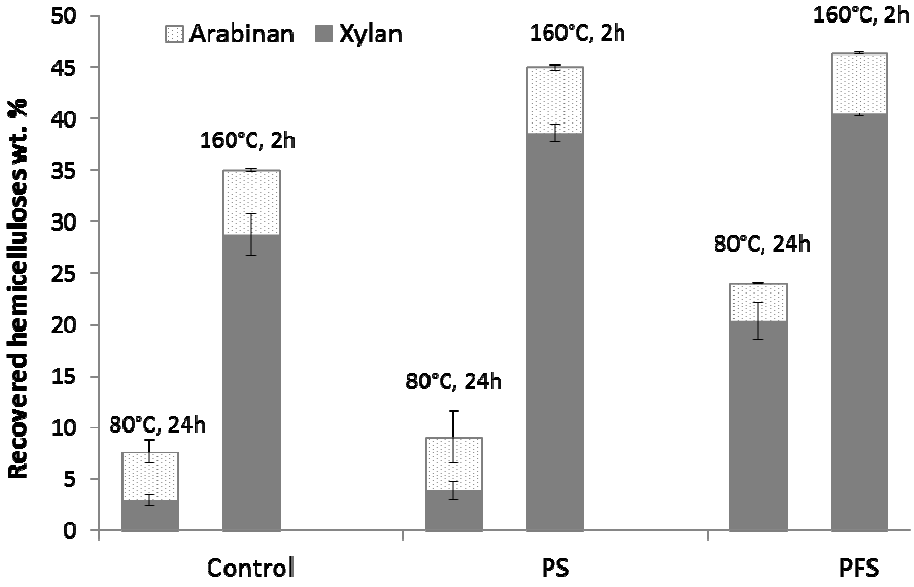

Very few monosaccharides were obtained after pretreatment of biomass with PFS or PS nanoparticles. PFS and PS solubilized the xylan fraction into its monomeric form at very low levels: 3.5 ± 0.1%, 1.0 ± 0.2% at 80 °C. Xylose monomer units were not detected in the solution for the control experiment. In the experiments carried out at 160 °C, only 0.3 and 1.2% of the original xylan was found in the solution as xylose for PFS and PS nanoparticles, respectively. From the initial arabinan, 49.5 ± 2.1% and 57.9 ± 11.2% was found as arabinose monomer in the pretreatment liquor of PS and PFS nanoparticles. In the control experiment, 36.0 ± 1.6 % of arabinan was hydrolyzed to the monomeric form. These results agree with previous findings in which acid-functionalized amorphous carbon was used to hydrolyze cellulose, the yield of monomers was only 4%, and most of the sugars obtained were in oligomeric form (Suganuma et al 2008). About 30% monomers yield was obtained from loblolly pine hemicelluloses using 1% sulfuric acid at 150 °C and 60% at 200 °C (Marzialetti et al 2008). At 160 °C, the low percentage of xylose found in the solution could be explained by degradation of the xylose units to other products such as furfural and formic acid (Antal et al 1991; Bonn and Bobleter 1983; Corma et al 2007; Dunlop 1948; Girisuta et al 2006); in this experiment, 16.0 ± 0.2, 20.0 ± 1.3, and 15.7 ± 1.2% of the original xylan was found in solution as furfural for PS, PFS, and control, respectively (Figure 3-7). The pretreatment was carried out at 160 °C for 2 h with a catalyst load of 0.25% and biomass load of 2.5%. The error bars represent the standard errors of two replicate experiments. Formic acid was also found in the pretreatment liquor, but it may have been a degradation product of either cellulose or xyloglucans. The results of this paper agree with the hemicellulose hydrolysis models proposed in the literature (Carrasco and Roy 1992; Grohmann et al 1986; Jacobsen and Wyman 2002; Kim et al 1987; Torget and Hsu 1994). These models suggest that either hemicelluloses or xylan are made of two different fractions that are hydrolyzed at different rates, one slow and one fast. In the present work, the fast-hydrolyzing fraction of hemicellulose is degraded to decomposition products, and that is why very few monomers were found in the pretreatment liquor. The slow-hydrolyzing fraction is found in solution as oligomers or remains in the non-hydrolyzed solid fraction.

Figure 3-7 Wheat straw hemicelluloses solubilized after pretreatment with PFS and PS acid-functionalized nanoparticles

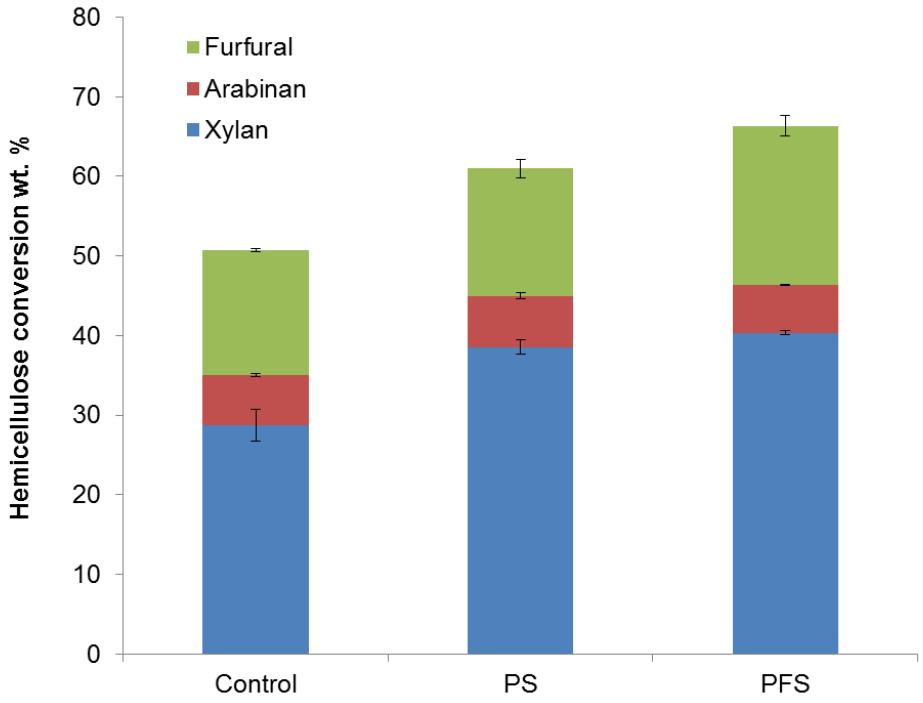

In the experiments performed at high temperature, a 0.25% (w/w) catalyst load was used; the PFS and PS nanoparticle dispersions are equivalent to using 0.003 and 0.002% (w/w) sulfuric acid solutions, respectively. The total hemicellulose (oligosaccharides and monosaccharides) recovered from wheat straw at 160 °C reached 46.3 ± 0.4% and 45.0 ± 1.2% using PFS and PS, respectively. The control experiment recovered 35.0 ± 1.8% of the original hemicellulose in the wheat straw sample. Most of the sugars found in solution came from the xylan fraction 38.6 ± 0.9% and 40.4 ± 0.2% using PS and PFS, respectively. Hemicellulose solubilization could have been affected by the buffering effect of the biomass, which has been said could reduce 1% (w/w) acid concentration in half (McMillan 1994). Low acid levels used are frequently used along with high temperatures; hemicellulose conversion from corn stover reached 97% (w/w) with 0.1% (w/v) sulfuric acid at 180 °C, but still more than 50% was oligomers of hemicellulose (Liu and Wyman 2004). At 175 °C, 96% (w/w) conversion of hemicellulose was obtained with 0.8% (w/v) sulfuric acid from yellow poplar sawdust (Allen et al 2001). PFS and PS nanoparticles

converted 66.3 ±1.7% and 61.0 ±1.2% of the hemicelluloses at acid levels 50 and 400 fold lower than those acid sulfuric solutions at 160 °C.

PFS and PS nanoparticles gave similar amounts of recovered hemicellulose; and both catalysts gave more sugars than the control. Because perfluorosulfonic acids are known as superacids and can be more acidic than sulfuric acid, we expected a better performance of PFS nanoparticles (Alvaro et al 2005; Corma and Garcia 2006; Grondin et al 1976). The acid strength of these acids has been explained by the electron-withdrawing properties of the Fluorine atoms (Corma et al 2004), but the leveling effect of water could have an effect on the catalytic activity of PFS nanoparticles (Corma et al 2004). Nanoparticles functionalized with alkyl-sulfonic acid show a significant improvement on hemicelluloses solubilization when using 160 °C instead of 80 °C, although the acid loading for this catalyst was relatively low. Similar acid capacity was reported previously for propyl-sulfonic acid-functionalized materials (Gill et al 2007). Low catalytic activity also could have been a consequence of the low water affinity observed for this catalyst in TGA experiments. These results agree with the findings of Van Rhijn et al. (Van Rhijn et al 1998), who synthesized mesoporuos silicas functionalized with propylsulfonic acid and obtained moisture contents of less than 1%. The aggregation of both PFS and PS nanoparticles also could have an effect on their capacity to hydrolyze hemicelluloses due to a considerable reduction of their surface area; however, the attachment of PFS and PS acid functions could have stabilized the acid and allowed moderate levels of hemicellulose hydrolysis compared with sulfuric acid solutions of similar acid strength.

3.4 Conclusions

Acid-functionalized magnetic nanoparticles were synthesized as catalysts for pretreatment and hydrolysis of lignocellulosic feedstock. TEM images confirmed that the synthesis of cobalt spinel ferrite yielded particles with diameters less than 10 nm. Coating the cobalt spinel ferrite particles did not significantly change the size distribution of the nanoparticles, although some particles agglomerated upon coating. FTIR spectra confirmed the covalent bonding between the magnetic core and the silica layer and the presence of sulfonic acid groups following functionalization. Analysis of sugars in the liquid fraction after pretreatment revealed a significant amount of oligosaccharides compared with the

hydrothermolysis when using PFS or PS nanoparticles at 160 °C. The acid-functionalized nanoparticles broke down the non-soluble polysaccharides into oligomeric forms.

Chapter 4 - Synthesis of propyl-sulfonic acid-functionalized nanoparticles for the catalysis of cellobiose[3]

Abstract

Functionalization of silica surfaces using organo-silanes is highly sensitive to reaction conditions. Silica-coated nanoparticles were functionalized with propyl-sulfonic acid groups (PS) under different synthesis conditions including, solvent (Ethanol, methanol, acetonitrile, and toluene), water in the reaction media (0 to 50%), 3-mercaptopropyl-trimethoxysilane concentration (MPTMS) (0.5 to 10%), and reaction time (6 to 16 h). The nanoparticles with a higher level of functionalization were obtained when there was a high water content in the reaction media (50%). A moderate level of functionalization (6–8% S) also can be obtained at low silane concentration (0.5%) with a long reaction time (15-16 h). The results showed that PS acid-functionalized nanoparticles are effective catalysts for the hydrolysis of cellobiose into glucose. The conversion of cellobiose increased as the functionalization level increased up to 6% S. The highest cellobiose conversion was 96.0%, which was significantly higher than 32.8% obtained with the control without catalyst 32.8%.

4.1 Introduction

One of the challenges in the production of renewable fuels and chemicals from lignocellulosic biomass is breaking down the complex structure of biomass into monomeric sugars. Biomass comprises a complex mixture of cellulose, hemicellulose, and lignin (Chang et al 1981). Cellulose is a polymer of glucose units linked by β-1,4-glycosidic linkages. Cellobiose, a disaccharide of glucose, is the true repeating unit of the cellulose polymer (Fleming et al 2001). The β-1,4 bonds between glucose units allow the formation of hydrogen bonds between adjacent chains and make the structure of the polymer highly stable and resistant to hydrolysis (Bobleter 1994; Gardner and Blackwell 1974; Okamura 1991). Currently, the most accepted process for production of cellulosic ethanol uses an acid hydrolysis to pretreat lignocellulosic biomass and an enzymatic hydrolysis to break the cellulose chains into monomer sugars (McMillan 1994).

[3] Paper has been submitted to Renewable Energy.

Cellulolytic enzymes are a big portion of the operational cost to produce cellulosic ethanol because they are expensive catalysts with limited reusability (Klein Marcuschamer et al 2012; Wooley et al 1999). These enzymes work optimally under a narrow set of conditions, plus reaction rates are slow (de Vries and Visser 2001; Xiros et al 2011). The efficiency of enzymatic hydrolysis of cellulose affects the economic feasibility of the process. Solid catalysts could act similarly to cellulolytic enzymes, with the additional benefits that these catalysts can be recovered and reused and could work well under a broad set of conditions (Chafin et al 2008; Harmer et al 1998; Harmer et al 2007; Yadav 2005). Although a number of articles have been published on the performance of heterogeneous catalysts on the hydrolysis of glycosidic bonds (Bootsma and Shanks 2007; Dhepe and Sahu 2010; Shimizu et al 2009; Vigier and Jerome 2010), research is in the early stage and more investigation is needed.

Organosilanes are broadly used for modification of surfaces to produce materials with special properties. Condensation of an organosilane on a surface gives the surface new attributes depending on its functional groups. Extensive literature is available on the modification of siliceous materials. This technology has been utilized in numerous coating applications on glass surfaces (Glass et al 2011; Hunter et al 1947; Norton 1944; Ulman 1996). Alkyl-silanes are attractive silica coupling agents because of the high stability of the Si-C bond. Silanating agents such as 3-mercaptopropyl-trimethoxysilane (MPTMS) have three leaving groups, and this feature gives the molecule the chance to anchor through more than one silanol group on siliceous surfaces (Corma and Garcia 2006).

One specific application of silica surface modification is to produce catalytic materials. The attachment of a catalytic group on a solid surface allows its recovery and reutilization. The catalytic groups are usually placed on porous materials because these materials can hold a larger number of the functional moieties. Propyl-sulfonic acid-functionalized silicas have been used on acid catalysis in several studies (Boveri et al 2003; Lai et al 2011b). Nevertheless, using heterogeneous catalysis brings about mass transfer issues that could decrease the efficiency of the catalysis. Nanocatalysts are a hybrid of heterogeneous and homogeneous catalysts. Functionalized nanoparticles can be used for catalysis of liquid and gas-phase reactions and can be separated and recovered from the reaction media (Fan and Gao 2006; Gao 2007; Phan and Jones 2006). At the same time, nanocatalysts have properties similar to those of homogeneous catalysts because they are very small and can be accessed easily by the reactants, circumventing

the diffusion problems that solid catalysts could present. Similar to silica surfaces, the surface of nanoparticles can be modified to confer them with desired chemical features (Raja and Thomas 2003).

Numerous studies have been reported on functionalization of nanoparticles for various applications (Fiurasek and Reven 2007; Hayashi 2009; Phan and Jones 2006; Shylesh et al 2009). In previous work, for instance, magnetic nanoparticles have been successfully coated with silica (Gill et al 2007; Peña et al 2012). These nanoparticles can be separated out of aqueous solutions using a magnetic field, and their silica surface can be further modified. The functionalization of silica-coated nanoparticles can be done using procedures similar to those reported on acid functionalization of silicas (Gill et al 2007; Siril et al 2007). Silica-coated nanoparticles could be treated in the same manner as siliceous materials because these nanoparticles have silanol groups sticking out from their surfaces. Although extensive work has been published in the area of coating with organosilanes, the production of a good film is a complex and delicate process. In aqueous solutions, the functionalization of silica with MPTMS occurs through a two-step reaction (Dubois and Zegarski 1993; Lee 1968; Plueddemann 1982; Tripp and Hair 1995). In the first step, the silane is hydrolyzed into hydrolyzate or alkyl-silanol, releasing three molecules of methanol (Figure 4-1, step 1). In the second step, the organosilanol condenses on the surface through the formation of silicon-oxygen bonds with the hydroxyl groups of the surface (Figure 4-1, step 2). Neighboring silanol groups (Si-OH) can crosslink and release water; this stabilizes the coating and prevent their detachment from the surface (Lee 1968). Then, the mercapto-propyl groups are oxidized to sulfonic acid groups using a hydrogen peroxide solution (Figure 4-1, step 3). Silanol solutions are unstable in the presence of water. Before they are linked to the surface, silanol molecules can condense with each other and then the solution becomes white (Mealey and Thomas 2005) (Figure 4-1, step 4). Stability of silane solutions can be determined by measuring the time it takes for the solution to haze to the point that a printed page cannot be read through a clear bottle (Plueddemann 1982). Another mechanism by which the modification could occur is through the condensation of siloxanols upon the surface (Tripp and Hair 1995). This physisorbed layer would be attached to the surface by weak linkages such as hydrogen bonds or van der Waals forces; it could be easily washed off by the solvent or hydrolyzed by water (Ishida and Koenig 1978; Tripp and Hair 1995).

The loading of functional groups on silica surfaces is greatly influenced by the presence of water, solvent polarity, silane concentration, and reaction time (Chirachanchai et al 1999; Plueddemann 1982). Glass et al. summarized a number of protocol parameters for organosilane deposition. Among others, the solvents used in these protocols were toluene, ethanol, isopropanol, acetone, and benzene. The reaction time varied from seconds up to 24 h, and the silane concentration varied from 0.1 up to 50% (Glass et al 2011). Such parameters are also expected to affect the number of acid sites placed on silica-coated nanoparticles. In this work, various synthesis conditions were used to functionalize silica-coated cobalt iron oxide nanoparticles with propyl-sulfonic acid groups. The objective of this research was to investigate the effect of synthesis conditions on the loading of organosilane on the nanoparticle surface and evaluate the performance of the functionalized nanoparticles for the hydrolysis of cellobiose into glucose.

Figure 4-1 Schematic of the preparation of propyl-sulfonic acid-functionalized nanoparticles

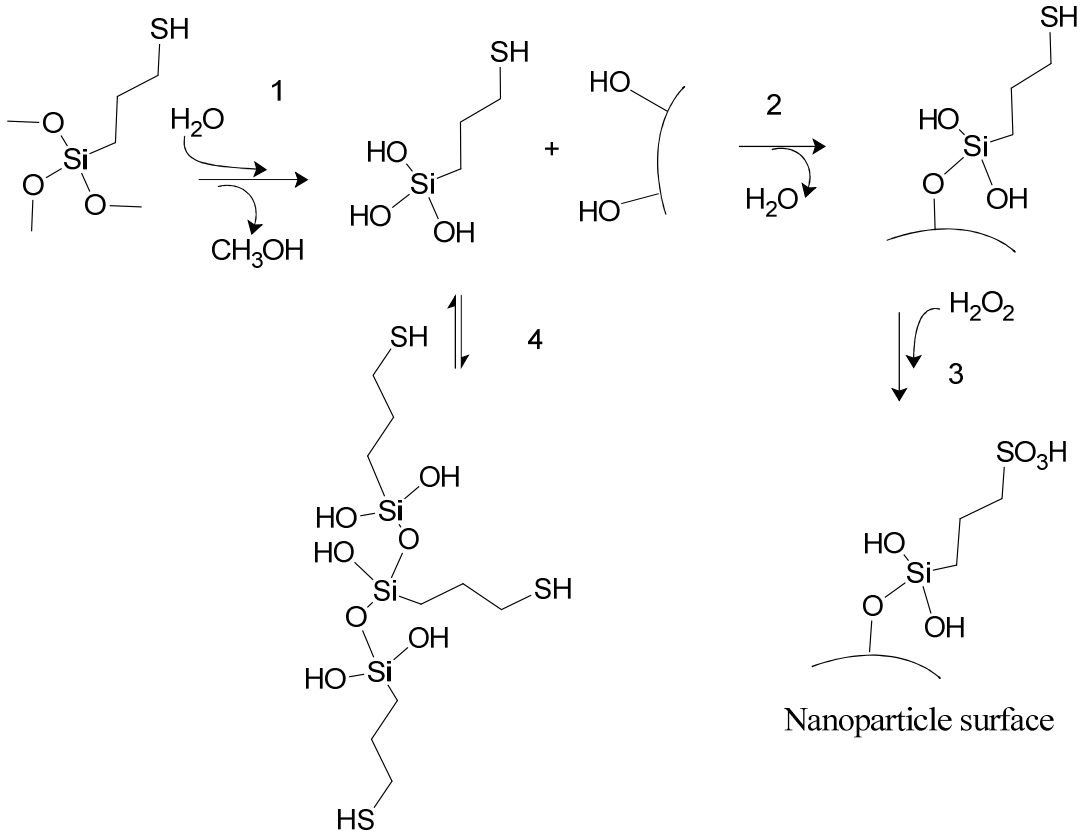

4.2 Methods and Materials

4.2.1 Materials

Cobalt (II) chloride hexahydrate (99%), D-(+)-Cellobiose (98%), iron (II) chloride tetrahydrate (99.99%), 3-mercaptopropyltrimethoxysilane (MPTMS) (95%), methylamine (40%w/w, 98.5%), sodium dodecyl sulfate (98.5%), and tetraethylorthosilicate (TEOS) (99.999%) were purchased from Sigma-Aldrich (St. Louis, Mo.). Acetonitrile, ammonium hydroxide, hydrogen peroxide, isopropanol, methanol, and toluene (A.C.S. reagent) were purchased from Fisher Scientific (Pittsburgh, Pa.). Ethanol (95%) was purchased from Decon Laboratories (King of Prussia, Pa.).

4.2.2 Synthesis of $CoFe_2O_4$

Cobalt iron oxide ($CoFe_2O_4$) was synthesized by precipitating salts of Co^{+2} and Fe^{+2} using a microemulsion method (Moumen et al 1996; Rondinone et al 1999). In a typical experiment, a solution was prepared with 4 mmol (0.9 g) of cobalt (II) chloride hexahydrate $CoCl_2 \cdot 6H_2O$, 10 mmol (1.9 g) of iron (II) tetrahydrate $FeCl_2 \cdot 4H_2O$, and 45 mmol (12.9 g) of sodium dodecyl sulfate (SDS). The salts and surfactant were dissolved in distilled water, mixed, and diluted to 1 L. One liter solution of 12 wt. % methylamine was also prepared. After stirring the first solution for 30 min at room temperature, both solutions were heated to 55–65˚C and then combined. The mixture was kept at 55–65˚C under rigorous mechanical stirring. After 3 h, the particles were magnetically separated and washed three times with water and once with ethanol, then stored in 100 mL of ethanol.

4.2.3 Silica coating of $CoFe_2O_4$

Cobalt iron oxide nanoparticles were coated with silica using the procedures reported in the literature (Gill et al 2007; Peña et al 2011; Shen et al 2004). The dispersion of $CoFe_2O_4$ in ethanol was sonicated for 1 h. Then about 15 ml of this solution were added to 550 ml of a mixture of isopropanol and water in a 9:1 ratio. This solution was sonicated and mechanically stirred for 30 min. One mL of tetraethylorthosilicate (TEOS) was diluted in 40 mL of isopropanol. After the 30-min stirring period, 50 mL of concentrated ammonium hydroxide were added, and the dilute TEOS solution was added dropwise at a rate of 0.3 ml/min. After the

addition of the TEOS solution, the mixture was sonicated for another hour. Then the silica-coated magnetic nanoparticles (SiMNPs) were magnetically separated, washed four to five times with water, and dried at 105°C in a forced-air convection oven.

4.2.4 Functionalization of silica-coated magnetic nanoparticles (SiMNPs)

Silanol groups in silica surfaces react with silane coupling agents by dehydration (Badley and Ford 1989; Brunel et al 2000; Rac et al 2006) or hydrolysis of the silane in the presence of water (Gill et al 2007). Solvent polarity, MPTMS concentration, and time affect the synthesis of mercaptopropyl-functionalized nanoparticles, and subsequently the loading of the sulfonic acid-functional group on propyl-sulfonic (PS) acid-functionalized nanoparticles (Chirachanchai et al 1999). PS nanoparticles were synthesized with the synthesis conditions shown in Table 4-1. In a typical experiment, 500 mg of dry SiMNPs were sonicated in the solvent for 1 h. After sonication, MPTMS was added, and the blend was refluxed and mechanically stirred. After the reaction, the nanoparticles were allowed to cool and then were magnetically separated from the reaction media. The mercaptopropyl-functionalized nanoparticles were washed three times with ethanol, isopropanol, or hexane according to the solvent used for the reaction. Then, the nanoparticles were placed in 60 ml solution with equal amounts of water, methanol, and hydrogen peroxide for oxidization of the mercapto groups. After 48 h in this solution, the nanoparticles were washed three times with distilled water and left overnight in 10 mL of 0.1 M sulfuric acid. The solution was then washed multiple times with distilled water until the pH remained constant. Then, the samples were dried at 105°C for 24 h.

Table 4-1 Synthesis conditions to obtain acid-functionalized nanoparticles

Parameter	Typical values
Water content (%)	0, 2, 10, 30, 50
MPTMS concentration (%)	0.5, 1, 2, 4, 5,10
Solvent	ethanol, methanol, acetonitrile, toluene
Time (h)	6,8,10,15,16

4.2.5 Characterization of PS-nanoparticles

The transmission electron microscope (TEM) images were used to estimate the size and size distribution of the nanoparticles. A TEM (model CM100, FEI Company, Hillsboro, Ore.) equipped with an AMT digital image capturing system was operated at 100 kV. The nanoparticles were placed onto Formvar/carbon-coated, 200-mesh copper grids (Electron Microscopy Sciences, Fort Washington, Pa.), then viewed by TEM. The size distribution of the nanoparticles was calculated using ImageJ software from the National Institutes of Health.

Fourier transform infrared (FTIR) spectra were used to confirm the presence of the propyl-sulfonic acid bonds in the synthesized nanoparticles. The spectra and peak positions were determined using an infrared spectrometer and its spectrum software (Spectrum 400, PerkinElmer Inc., Waltham, Mass.). The measurement was carried out in the wave number range 500–4000 cm^{-1}, with 4 cm^{-1} resolution and 32 scans per sample.

Hydronium ion concentration per unit mass of catalyst was determined with an ion-exchange titration method (Badley and Ford 1989; Melero et al 2002). To withdraw the hydronium ions from the catalyst, 0.05 g of catalyst was added to 20 ml of sodium chloride (NaCl, 2 mM). The nanoparticle suspensions were homogenized, sonicated, and left overnight at room temperature. After 24 h, the particles were separated from the solution using centrifugation. The particles were re-dispersed in another 20 ml of sodium chloride, and the previous salt solution was set aside. Again the particles were homogenized, sonicated, and left overnight. Then, the particles were separated from the solution. Finally, the salt solutions were titrated to neutrality with a 0.01 M NaOH solution. Samples were analyzed after each synthesis batch in duplicate.

Sulfur content was used as an indicator of the silane grafting level on the nanoparticles, and it was determined by an elemental analyzer (Model 2400 SeriesII, PerkinElmer Inc.). The percentage of sulfur involved in sulfonic acid groups was calculated from the ion exchange capacity values by multiplying the milimoles of hydronium ions by the atomic mass of sulfur.

4.2.6 Hydrolysis of Cellobiose

The catalytic ability of the PS nanoparticles to hydrolyze the β-1-4 glycosidic bond was evaluated using 4 mg/ml cellobiose solutions with 1% (w/w) PS nanoparticles. The dispersions were sonicated for 20 min, then placed in a 60-ml Swagelok tube reactor (Swagelok, Kansas City

Valve & Fitting Co., Kan.) made from 316-L stainless steel with a measured internal volume of 75 mL (outside diameter of 38.1 mm, length of 125 mm, and wall thickness of 2.4 mm) (Kitano et al 2009; Zeng et al 2012). The reaction was carried out at 175°C for 30 min in a sand bath (Techne, Inc., Princeton, N.J.). Two replicates were run for all experiments. The control experiment was carried out under the same conditions as the experiments using PS nanoparticles. The control experiment had no catalyst and was referred to as hydro-thermolysis. After the reaction, the solutions were analyzed by HPLC to determine the glucose yield and residue cellobiose using a RCM-Ca+2 monosaccharide column (300 x 7.8mm; Phenomenex, Torrance, Calif.) and refractive index detector. Samples were run at 80°C at 0.6 ml/min with water as mobile phase.(Sluiter et al 2008a) To calculate the glucose yield, the moles of glucose in the solution were divided by the theoretical amount of glucose that could have been obtained from cellobiose.

4.3 Results and Discussion

The acid loading in PS nanoparticles varied from 0.02–0.59 mmol H^+/g among all solvents used (Table 4-2). The range of the acid loading values from this research agrees with values previously reported for propyl-sulfonic acid-functionalized silicas (Cano Serrano et al 2003); however, the acid capacity of some of the nanoparticles was probably underestimated because the nanoparticles could not be dispersed in the NaCl solution. Nanoparticles that gained a high load of propyl groups floated on the top of the solution and were difficult to disperse in aqueous solutions, so not all of the hydronium ions could be released into the solution. This problem was evidenced by the low hydronium ion concentrations compared with the total sulfur content (p.e. for toluene the acid capacity should have been around 0.4 mmol H^+/g instead of 0.05 mmol H^+/g according to its final sulfur content of 0.77%). Because ion exchange titrations are sensitive to the final wettability of the sample, the total sulfur content on the PS nanoparticles was used as the main indicator of the level of functionalization of these nanoparticles. Besides being a more robust method, elemental analysis can detect small differences in the number of functional groups that were attached.

Table 4-2 Sulfur analysis and ion exchange titration results by solvent used during grafting

	$\%S_{total}$	mmol H^+/g	% S_{-SO3H}
Toluene	0.77	0.05	0.16
Acetonitrile	0.26	0.02	0.05
Ethanol	0.41	0.08	0.26
Methanol	3.15	0.07	0.21
Ethanol/Water	18.59	0.59	1.88

The sulfur content ($\%S_{total}$) of PS nanoparticles functionalized under different synthesis conditions varied from 0.26% to 18.59% (Table 2). Sulfur and carbon were not detected in $CoFe_2O_4$ or in silica-coated nanoparticles. Badley et al. reported %S values from 3.25% to 8.32% for propyl-sulfonic acid-functionalized silicas (Badley and Ford 1989). Other work reported 1.17 mEq S/g (3.7%) for propyl-sulfonic modified SBA-15 (Melero et al 2010) and 10.88 %S on thiol-MCM-41 (Lim et al 1998). The %S calculated from the ion exchange capacity values were lower than %S obtained from the chemical analysis, which indicates that not all the incorporated sulfur ($\%S_{total)}$ was oxidized to the sulfonic acid form ($\%S_{—SO3H}$) . In this study, up to 63% of the total sulfur was oxidized to sulfonic acid, but for most samples was less than 20%. Badley and Ford reported that only 34% of the sulfur incorporated was in the sulfonic acid form (Badley and Ford 1989). Cano-Serrano et al. reached 57% for the best scenario (Cano-Serrano et al 2003). The acid capacity of the nanoparticles could increase significantly if the mercapto-propyl groups were completely oxidized, but using stronger oxidizing conditions could detach the mercapto-propyl group (Badley and Ford 1989; Cano Serrano et al 2003). Some of the thiol groups could also have reacted with each other to form S-S bridges before the oxidation step was carried out (Boveri et al 2003; Diaz et al 2000). Moreover, some PS nanoparticles had a lot of thiol groups buried in lower molecular layers due to high loads of MPTMS and were not exposed to the oxidizing agent.

It has been calculated that 0.25% silane gives about eight molecular layers and 2% silane generates about 70 (Sterman and Bradley 1961). Low concentrations of MPTMS are preferred because the extent of the polymerization reaction is easier to control. 0.5% MPTMS provided sufficient organosilane to reach about 5–8% S on the PS nanoparticles when given enough time

to react (Figure 4-2). Condensation of multiple layers of silane was expected when concentrations up to 4 or 5% of MPTMS were used. Deposition of multiple molecular layers could prevent oxidation of thiol groups in deeper layers. On the other hand, low silane concentrations could result in poor and uneven coverage of the surface with some areas of scarce functionalization.

Figure 4-2 Effect of silane concentration on the total sulfur incorporated after functionalization of silica-coated nanoparticles. The grafting reactions were carried out in a 1:1 blend of ethanol and water for 16h

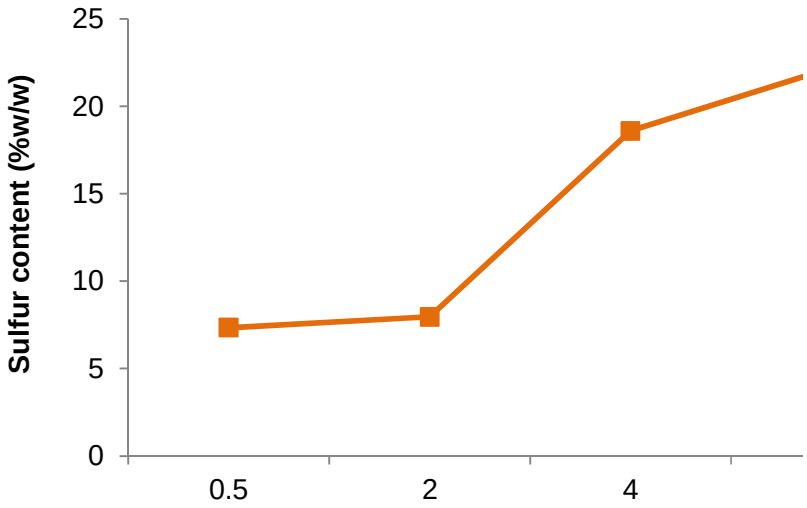

The effect of water concentration on silanol deposition was studied using various blends of ethanol and water (0–50% water in ethanol). Although several authors have recommended the use of only traces of water during the modification of surfaces with organosilanes, we found that the level of functionalization when using water concentrations under 20% was less than 1% (Fig. 3). To obtain sulfur contents of about 5–7%, more than 33% water concentration had to be used in the synthesis setup.

Figure 4-3 Effect of water concentration in the reaction media on the total sulfur incorporated after functionalization of silica-coated nanoparticles with 4% MPTMS. The grafting reactions were carried out in ethanol

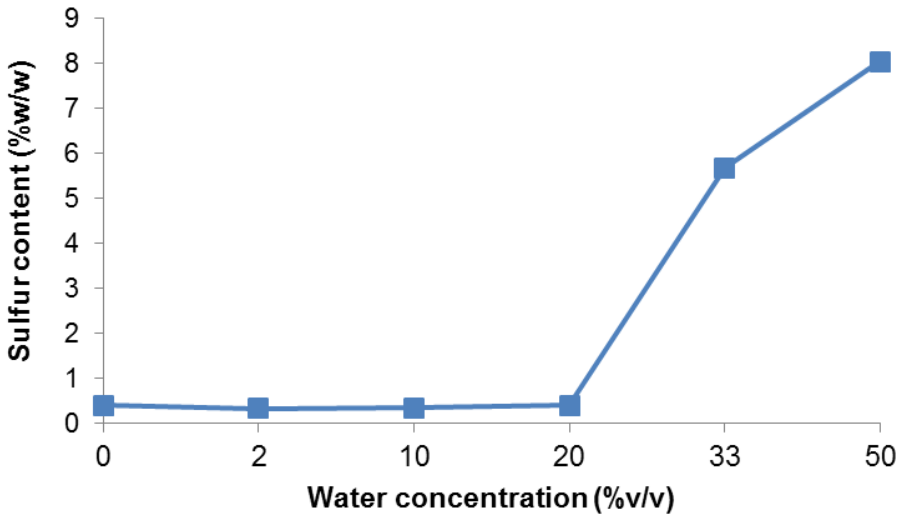

All pure solvents yielded very low levels of acid functionalization (Table 4-2). Using non-polar solvents such as toluene is good to control silanol polymerization, but the hydrolysis and condensation reaction rates are too slow. We expect that longer reaction times would be needed to improve acid functionalization if non-polar solvents are used. The moisture in the SiMNPs did not provide sufficient water to catalyze the reaction. Acetonitrile did not help the functionalization of the nanoparticles; the reaction media did not haze, which could be an indicator that MPTMS was not hydrolyzed. Methanol accelerated the reaction and helped the silanol groups react with each other before they attached to the surface. Some chunks of polysiloxane were observed, which were separated from the nanoparticles using a 500-mesh sieve; the polysiloxane deposits were retained, and the nanoparticle dispersion passed through it. Ethanol alone could not catalyze the hydrolysis of MPTMS into propyl-silanols; at least 33% water is needed to yield nanoparticles with a considerable number of functional groups. To some degree, ethanol controls the hydrolysis and condensation reactions since these reactions occurred when the reaction time was longer than 12 h.

To obtain at least 6% S on the nanoparticles, at least 15 h of reaction time was needed when using 0.5% MPTMS and 50% water (Figure 4-4). The level of functionalization increased

with time of exposure of the nanoparticles to the silanol solution. Reducing reaction time may require higher concentrations of MPTMS in the solution, but then reaction 4 in Figure 4-1 could be favored.

Figure 4-4 Effect of time on the total content of sulfur after functionalization with 0.5% MPTMS in a blend of ethanol and water (1:1)

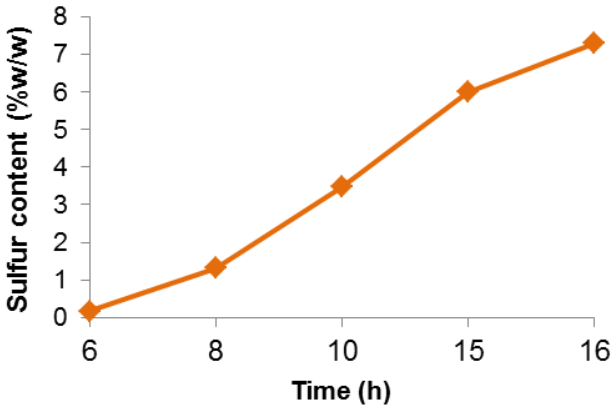

FTIR spectra of the acid-functionalized nanoparticles with two different levels of functionalization are shown in Figure 4-5. More intense bands are seen in the nanoparticles with larger % S. The peaks at 1620 cm^{-1} and 3400 cm^{-1} observed on the spectra have been attributed to the O–H vibration and stretching vibrations of physisorbed water (Hair 1975; Phan and Jones 2006). The weak peak at 3640 cm^{-1} corresponds to surface hydroxyl groups that are forming hydrogen bonds with other neighboring silanol groups (Brunel et al 2000; Hair 1975); these silanol groups are not available for reaction with MPTMS. This could be advantageous because it maintains the hydrophilic properties of the silica surface. Wettability of the surface is preferred when the targeted reactions are carried out in aqueous solutions, because it is expected that MPMTS would cause an increase in the hydrophobicity of the surface (Cano Serrano et al 2003; Chirachanchai et al 1999). The peaks at 1850–1929 cm^{-1} are associated with symmetric and asymmetric vibrations of the C–H bonds in the propyl chain, respectively (Brunel et al 2000; Colilla et al 2010; Dubois and Zegarski 1993). Deformation vibrations bands of $–CH_2$ are also observed at 1440 cm^{-1} (Rac et al 2006). The peaks at 1410 cm^{-1} in both spectra have been assigned to the stretching vibrations of S=O from undissociated acid sulfonic groups (Alvaro et al 2005; Buzzoni et al 1995). The doublet at 1300–1340 cm^{-1} in the upper spectra has been

attributed to stretching vibrations of $–SO_3^-$ species (Buzzoni et al 1995). The peak at 2520 cm^{-1} in the upper spectra can be associated with thiol groups from the mercaptopropyl groups that were not oxidized (Cano-Serrano et al 2003). The peaks associated with the C–H bonds as well as the peaks corresponding the O=S=O and $–SO_3H$ bonds had larger intensities for PS nanoparticles that had larger % S.

Figure 4-5 FT-IR spectra of PS nanoparticles with high and low levels of functionalization

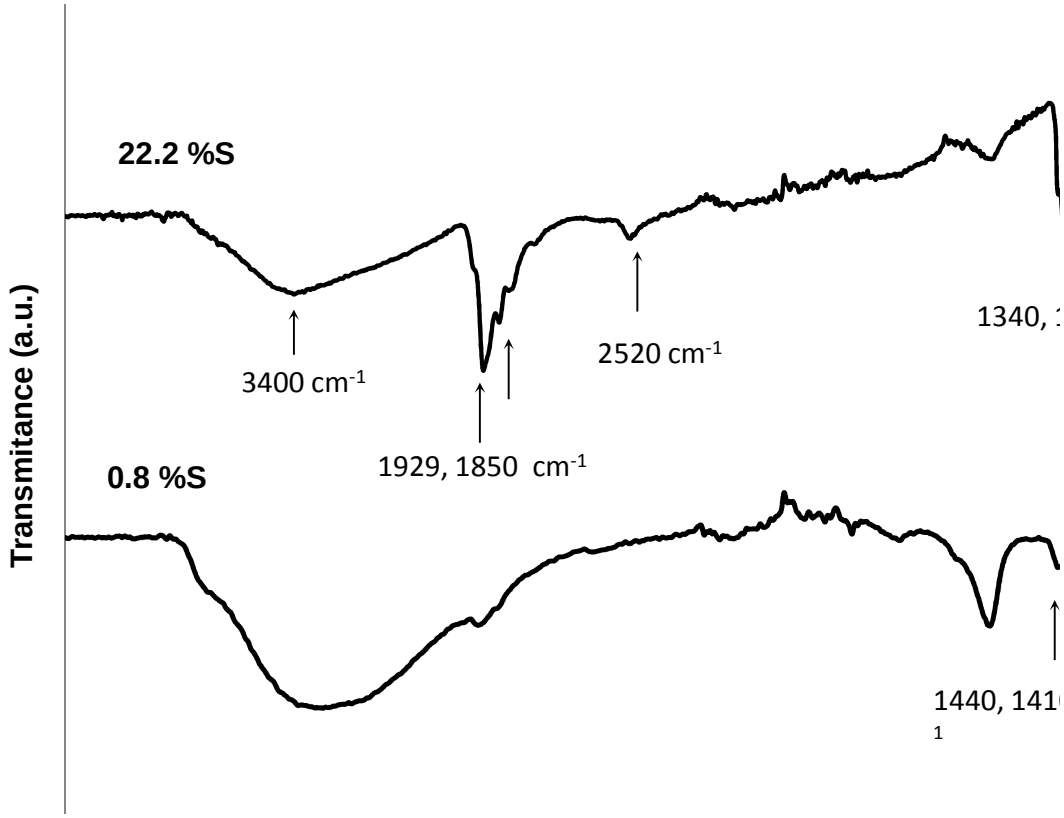

Before MPTMS modification, SiMNPs had an average particle size of 3.5 ± 1.6 nm (Figure 4-6, image A,). After functionalization with MPTMS, the size of the nanoparticles increased with the incorporated %S, indicating that the silanol has been deposited on their surface (Figure 4-6, image E). PS nanoparticles with a low level of functionalization (0.77% S) had an average Feret size of 7.7 ± 7.8 nm (Figure 4-6, image B). Surface modification carried out in toluene yielded small particles with low % S. The condensation of MPTMS on the surface of

the silica-coated nanoparticles was better controlled in anhydrous conditions even at high silane concentration (10%). This can be explained by the fact that using nonpolar solvents such as toluene prevents excessive condensation of MPMTS (Bossaert et al 1999; Chirachanchai et al 1999; Tripp and Hair 1995). PS nanoparticles with a medium level of functionalization (7.42 % S), which were synthesized in a 1:1 blend of water and ethanol with 2.5% MPTMS are shown in Figure 4-6, image C. Their average size was 26.4 ± 9.8 nm. PS particles synthesized with 5% MPTMS in a 1:1 blend of water and ethanol had the highest sulfur content 22.2% S obtained in this study. These particles also had the largest particle size. Their average size was 42.5 ± 44.5 nm (Fig. 6, image D). MPTMS is effectively hydrolyzed by water and reacts readily with Si-OH groups that are available (Chirachanchai et al 1999). Therefore, it was expected to observe that high water and silane concentrations promoted the condensation of the hydrolyzate into a thick silica layer on the surface of the nanoparticles. Although, PS remained in the nanoscale at the high modification levels (e.g., 22.2 %S), excessive MPTMS condensation gives hydrophobic nanoparticles (Macquarrie et al 1999). In aqueous conditions, hydrophobic nanoparticles agglomerate to reduce the surface area in contact with water molecules. The formation of nanoparticle aggregates in the reaction solution can hamper the catalytic activity of these nanoparticles by lowering the surface area available for reaction.

Figure 4-6 TEM images of propyl-sulfonic acid-functionalized nanoparticles. Image A depicts nanoparticles before MPTMS modification. Image B depicts PS nanoparticles with low sulfur content (0.77%); image C depicts particles with a total sulfur content of 8.82%, and image D depicts particles with 22.21% S. The scale in all the images is 100 nm except for image A, which is 20 nm. Image E depicts the relationship between incorporated sulfur vs. mean Feret size

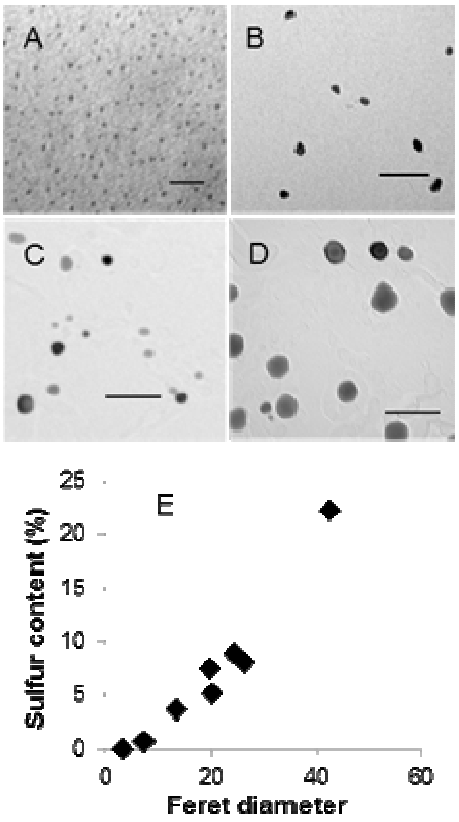

Results from the cellobiose hydrolysis using PS nanoparticles are shown in Figure 4-7. Increments in cellobiose conversion when the level of sulfur incorporated on the nanoparticles increased from 0.26 to 6. 0% S can be observed. The conversion of cellobiose reached up to 96.0 ± 0.7%. The control experiment without nanoparticles gave a cellobiose conversion of 32.8% ± 8.7. The hydrolysis of cellobiose was catalyzed with dispersions of PS nanoparticles that were equivalent to sulfuric acid solutions with concentrations less than 0.06% (w/w). Although the acid concentration provided by the nanoparticles was rather low, the results are promising and

showed significant improvement in the conversion of cellobiose using acid-functionalized nanoparticles compared with the control.

Figure 4-7 Cellobiose conversion at 175˚C for 30 min. Before the reaction, reacting solutions were prepared with 1% (w/w) catalyst and 4% (w/v) cellobiose

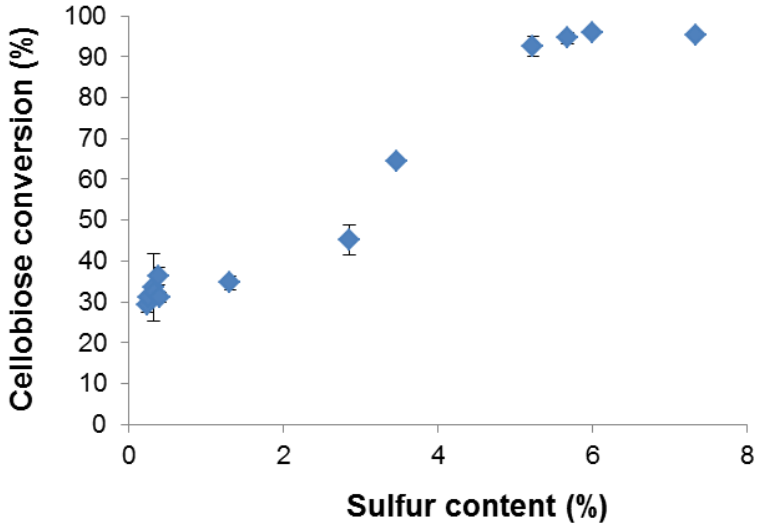

A comparison of the size and morphology of the nanoparticles was done with TEM images of PS nanoparticles before and after cellobiose hydrolysis Figure 4-8. The size of the nanoparticles did not change after reaction, but the particles looked cleaner after reaction. It is possible that the reaction temperature (175°C) served as a cleaning treatment, and removed material left after synthesis. The PS nanoparticles analyzed in these images had 8.82% S ± 1.1 before and 9.25 ±1.4 %S after hydrolysis, but in most cases, the catalyst lost about 30-49% of the incorporated sulfur after the hydrolysis reaction. More research is required to find a post-grafting curing method to avoid leaching the acid functional groups.

Figure 4-8 TEM image of PS nanoparticles before (A) and after (B) cellobiose hydrolysis

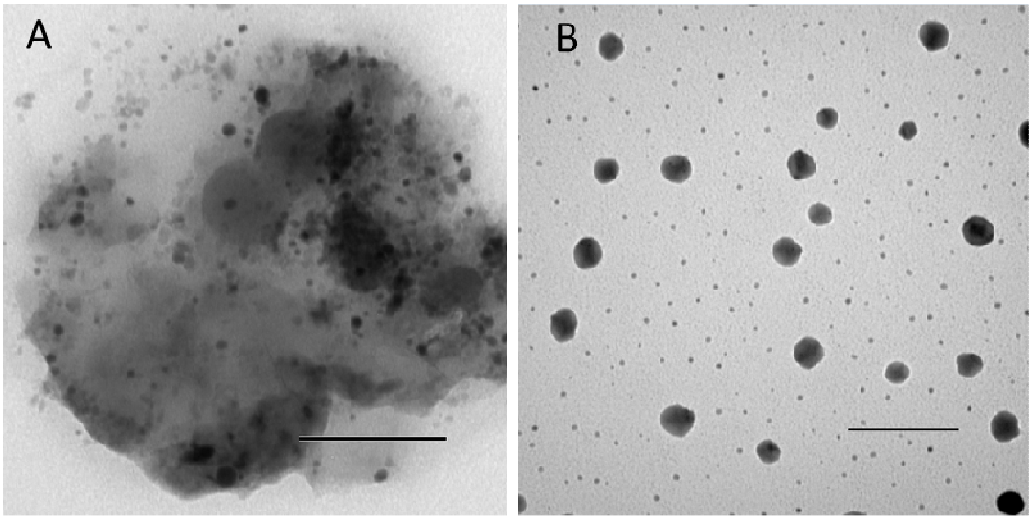

4.4 Conclusions

Silane concentration, water content in the reaction media, and acid functionalization time had a significant effect on propyl sulfonic acid-functionalized nanoparticles. The most active nanoparticles had 5–7% S, and were synthesized with 0.5% MPTMS, water (30–50%) and 15–16 h of reaction time. Propyl-sulfonic acid-functionalized nanoparticles effectively hydrolyzed cellobiose (96.0%), which was significantly higher than the conversion of the control without catalyst (32.8%).

Chapter 5 - Propyl-Sulfonic Acid Functionalized Nanoparticles as Catalyst for Pretreatment of Corn Stover

Abstract

Propyl-sulfonic (PS) acid-functionalized nanoparticles were synthesized, characterized, and evaluated as catalysts for pretreatment of corn stover. Silica-coated nanoparticles were functionalized with 0.5% mercaptopropyltrimethoxysilane (MPTMS) at neutral pH in a mixture of water and ethanol. Sulfur content of acid functionalized nanoparticles measured in a CHNS analyzer varied from 6-10%, and the acid load ranged from 0.040 to 0.066 mmol H^+/g. Pretreatment of corn stover was carried out at three temperature levels, 160, 180, and 200°C, for 1 h. Three levels of catalyst load were used: 0.1, 0.2, and 0.3 g of catalyst per gram of biomass. Hydro-thermolysis controls were carried out at each temperature level. The catalyst load did not affect glucose yield at 160°C, and the average glucose yield obtained at this temperature was 59.0%. The glucose yield was linearly correlated to the catalyst load during pretreatment at 180°C. The maximum glucose yield obtained at 180°C was 90.9%. Complete hydrolysis of glucose was reached at 200°C, but the average xylose yield was 4.6%, and approximately 20.2% of the combined glucose and xylose were lost as hydroxymethylfurfural and furfural. Results showed that acid-functionalized nanoparticles can be potential catalysts for the pretreatment of biomass for its later conversion to ethanol.

5.1 Introduction

One of the challenges in the production of bioethanol and chemicals from lignocellulosic biomass is breaking down the complex structure of biomass into monomeric sugars. Biomass has a complex mixture of cellulose, hemicellulose, and lignin. A pretreatment step is required to make the biomass cellulose fraction more susceptible to an enzymatic hydrolysis. Studies have shown that the removal of lignin and the consequent solubilization of hemicelluloses favor the enzymatic digestion of cellulose (Chang and Holtzapple 2000; Chang and Holtzapple 2000). The most accepted method for pretreatment of lignocellulosic biomass uses corrosive catalysts such as hydrochloric acid or sulfuric acid (Gonzalez et al 1986; Herrera et al 2004; Lee and Kim 2002; Viola et al 2007; Wyman et al 2005). The use of corrosion-resistant materials demands

higher capital investment than the capital needed when using less corrosive catalysts. Thermochemical pretreatment of biomass generates decomposition products such as hydroxymethylfurfural (HMF) and furfural. Pretreated biomass must be detoxified to remove these products because they could inhibit the microorganisms used during sugar fermentation to ethanol (Delgenes 1996). Chemical pretreatment of lignocellulosic biomass incurs additional costs for disposal of residues from neutralization and biomass conditioning. Solid acids provide similar catalytic properties to their liquid counterparts, with the advantages of being recoverable and reusable (Chafin et al 2008; Harmer et al 1998; Harmer et al 2007; Yadav 2005). Solid acids in the nanoscale prevent mass transfer problems that common heterogeneous catalysts generate. Acid functionalized nanoparticles could be used to replace mineral acids during biomass pretreatment for cellulosic ethanol production. Silica-coated nanoparticles (SiMNPs) can be modified to confer these nanoparticles with desired chemical properties (Raja and Thomas 2003)(Raja and Thomas 2003). 3-mercaptopropyltrimethoxysilane (MPTMS) is commonly used to graft sulfonic acid functional groups on silica materials. SiMNPs can be functionalized using similar procedures to those reported of silica acid functionalization (Gill et al 2007; Siril et al 2007). Acid functionalized silica materials have been used to catalyze α-1,4-glycosidic bonds in sucrose and starch (Dhepe et al 2005) and β-1,4-glycosidic in cellobiose (Bootsma and Shanks 2007). Acid functionalized nanoparticles were previously used for cellobiose hydrolysis (Peña et al 2011) and hemicellulose solubilization (Peña et al 2012). In this work, silica-coated cobalt iron oxide nanoparticles functionalized with propyl-sulfonic acid groups were synthesized and used as catalyst for the pretreatment of corn stover.

5.2 Methods and Materials

5.2.1 Materials

Cobalt (II) chloride hexahydrate (99%), D-(+)-Cellobiose (98%), iron (II) chloride tetrahydrate (99.99%), MPTMS (95%), methylamine (40%w/w, 98.5%), sodium dodecyl sulfate (98.5%), and tetraethylorthosilicate (TEOS) (99.999%) were purchased from Sigma-Aldrich (St. Louis, Mo., USA). Ammonium hydroxide, toluene, and isopropanol (A.C.S. reagent) were purchased from Fisher Scientific (Pittsburgh, Pa., USA). Ethanol (95%) was purchased from Decon Laboratories (King of Prussia, Pa., USA). Corn stover was harvested from the Kansas

State University Agronomy Farm in October 2011 (Manhattan, Kan.). Corn stover was ground in a cutting mill (SM2000, Retsch, Inc., Newtown, Pa.) to pass a 1 mm mesh.

5.2.2 Synthesis of SiMNPs

Cobalt iron oxide nanoparticles were synthesized by precipitating salts of Co^{+2} and Fe^{+2} using a microemulsion method (Moumen et al 1996; Rondinone et al 1999). In a typical experiment, a solution was prepared with 4 mmol (0.9 g) of cobalt (II) chloride hexahydrate $CoCl_2 \cdot 6H_2O$, 10 mmol (1.9 g) of iron (II) tetrahydrate $FeCl_2 \cdot 4H_2O$, and 45 mmol (12.9 g) of sodium dodecyl sulfate (SDS). The salts and surfactant were dissolved in distilled water, mixed, and diluted to 1 L. One liter solution of 12 wt. % methylamine was also prepared. After stirring the first solution for 30 min at room temperature, both solutions were heated to 55-65˚C and then combined. The mixture was kept at 55-65˚C under rigorous mechanical stirring. After three hours, the particles were magnetically separated and washed three times with water and once with ethanol. Then, the particles were stored in 100 mL of ethanol.

Cobalt iron oxide nanoparticles were coated with silica using procedures reported in the literature (Gill et al 2007; Peña et al 2011; Shen et al 2004). The dispersion of $CoFe_2O_4$ in ethanol was sonicated for 1 h. Approximately 15 ml of this solution were added to 550 ml blend isopropanol and water 9:1. This solution was sonicated and mechanically stirred for 30 min. One mL of tetraethylorthosilicate (TEOS) was diluted in 40 mL of isopropanol. After stirring, 50 mL of concentrated ammonium hydroxide were added and the dilute TEOS solution was added at a rate of 0.3 ml/min. After the addition of the TEOS solution, the mixture was sonicated for another hour. Then, the silica-coated magnetic nanoparticles (SiMNPs) were magnetically separated, washed four to five times with water, and dried at 40°C in a forced air convection oven.

5.2.3 Functionalization of SiMNPs

Propyl-sulfonic (PS) acid grafting upon silica-coated nanoparticles was done using procedures similar to those used for silica functionalization (Badley and Ford 1989; Cano-Serrano et al 2003; Gill et al 2007; Hamoudi et al 2004; Morales et al 2008; Siril et al 2007). Approximately 500 mg of dry SiMNPs and 1 ml of MPTMS were sonicated in 100 ml of ethanol for 1 h. After sonication, 100 ml of 100 mM acetate buffer at pH 4.8 was added, and the mixture

was heated and mechanically stirred at 75 °C. After 16 h of reaction, the mercaptopropyl-functionalized nanoparticles were separated magnetically and washed three times with ethanol. Then, the nanoparticles were placed in a 60 ml solution with equal amounts of water, methanol, and hydrogen peroxide for oxidization of the mercapto groups. After 48 h in the oxidizing solution, the nanoparticles were washed three times with distilled water and placed in 100 mL of 0.01 N HCl for 48 h. After protonation, the PS nanoparticles were separated out of the acid solution and washed multiple times with distilled water. Then, the PS nanoparticles were dried at 120°C for 3 h.

5.2.4 Characterization of the nanoparticles

Fourier transform infrared (FTIR) spectra were used to confirm the presence of propyl-sulfonic acid gruops in functionalized nanoparticles. The measurement was carried out in two wave number range 500–4000 cm^{-1}, with a resolution of 4 cm^{-1} and 32 scans per sample. Spectra and peak positions were determined using an infrared spectrometer and spectrum software (Spectrum 400, PerkinElmer Inc., Waltham, Mass.).

Sulfur content was used as an indicator of the silane grafting level on the nanoparticles. Sulfur content (wt. %) was determined in an elemental analyzer (Model 2400 SeriesII, PerkinElmer Inc., Waltham, Mass.). The concentration of hydronium ions was calculated as percentage of sulfur divided by the molecular weight of the sulfur atom and the working volume.

5.2.5 Pretreatment of Corn Stover

Before pretreatment, corn stover samples were analyzed for composition following the NREL LAP TP-510-42618 (Sluiter et al 2008b) (Table 5-1). PS nanoparticles were used to pretreat corn stover and evaluate their ability to increase biomass susceptibility to an enzymatic hydrolysis. A scheme of the steps followed to pretreat biomass using acid functionalized nanoparticles is shown in Figure 5-1. A Box–Behnken design was employed to calculate the minimum number of experiments required to obtain an estimate of the surface response for temperature, catalyst load, and %S content of the catalyst. A minimum of 17 experiments was calculated, and the results from 34 runs were analyzed using Design Expert (Stat-Ease, Inc., Minneapolis, Minn., USA). The pretreatment was carried out at 160, 180, and 200°C. In a typical experiment, 0.1-0.3 g of PS nanoparticles and 1.0 g of corn stover (both weighted to the nearest 0.1 mg) and 39 ml of distilled water were placed in a 60 ml Swagelok tube (Swagelok, Kansas

City Valve & Fitting Co., Kan.). Then, the tube was sonicated for 30 min to disperse the nanoparticles. After sonication, the tube was placed in a sand bath previously heated at the pretreatment temperature. After 60 min of reaction, the tube was cooled to room temperature in approximately 5 min. The control experiments had no catalyst and were carried out under the same conditions as experiments using PS nanoparticles. After pretreatment, the solid and liquid fractions were separated via vacuum filtration using a Büchner funnel. The pretreated solids and PS nanoparticles were retained in the paper filter and the solubilized sugars passed as filtrate. The solid material was washed with approximately 200 ml of distilled water to remove all soluble sugars, as described in (Sluiter et al 2008c). Then, the solid fraction was hydrolyzed for 24 h following the NREL LAP TP-510-42629 (Selig et al 2008). In a typical experiment, approximately 2.5 g of wet biomass were placed in 30 ml of distilled water and 30 ml of 100 mM acetate buffer at pH 4.8; after 2 ml of Accelerase® 1500 were added to the slurry, the samples were kept at 50°C for 24 h. After hydrolysis, the solutions were analyzed by HPLC to account for glucose and xylose using a RCM-Ca+2 monosaccharide column (300 x 7.8mm; Phemomenex®, Torrance, Calif., USA) and refractive index detector. Samples were run at 80°C at 0.6 ml/min with water as mobile phase. The PS nanoparticles were then separated from the enzymatically treated solution. A 400 mesh was used to retain the solid fraction remaining after enzymatic hydrolysis and, a magnet was used to wash the nanoparticles. The nanoparticles were then dried and analyzed by FTIR. The filtrate was passed over a filter membrane of 0.2 µm. The sample was then analyzed for sugars following NREL LAP TP-510-42623 (Sluiter et al 2008a). Decomposition products of glucose and xylose, such as HMF, and furfural were measured using an ROA-organic acid column (300 x 7.8 mm; Phemomenex®, Torrance, Calif.) and a UV detector. Samples were run at 65°C at 0.6 ml/min with 5 mM H_2SO_4 for 55 min. The percentage of glucose converted to HMF was calculated by multiplying the concentration of HMF by 1.429. The percentage of xylose converted to furfural was calculated by multiplying the concentration of furfural by 1.562.

Table 5-1 Corn stover composition (dry basis)

Biomass constituents	Corn stover
95% ethanol extractives	21.8 ± 3.8
Glucan (%)	30.2± 2.6
Xylan (%)	18.4± 2.3
Arabinan (%)	1.9± 0.3
Acid-soluble lignin (%)	1.0± 0.1
Acid-insoluble lignin (%)	14.5± 0.4
Total lignin (%)	15.4± 0.5
Acid-insoluble ash (%)	2.1± 0.3

Figure 5-1 Schematic of sugar recovery from corn stover using propyl-sulfonic acid functionalized nanoparticles during pretreatment

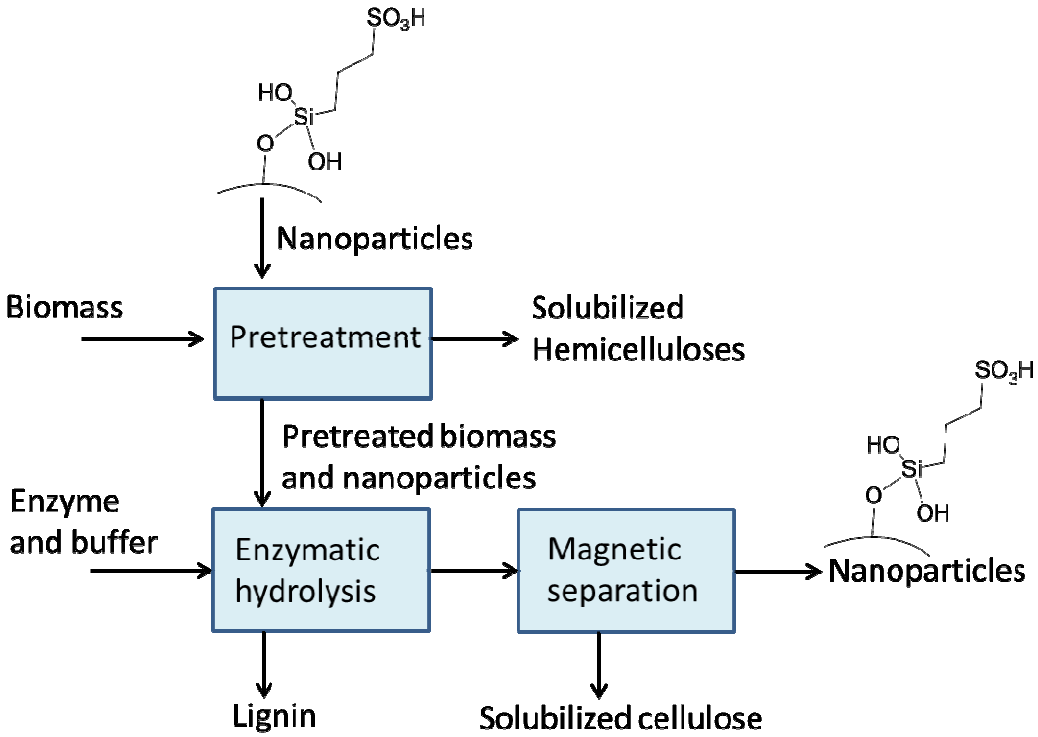

5.2.6 Recyclability experiments

Stability of the PS nanoparticles was evaluated using cellobiose hydrolysis as model reaction of biomass pretreatment. Solutions of 4 mg/ml of cellobiose and 1% PS nanoparticles

were placed in a 60 ml Swagelok tube (Swagelok, Kansas City Valve & Fitting Co., Kan.). The tubes were kept at 175°C for 30 min in a sand bath. The sugar solution and PS nanoparticles were separated using a neodymium magnet and dried at 105°C. PS nanoparticles were analyzed with the elemental analyzer as described above.

5.3 Results and Discussion

FTIR spectra taken to the acid-functionalized nanoparticles are shown in Figure 5-2. The peaks at 1620 cm^{-1} and 3400 cm^{-1} on the spectra have been attributed to the O-H vibration and stretching vibrations of physisorbed water. These bands could also be associated with silanol groups of the SiMNPs (Brunel et al 2000; Hair 1975) that did not react with MPTMS. It has been reported that only one hydroxyl group from silanols attaches to silica surfaces (Goerl 1997); therefore, hydroxyl groups of the propylsilanol moieties can also generate bands at 3400 cm^{-1}. Peaks at 1950-1929 cm^{-1} are associated with symmetric and asymmetric vibrations of the C-H bonds in the propyl chain, respectively (Brunel et al 2000; Colilla et al 2010; Dubois and Zegarski 1993). Deformation vibrations bands of $–CH_2$ are also observed at 1457 cm^{-1} (Rac et al 2006). In the fingerprint region, bands attributed to Si-O-Si, Si-OH, and Si-O at 1078, 956, 800 cm^{-1} are observed (Colilla et al 2010; Smith 1960; Tripp and Hair 1995; Zhao et al 2000). Peaks at 1414 cm^{-1} in the spectra for PS nanoparticles have been assigned to the stretching vibrations of S=O from undissociated acid sulfonic groups (Alvaro et al 2005; Buzzoni et al 1995). The doublet at 1350 and 1310 cm^{-1} has been attributed to stretching vibrations of $–SO_3^-$ species (Buzzoni et al 1995). The peak at 2520 cm^{-1} (Diaz et al 2000) associated to thiol groups from the mercaptopropyl groups was not observed, meaning that all groups were oxidized either to sulfonic acid groups or to other S species. Other authors have found evidence of the formation of S-S bridges when working with MPTMS; however, bands associated with S-S were not observed in this study. Bands at 743 and 691 cm^{-1} may be attributed to S-OR species.

Figure 5-2 FT-IR spectra of propyl-sulfonic acid functionalized nanoparticles

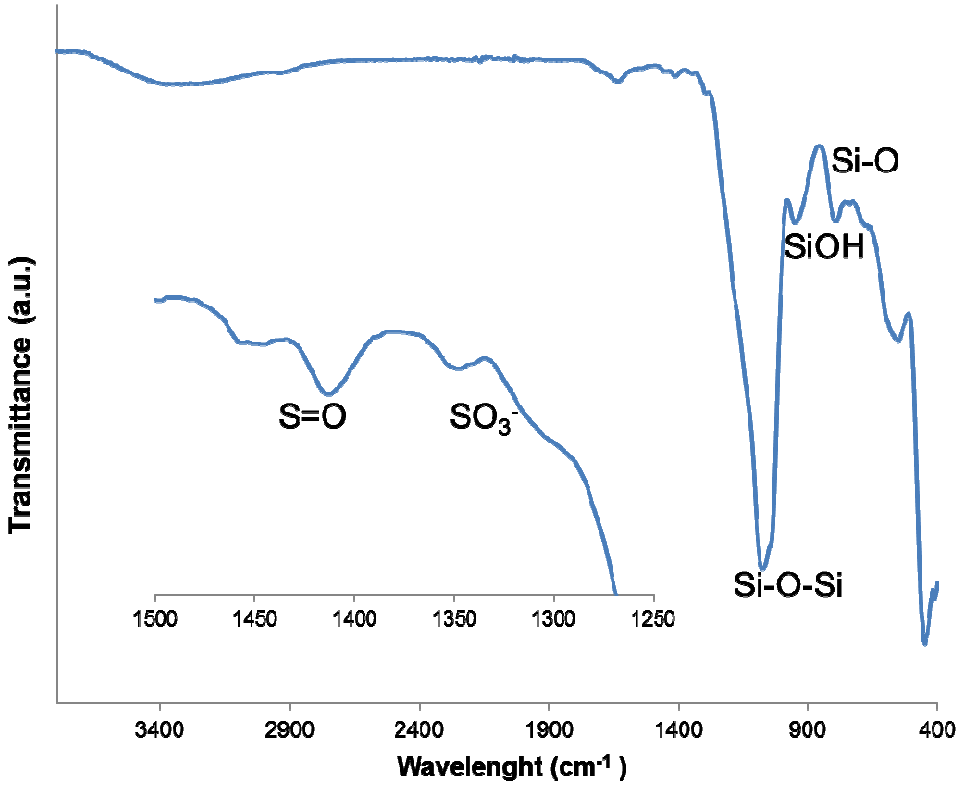

The sulfur content %S of PS nanoparticles varied from 5.01% to 9.94%. Badley et al. (1989) reported values of %S between 3.25% and 8.32% for propyl-sulfonic acid functionalized silicas (Badley and Ford 1989). Other works reported 1.17 meq S/g (3.7 %) for propyl-sulfonic modified SBA-15 (Melero et al 2010) and 10.88 S% on thiol-MCM-41 (Lim et al 1998). However, the possibility exists that only part of the sulfur is in the sulfonic acid form even though the bands associated with S-S bridges or non-oxidized –SH groups were not observed in the FTIR spectra of PS nanoparticles.

Predicted total glucose yield from corn stover is shown in Figure 5-3. The red dots indicate design points as a function of pretreatment temperature and catalyst loading. At 160°C, PS nanoparticles did not show significant improvement in biomass digestibility. The average glucose yield obtained at this temperature was 59.02% (± 5.48) out of 11 experiments using various catalyst load levels. Even though PS nanoparticles were effectively modified (5-9% S), at 160°C, the sugar yield was not significantly different from the yield obtained in the hydro-

thermolysis (0 mg S/g biomass). Aggregation of the particles could have caused limited availability of catalytic sites for reaction with carbohydrate-lignin bonds in biomass. However, at 200°C, complete sugar hydrolysis occurred, and differences between control and catalyst performance experiments were not detected.

Figure 5-3 Contour graph of the model for total glucose yield from corn stover

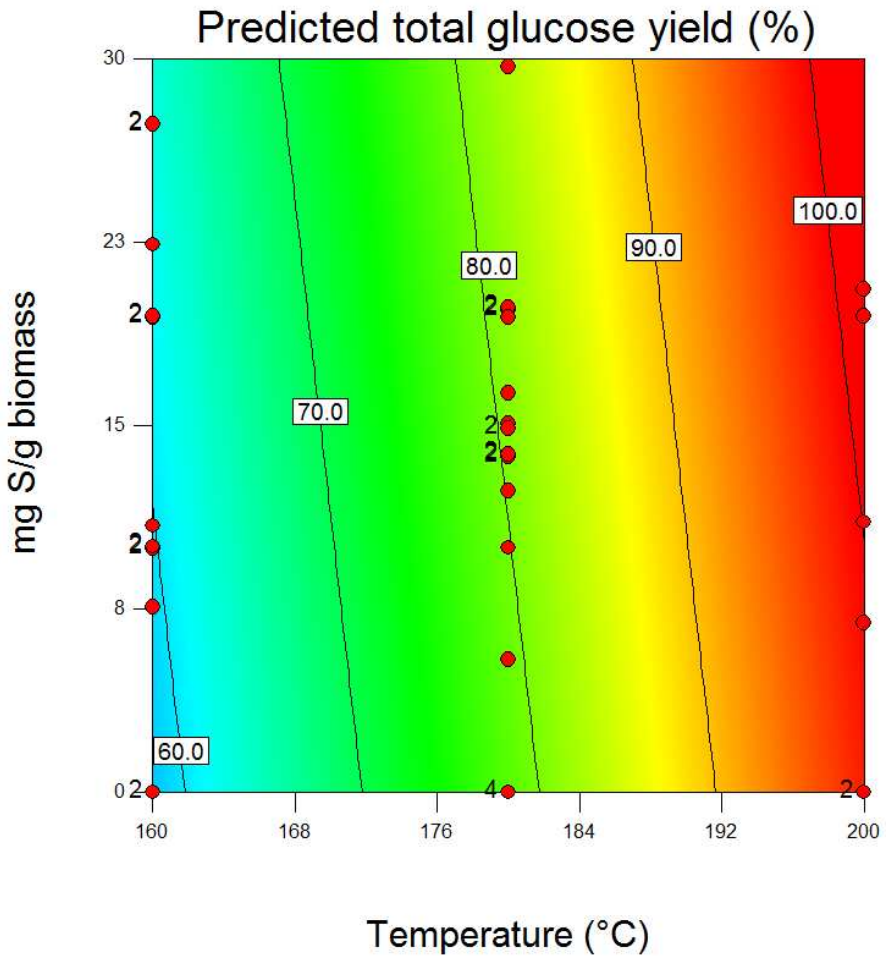

At 180°C, the total glucose yield was linearly correlated to the load of catalyst indicated in terms of total sulfur mass (Figure 5-4). For this correlation, a Bonferroni correction was applied for which a P-value of 0.025 was used as criteria for significance. A maximum glucose yield of 90% was reached when using 0.2 g of PS nanoparticles with a total sulfur content of 6.1%.

Figure 5-4 Total glucose yield from corn stover as a function of catalyst loading at 180˚C for one hour

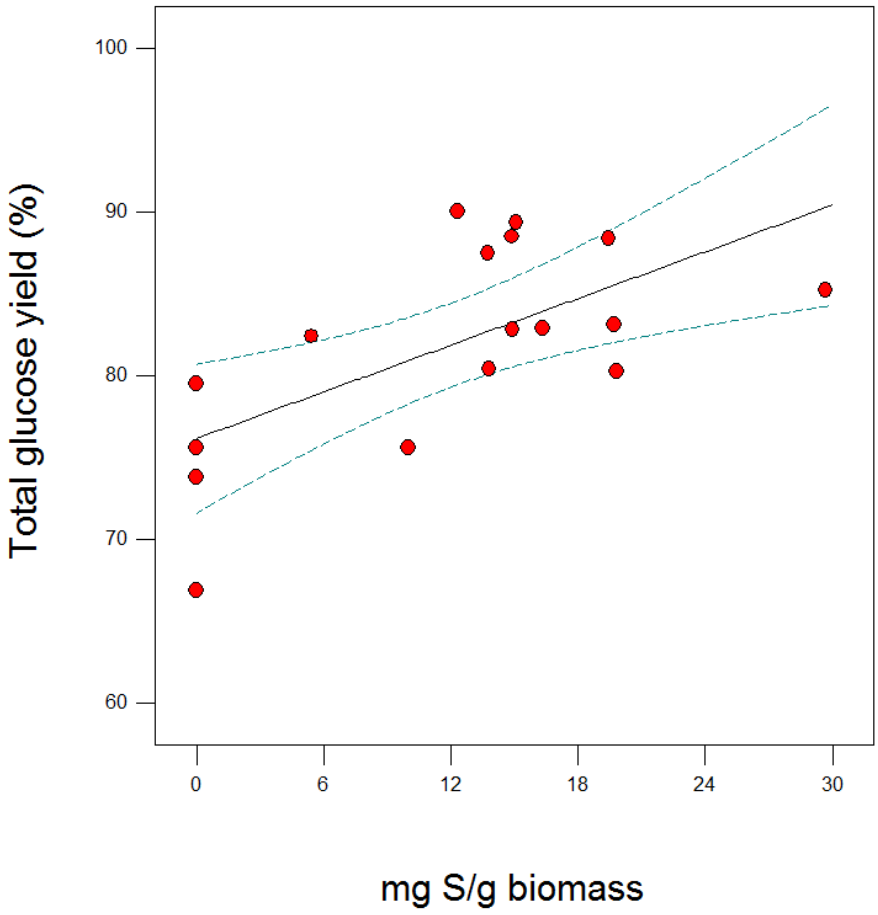

Modeled xylose yield predicts that a maximum xylose yield could be reached with a catalyst load of 6 mg S/g biomass between 165 and 175°C (Figure 5-5). At 160°C, a load of catalyst higher than 30mg/ml would be required in order to increase the xylose yield over 50%. Xylose yield increased with increasing temperature; however, after 175°C, the xylose yield decreased rapidly because at these temperatures pentose sugars can be degraded to other products such furfural and formic acid (Bobleter 1994). At 160°C, PS nanoparticles did not have a significant effect on the xylose yield, and at 200°C, the xylose yield decreased with the catalyst load. At 200°C, the xylose recovery was less than 6%, which can be explained by the fact that PS nanoparticles can catalyze the production of xylose-derived products.

Figure 5-5 Contour graph of the model for total xylose yield as a function of pretreatment temperature and catalyst loading

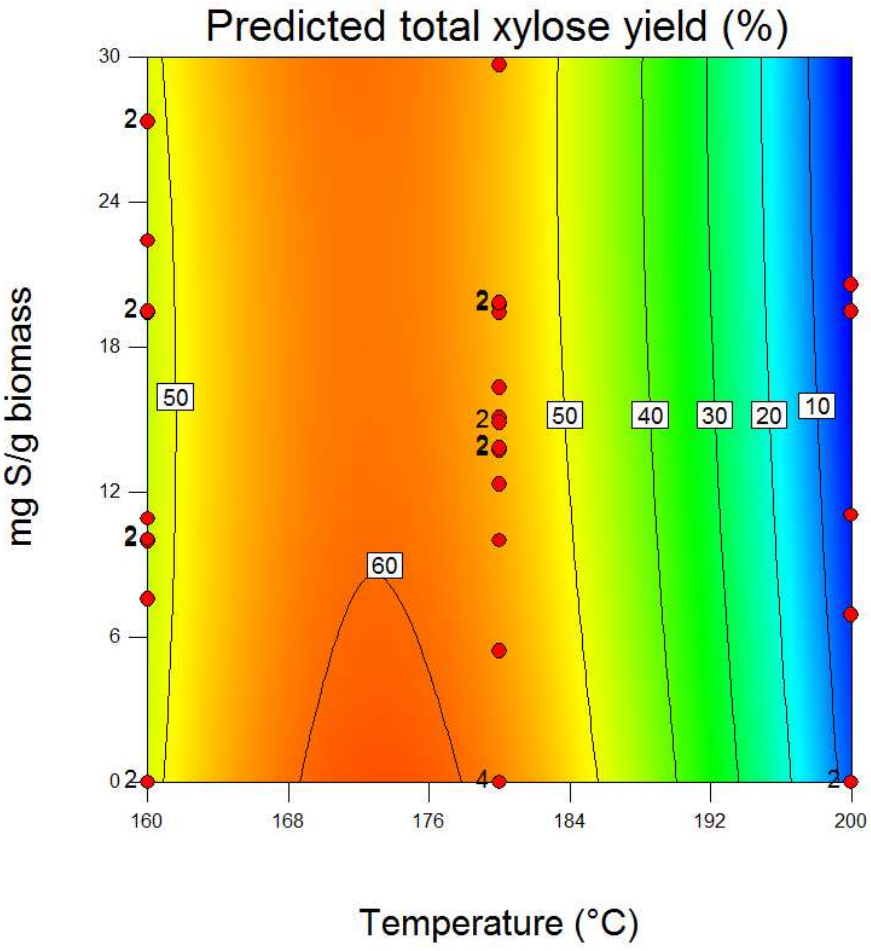

Various works have discussed the use of supported acids to produce carbohydrate-derived products such as HMF and furfural (Moreau 1998; Ordomsky, 2012). The predicted amount of glucose lost as HMF is shown is Figure 5-6. The HMF formation increased with the catalyst load and temperature. At 160°C, the amount of glucose lost was less than 2% for all catalyst loadings tested. At 200°C, approximately 11% of total glucose in the corn stover samples was lost at the highest catalyst load.

Figure 5-6 Contour graph of the model for the percentage of glucose lost as HMF as a function of pretreatment temperature and catalyst loading

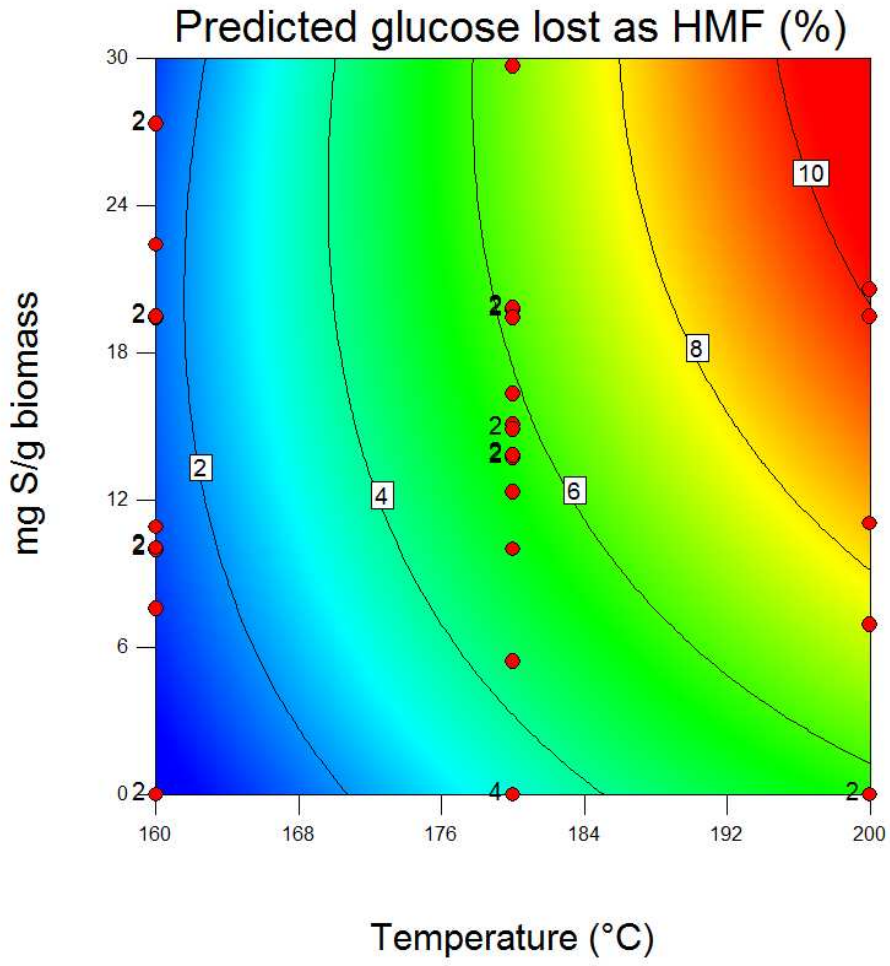

The amount of xylose lost as furfural is shown in Figure 5-7. The amount of xylose lost because of furfural formation increased with the catalyst load and temperature. When PS nanoparticles were used at a load of 30 mg S/g biomass and at a temperature of 160°C, less than 1% xylose was lost as furfural. At 200°C and 30 mg S/g biomass, the amount of xylose lost as furfural reached 30%.

Figure 5-7 Contour graph of the model for the percentage of xylose lost as furfural as a function of pretreatment temperature and catalyst loading

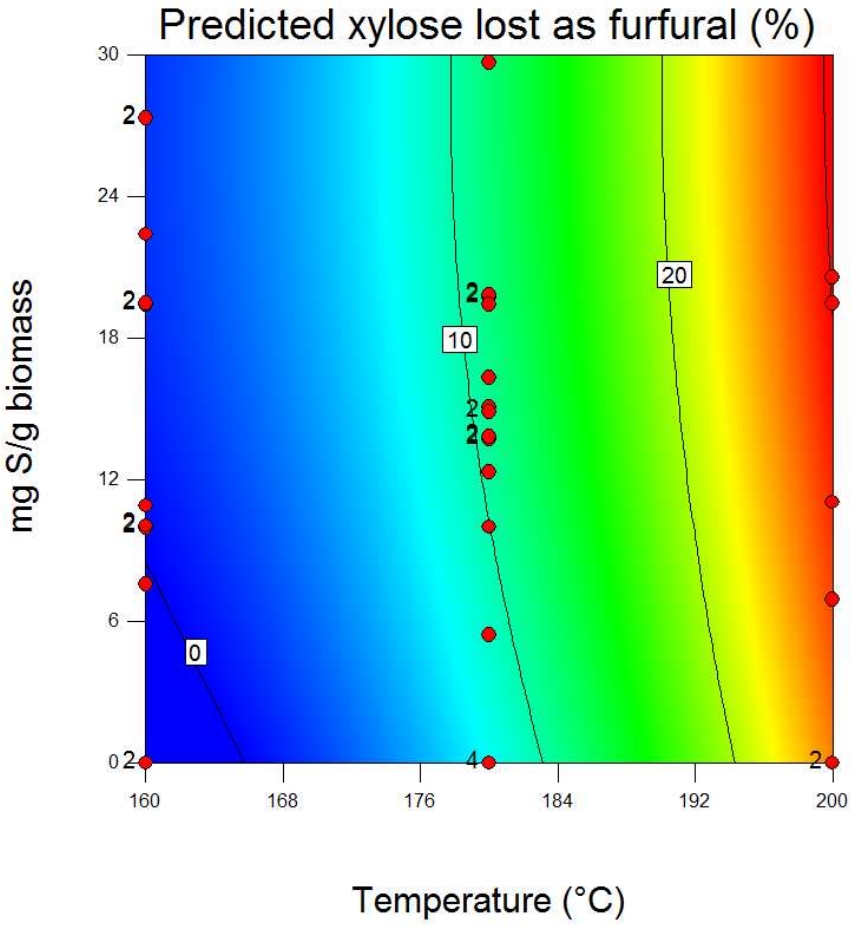

Pretreatment of corn stover with PS nanoparticles could have given higher sugar yields at lower temperatures if they did not aggregate and form clumps. Aggregation of the nanoparticles hides the catalytic sites and makes them unavailable for reaction. The possibility also exists that sulfate salts were formed with ions derived from trace minerals in biomass. PS nanoparticles appeared to have affinity towards pretreated biomass; complete separation of biomass and nanoparticles was difficult as evidenced by the increment in carbon content in PS nanoparticles after pretreatment (Table 5-2). PS nanoparticles did not block enzyme access to the carbohydrate fraction PS nanoparticles. This conclusion is made because complete glucose recovery was reached for some experiments, even though the nanoparticles were present during enzymatic hydrolysis.

Table 5-2 Elemental Analysis of PS nanoparticles before and after cellobiose hydrolysis and pretreatment at 175°C

PS nanoparticles	% C	% H	%N	% S
Before cellobiose hydrolysis	11.86	2.39	-	9.81
After cellobiose hydrolysis	11.10	2.33	-	9.00
Before pretreatment	11.43	2.62	-	9.59
After pretreatment	24.67	3.32	2.21	3.13

Hydrolysis of cellobiose has been used as model reaction of cellulose hydrolysis to its glucose units (Bootsma and Shanks 2007; Lai et al 2011a; Shimizu et al 2009). In this work, the cellobiose hydrolysis reaction was used to analyze stability of propyl-sulfonic acid groups in PS nanoparticles. To assess the loss of functional groups during reaction, sulfur content of the nanoparticles was measured before and after cellobiose hydrolysis (Table 2). The PS nanoparticles lost approximately 1% of their sulfonic acid groups after hydrolysis of cellobiose at 175°C, indicating that PS nanoparticles retained most of their functional groups and that these groups are stable during catalysis in aqueous media reactions at high temperatures. Elemental analysis was also performed on PS nanoparticles after pretreatment. However, it was difficult to remove all the biomass left after pretreatment. Organic content of the nanoparticles increased, and determination of the real percentage of sulfonic groups after pretreatment was difficult. An FTIR spectrum was also taken after pretreatment with PS nanoparticles (Figure 5-8). The band at 1510 cm^{-1} characteristic of lignin (Gosselink et al 2004) was observed, as well as an increment in the band intensity associated with C-H bonds at 1457 cm^{-1}. Although, the absorption of material is not a desired condition, it can be an indicator of the affinity of these nanoparticles towards cellulose-derived materials, necessary for effective catalysis.

Figure 5-8 FT-IR spectra of propyl-sulfonic acid functionalized nanoparticles after pretreatment

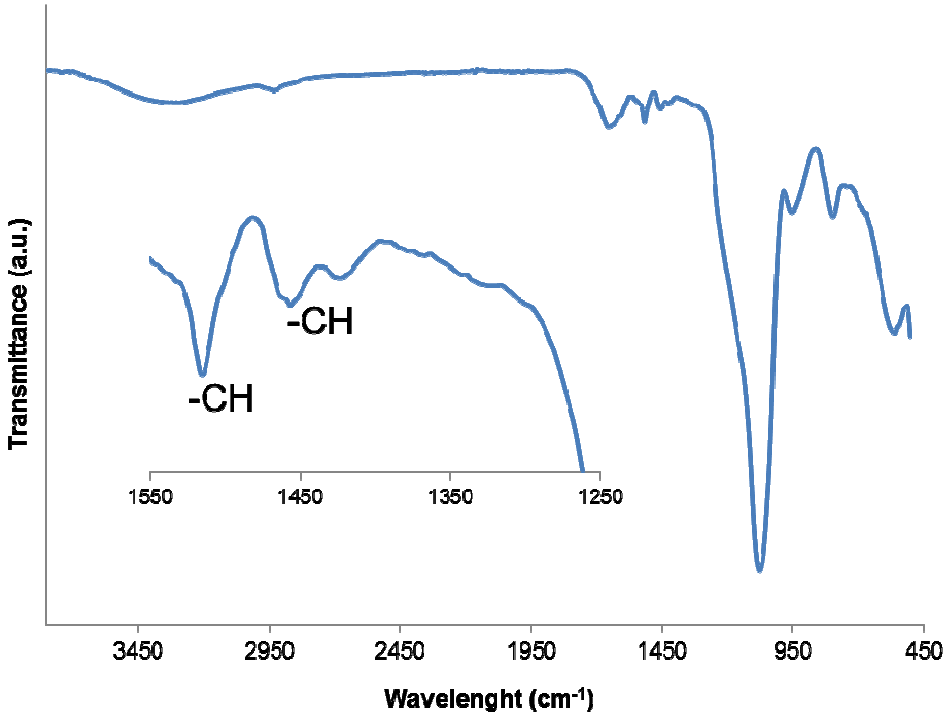

5.4 Conclusions

For corn stover, the highest glucose yield of more than 90% was obtained at a pretreatment temperature of 180°C, and the average glucose yield was linearly correlated to the load of PS nanoparticles at 180°C. At lower temperatures, the amount of PS nanoparticles required to increase glucose yield above 59.0% must be higher than 30 mg S/g biomass, equivalent to 24 mmol H^+/L. At 200°C, complete cellulose hydrolysis to glucose was achieved, but 96% of corn stover hemicelluloses were lost as degradation products. PS nanoparticles retained 99% of their propyl-sulfonic acid load after hydrolysis of cellobiose at 175°C.

Chapter 6 - Conclusions

Silica-coated maganetic nanoparticles (SiMNPs) were functionalized with prefluoroalkylsulfonic (PFS), alkylsulfonic (AS), and butylcarboxylic (BCOOH) acid functions. Feret diameters were calculated from TEM images as 2.0, 6.9, and 2.0 nm, respectively. Total organic content was 32.5%, 12.6%, and 25.9% for PFS, AS, and BCOOH, respectively, determined as loss weight from 200 to 600°C. The sulfur content of PFS and AS was measured as 3.1% and 4.9%, respectively. The carbon content of PFS, AS, and BCOOH was 12.4%, 6.1%, and 19.5%, respectively. The FTIR spectra for all nanoparticles had a broad Si-O band. A band at 1929 cm^{-1} associated with C-H was observed in the PFS and BCOOH spectra. Peaks associated to undissociated sulfonic acid (1420 cm^{-1}) and to O=S=O groups (1377 cm^{-1}) were observed in PFS and AS spectra. A band at 1738 cm^{-1} corresponding to the carbonyl group was observed in the BCOOH spectrum.

Hydrolysis of cellobiose using AS and PFS acid functionalized nanoparticles (0.2 g catalyst/g cellobiose) yielded 77.8% and 74.6% cellobiose conversion at 175°C for 1 h, respectively. Glucose yields hydrolyzed by PS and PFS nanoparticles were 49.5% and 45.8%, respectively. Low glucose yields were due to thermal degradation of the sugar. PS nanoparticles retained approximately 60% of its propyl-sulfonic acid groups and 75% of its original catalytic activity, which resulted in 47% cellobiose conversion after a third cycle. PFS nanoparticles lost catalytic activity, since cellobiose conversion was 47% after the third cycle. Hydrolysis using BCOOH nanoparticles yielded 58.1% cellobiose conversion, and the conversion rate of control was 51.9%.

Synthesis conditions used to functionalize SiMNPs with propyl-sulfonic acid groups affected the catalytic properties of PS nanoparticles. The most active PS nanoparticles had 5–7% S, and they were synthesized with 30–50% water, 0.5% MPTMS, and 15–16 h of reaction time. The performance of PS nanoparticles was evaluated on the hydrolysis of cellobiose at 175°C for 30 min and 2.5 g PS nanoparticles/g cellobiose. PS nanoparticles synthesized at these conditions hydrolyzed 96% of the initial amount of cellobiose, which was significantly higher than the conversion of the control without catalyst (32.8%).

AS and PFS acid-functionalized nanoparticles were used as pretreatment catalysts of wheat straw. The pretreatment was carried out at 160°C for 2 h using 0.1 g catalyst/g biomass. PFS and PS nanoparticles solubilized 46.3% and 45.0% of wheat straw hemicelluloses, respectively. These values are significantly higher than sugars solubilized in the control experiment (35.0%). The acid-functionalized nanoparticles broke down the non-soluble polysaccharides into oligomers, and the monomers were degraded to furfural at these pretreatment conditions.

At 180°C treatment, a total glucose yield greater than 90% was obtained from corn stover and the glucose yield was linearly correlated to the load of PS nanoparticles. At lower temperatures, the amount of PS nanoparticles required to increase the glucose yield above 59% must be higher than 30 mg S/g biomass, equivalent to 0.43 g catalyst/biomass for PS particles with 7%S and a 24 mmol H^+/L acid solution. At 200°C, complete cellulose hydrolysis to glucose was achieved, but 96% of corn stover hemicelluloses were lost as degradation products. PS nanoparticles retained 99% of their propyl-sulfonic acid load after hydrolysis of cellobiose at 175°C.

In order to use acid-functionalized nanoparticles for pretreatment of lignocellulosic biomass, several problems must be addressed, such as the low density of acid sites, acid sites leaching, and agglomeration. Acid sites density of the nanoparticles is low; the weight of PS nanoparticles must be 100 times larger than the weight of sulfuric acid in order to prepare acid solutions with equivalent acid strength. For example, to prepare a 1 mmol H^+/L solution, 0.049 g of sulfuric acid are needed; to prepare the same solution with PS nanoparticles, 5 g of the catalyst are needed. Some of the functional groups are lost into the solution, so the catalysis could be equivalent to a homogeneous catalysis. Acid functionalized nanoparticles must be recyclable in order to become substitutes of traditional homogeneous acid catalysts. Moreover, the nanoparticles aggregate; the area available for reaction is reduced and not all catalytic sites are exposed and available to the reactants.

Future work

To reduce the acid density of acid-functionalized SiMNPs, an alternative magnetic core may be utilized, such as iron oxide nanoparticles. Nanoparticles with a size distribution under 6 nm can be obtained when synthesizing iron oxide nanoparticles (Estephan et al 2013). Also, a

solvothermal-assisted transfer method could be used to synthesize $CoFe_2O_4$.This method controlled average particle size between 2-6 nm (Feng et al 2013). Smaller nanoparticles would reduce the weight of the metallic core which is the heaviest one, and will give the nanoparticles a higher ratio of hydronium ions to mass unit.

Even though extensive work has been published on silane grafting on silica surfaces, few works have been reported on the silanization of nanoparticle surfaces. Reaction mechanisms must be understood to know how to improve the stability of ligand-surface bonds on nanoparticles. Stability of these linkages is critical to catalyst recyclability.

Solvents other than water may have to be used during pretreatment. Water can break bonds between surface hydroxyls of SiMNPs and the nanoparticle's acid-functional groups. Siloxane bonds are water susceptible; in acidic environments, siloxane bonds can be hydrolyzed to silanol (Cypryk and Apeloig 2002). The use of alternative solvents during pretreatment could prevent the hydrolysis of Si-O-Si bonds. Furthermore, solvents with higher affinity towards non-polar molecules could help the depolymerization of lignin during pretreatment. Using the organosolv method, solvents such as ethanol, methanol, and acetone have effectively been used for the pretreatment of biomass (Cheng et al 2013; Wildschut et al 2013).

Perfluoropropylsulfonic acid groups could be used as catalysts of biomass pretreatment because they are strong acid catalysts; however, as was demonstrated in this work, the bonds that link perfluoropropylsulfonic acid groups to the surface are too weak, at least in aqueous solutions. A solution to this problem could be the polymerization of Nafion resins on nanoparticles surfaces. Nafion has been successfully used as a catalyst of organic reactions (Climent et al 2013)(Cheng et al 2013)(Cheng et al 2013){{586 Cheng, Shuna 2013}} and could be an effective catalyst for hydrolysis of lignin carbohydrate bonds.

Hemicelluloses solubilization and lignin removal require breaking various bonds that link carbohydrates and lignin, thus various functional groups should be used during the acid catalysis of these bonds. Nanoparticles' surface could be modified simultaneously with various functional groups, such as carboxylic and sulfonic acids. Nanoparticles could also be functionalized with molecules having two functional groups in the same attached molecule. Nanoparticles functionalized with multiple functional groups could synergistically affect the catalysis of biomass pretreatment.

References

Allen, S., Schulman, D., Lichwa, J., Antal, M., and Jennings, E. 2001. A comparison of aqueous and dilute-acid single-temperature pretreatment of yellow poplar sawdust. Industrial engineering chemistry research. 40:2352-2361

Allred, C. S., Arnold, D., Barrett, T. J., Beehler, A., Bement, A., Buchanan, G., Dorr, T. C., Gray, G., Hays, S., Karsner, A., Orbach, R., Swagel, P., and Turner, J. 2008. National Biofuels Action Plan

Alvaro, M., Corma, A., Das, D., Fornes, V., and Garcia, H. 2005. "Nafion"-functionalized mesoporous MCM-41 silica shows high activity and selectivity for carboxylic acid esterification and Friedel-Crafts acylation reactions. J. Catal. 231:48

Antal, M. J., Leesomboon, T., Mok, W. S., and Richards, G. N. 1991. Kinetic-studies of the reactions of ketoses and aldoses in water at high temperature. 3. Mechanism of formation of 2-furaldehyde from D-xylose. Carbohydr.Res. 217:71-85

Bacic, A., and Stone, B. 1980. A (1-]3)-linked and (1-]4)-linked beta-D-glucan in the endosperm cell-walls of wheat. Carbohydr.Res. 82:372-377

Badley, R., and Ford, W. 1989. Silica-bound sulfonic-acid catalysts. J.Org.Chem. 54:5437-5443

Bautista, L., Morales, G., Sanz, R., and Bautista, F. 2010. Immobilization strategies for laccase from Trametes versicolor on mesostructured silica materials and the application to the degradation of naphthalene. Bioresour.Technol. 101:8541-8548

Bayer, E., Chanzy, H., Lamed, R., and Shoham, Y. 1998. Cellulose, cellulases and cellulosomes. Curr.Opin.Struct.Biol. 8:548-557

Beamson, G., and Alexander, M. 2004. Angle-resolved XPS of fluorinated and semi-fluorinated side-chain polymers. Surf.Interface Anal. 36:323-333

Bell, A. 2003. The impact of nanoscience on heterogeneous catalysis. Science. 299:1688-1691

Bernal, C., Mesa, M., and Sierra, L. 2012. Synthesis of new silicas with high stable and large mesopores and macropores for biocatalysis applications. Materials science engineering.C, Biomimetic materials, sensors and systems. 32:1380-1385

Biloiu, C., Biloiu, I. A., Sakai, Y., Suda, Y., and Ohta, A. 2004. Amorphous fluorocarbon polymer (a-C : F) films obtained by plasma enhanced chemical vapor deposition from

perfluoro-octane (C8F18) vapor I: Deposition, morphology, structural and chemical properties. J. Vac. Sci. Technol. A. 22:1158-1165

Blanco Brieva, G., Campos Martin, J., de Frutos, M., and Fierro, J. 2008. Preparation, Characterization, and Acidity Evaluation of Perfluorosulfonic Acid-Functionalized Silica Catalysts. Industrial engineering chemistry research. 47:8005-8010

Bobleter, O. 1994. Hydrothermal degradation of polymers derived from plants. Prog. Polym. Sci. 19:797-841

Bonn, G., and Bobleter, O. 1983. Determination of the hydrothermal degradation products of D-(U-C14) glucose and D-(U-C-14) fructose by TLC. J. Radioanal. Chem. 79:171-177

Bootsma, J. A., and Shanks, B. H. 2007. Cellobiose hydrolysis using organic-inorganic hybrid mesoporous silica catalysts. Appl. Catal. A-Gen. 327:44-51

Bossaert, W., De Vos, D., Van Rhijn, W., Bullen, J., and Grobet, P. 1999. Mesoporous sulfonic acids as selective heterogeneous catalysts for the synthesis of monoglycerides. Journal of catalysis. 182:156-164

Boveri, M., Agundez, J., Diaz, I., Perez Pariente, J., and Sastre, E. 2003. Synthesis and characterisation of ordered mesoporous acid catalysts for synthesis of biodegradable surfactants. Collect.Czech.Chem.Commun. 68:1914-1926

Brown, R. 2003. Cellulose structure and biosynthesis: What is in store for the 21st century?. Journal of polymer science.Part A, Polymer chemistry. 42:487-495

Brunel, D., Cauvel, A., Di Renzo, F., Fajula, F., and Fubini, B. 2000. Preferential grafting of alkoxysilane coupling agents on the hydrophobic portion of the surface of micelle-templated silica. New journal of chemistry. 24:807-813

Bucsi, I., and Olah, G. 1992. Catalysis by solid superacids .27. Oligomerization of 2-methylpropene and transformation of 2,4,4-trimethyl-2-pentene over supported and unsupported perfluorinated resinsulfonic acid catalysts. Journal of catalysis. 137:12-21

Buruiana, T., Melinte, V., Stroea, L., and Buruiana, E. 2009. Urethane Dimethacrylates with Carboxylic Groups as Potential Dental Monomers. Synthesis and Properties. Polym.J. 41:978

Buzzoni, R., Bordiga, S., Ricchiardi, G., Spoto, G., and Zecchina, A. 1995. Interaction of H_2O, CH_3OH, $(CH_3)(_2)O$, CH_3CN, and pyridine with the superacid perfluorosulfonic membrane nafion: an IR and Raman study. J.Phys.Chem. 99:11937-11951

Cano Serrano, E., Campos Martin, J., and Fierro, J. 2003. Sulfonic acid-functionalized silica through quantitative oxidation of thiol groups. Chem. Commun.:246-247

Capehart, T., Allen, E., and Bond, J. K. 2012. Feed Outlook: August 2012. FDS-12H

Carrasco, F., and Roy, C. 1992. Kinetic-Study of Dilute-Acid Prehydrolysis Of Xylan-Containing Biomass. Wood Sci.Technol. 26:189-208

Carvalheiro, F., Duarte, L., Medeiros, R., and Girio, F. 2004. Optimization of brewery's spent grain dilute-acid hydrolysis for the production of pentose-rich culture media. Appl.Biochem.Biotechnol. 113:1059-1072

Cejpek, K., Velisek, J., and Novotny, O. 2008. Formation of carboxylic acids during degradation of monosaccharides. Czech journal of food science. 26:113-131

Chafin, S., Pennybaker, K., Fahey, D., Subramaniam, B., and Gong, K. 2008. Economic and Environmental Impact Analyses of Solid Acid Catalyzed Isoparaffin/Olefin Alkylation in Supercritical Carbon Dioxide. Industrial engineering chemistry research. 47:9072

Chang, M. M., Chou, T. Y. C., and Tsao, G. T. 1981. Structure, pretreatment and hydrolysis of cellulose. Pages 15-42 in: Bioenergy. A. Fiechter ed. Springer Berlin Heidelberg

Chang, V., and Holtzapple, M. 2000. Fundamental factors affecting biomass enzymatic reactivity. Appl.Biochem.Biotechnol. 84-86:5-37

Chanzy, H. 1990. Aspects of cellulose structure. Pages 3-3-12 in: Cellulose sources and exploitation: industrial utilization, biotechnology and physico-chemical properties . J. F. Kennedy, G. O. Philips and P. A. Williams eds. Ellis Horwood: Chichester, UK

Cheng, S., Yuan, Z., Leitch, M., Anderson, M., and Xua, C. 2013. Highly efficient de-polymerization of organosolv lignin using a catalytic hydrothermal process and production of phenolic resins/adhesives with the depolymerized lignin as a substitute for phenol at a high substitution ratio. Industrial crops and products. 44:315-322

Chirachanchai, S., Chungchamroenkit, R., and Ishida, H. 1999. Adsorption of tetrasulfide-functional silane on high surface area silica treated with aqueous and non-aqueous solutions. Composite interfaces. 6:155-167

Climent, M., Corma, A., Iborra, S., Martinez-Silvestre, S., and Velty, A. 2013. Preparation of glycerol carbonate esters by using hybrid Nafion-silica catalyst. ChemSusChem. 6:1224-34

Colilla, M., Izquierdo-Barba, I., Sanchez-Salcedo, S., Fierro, J., Hueso, J., and Vallet-Regi, M. 2010. Synthesis and Characterization of Zwitterionic SBA-15 Nanostructured Materials. Chem. Mater. 22:6459-6466

Corma, A., Das, D., Fornes, V., Garcia, H., and Alvaro, M. 2004. Single-step preparation and catalytic activity of mesoporous MCM-41 and SBA-15 silicas functionalized with perfluoropropylsulfonic acid groups analogous to Nafion (R). Chem. Commun.:956-957

Corma, A., and Garcia, H. 2006. Silica-bound homogeneous catalysts as recoverable and reusable catalysts in organic synthesis. Adv.Synth.Catal. 348:1391-1412

Corma, A., Iborra, S., and Velty, A. 2007. Chemical routes for the transformation of biomass into chemicals. Chem.Rev. 107:2411-2502

Corredor, D. Y., Sun, X. S., Salazar, J. M., Hohn, K. L., and Wang, D. 2008. Enzymatic hydrolysis of soybean hulls using dilute acid and modified steam-explosion pretreatments. J. Biobased Mater. Bio. 2:43-50

Cypryk, M., and Apeloig, Y. 2002. Mechanism of the Acid-Catalyzed Si-O Bond Cleavage in Siloxanes and Siloxanols. A Theoretical Study. Organometallics. 21:2165-2175

Dale, B., and Lau, M. 2009. Cellulosic ethanol production from AFEX-treated corn stover using Saccharomyces cerevisiae 424A(LNH-ST). Proc.Natl.Acad.Sci.U.S.A. 106:1368

de Vries, R., and Visser, J. 2001. Aspergillus enzymes involved in degradation of plant cell wall polysaccharides. Microbiology and molecular biology reviews. 65:497-522

Delgenes, J. 1996. Effects of lignocellulose degradation products on ethanol fermentations of glucose and xylose by Saccharomyces cerevisiae, Zymomonas mobilis, Pichia stipitis, and Candida shehatae. Enzyme and microbial technology. 19:220-225

Dhepe, P. L., Ohashi, M., Inagaki, S., Ichikawa, M., and Fukuoka, A. 2005. Hydrolysis of sugars catalyzed by water-tolerant sulfonated mesoporous silicas. Catal. Lett. 102:163

Dhepe, P., and Sahu, R. 2010. A solid-acid-based process for the conversion of hemicellulose. Green Chem. 12:2153-2156

Diaz, I., Marquez-Alvarez, C., Mohino, F., Perez-Pariente, J., and Sastre, E. 2000. Combined Alkyl and Sulfonic Acid Functionalization of MCM-41-Type Silica Part 1. Synthesis and Characterization. Journal of catalysis. 193:283-294

Dien, B., Jung, H., Vogel, K., and Casler, M. 2006. Chemical composition and response to dilute-acid pretreatment and enzymatic saccharification of alfalfa, reed canarygrass, and switchgrass. Biomass Bioenergy. 30:880-891

Dube, D., Rat, M., Shen, W., Beland, F., and Kaliaguine, S. 2009a. Perfluoropropylsulfonic acid-functionalized periodic mesostructured organosilica: a strongly acidic heterogeneous catalyst. Journal of materials science. 44:6683-6692

Dube, D., Rat, M., Shen, W., Nohair, B., Beland, F., and Kaliaguine, S. 2009b. Perfluorinated alkylsulfonic acid functionalized periodic mesostructured organosilica: A new acidic catalyst. Applied catalysis.A, General. 358:232-239

Dubois, L., and Zegarski, B. 1993. Bonding of Alkoxysilanes to Dehydroxylated Silica Surfaces - A New Adhesion Mechanism. J.Phys.Chem. 97:1665-1670

Dunlop, A. P. 1948. Furfural formation and behavior. Industrial engineering chemistry. 40:204-209

El-Okr, M. M., Salem, M. A., Salim, M. S., El-Okr, R. M., Ashoush, M., and Talaat, H. M. 2011. Synthesis of cobalt ferrite nano-particles and their magnetic characterization. J Magn Magn Mater. 323:920-926

Estephan, Z., Hariri, H., and Schlenoff, J. 2013. One-pot, exchange-free, room-temperature synthesis of sub-10 nm aqueous, noninteracting, and stable zwitterated iron oxide nanoparticles. Langmuir. 29:2572-9

Fan, J., and Gao, Y. 2006. Nanoparticle-supported catalysts and catalytic reactions - a mini-review. J.Exp.Nanosci. 1:457-475

Feng, X., Mao, G. Y., Bu, F. X., Cheng, X. L., Jiang, D. M., and Jiang, J. S. 2013. Controlled synthesis of monodisperse $CoFe_2O_4$ nanoparticles by the phase transfer method and their catalytic activity on methylene blue discoloration with H_2O_2. J Magn Magn Mater. 343:126-132

Fiurasek, P., and Reven, L. 2007. Phosphonic and sulfonic acid-functionalized gold nanoparticles: A solid-state NMR study. Langmuir. 23:2857

Fleming, K., Gray, D., and Matthews, S. 2001. Cellulose crystallites. Chemistry - A European Journal. 7:1831-1835

Gao, Y. 2007. Nano-reagents with cooperative catalysis and their uses in multiple phase reactions. U.S.Pat.Appl.Publ. 2007-668151; 2006-763123:27

Gardner, K. H., and Blackwell, J. 1974. Structure of Native Cellulose. Biopolymers. 13:1975-2001

Gill, C. S., Price, B. A., and Jones, C. W. 2007. Sulfonic acid-functionalized silica-coated magnetic nanoparticle catalysts. J.Catal. 251:145-152

Girio, F. M., Fonseca, C., Carvalheiro, F., Duarte, L. C., and Marques, S. 2010. Hemicelluloses for fuel ethanol: A review. Bioresour.Technol. 101:4775-4800

Girisuta, B., Janssen, L., and Heeres, H. 2006. A kinetic study on the conversion of glucose to levulinic acid. Chem.Eng.Res.Design. 84:339-349

Glass, N., Tjeung, R., Chan, P., Yeo, L., and Friend, J. 2011. Organosilane deposition for microfluidic applications. Biomicrofluidics. 5:036501

Goerl, U., Hunsche, A., Mueller, A. Koban,H G. 1997. Investigations into the Silica/Silane Reaction System. Rubber chemistry and technology. 70:608-623

Gonzalez, G., LopezSantin, J., Caminal, G., and Sola, C. 1986. Dilute acid-hydrolysis of wheat straw hemicellulose at moderate temperature - a simplified kinetic-model. Biotechnol.Bioeng. 28:288-293

Gosselink, R., van Dam, J., Boeriu, C., and Bravo, D. 2004. Characterisation of structure-dependent functional properties of lignin with infrared spectroscopy. Industrial crops and products. 20:205-218

Grohmann, K., Torget, R., and Himmel, M. 1986. Optimization of dilute acid pretreatment of biomass. Biotechnol. Bioeng. Symp. 15:59-80

Grohmann, K., Himmel, M., Rivard, C., Tucker, M., and Baker, J. 1984. Chemical-mechanical methods for the enhanced utilization of straw. Biotechnol.Bioeng.:137-157

Grondin, J., Sagnes, R., and Commeyras, A. 1976. Perfluorosulfonic acids-3. Hammett acidity functions of perfluoroalkanesulfonic acids and of their mixtures with SbF_5. Bulletin de la Société chimique de France:1779-1783

Haddad, P. S., Duarte, E. L., Baptista, M. S., Goya, G. F., Leite, C. A. P., and Itri, R. 2004. Synthesis and Characterization of silica-coated magnetic nanoparticles. Progress in Colloid and Polymer Science. 128:232-238

Hair, M. 1975. Hydroxyl-Groups on Silica Surface. J.Non Cryst.Solids. 19:299-309

Hamoudi, S., Royer, S., and Kaliaguine, S. 2004. Propyl- and arene-sulfonic acid functionalized periodic mesoporous organosilicas. Microporous and mesoporous materials. 71:17-25

Harmer, M. A., Sun, Q., Vega, A. J., Farneth, W. E., Heidekum, A., and Hoelderich, W. F. 2000. Nafion resin-silica nanocomposite solid acid catalysts. Microstructure-processing-property correlations. Green Chem. 2:7-14

Harmer, M. A., Farneth, W. E., and Sun, Q. 1998. Towards the sulfuric acid of solids. Adv. Mater. 10:1255

Harmer, M. A., Sun, Q., Michalczyk, M. J., and Yang, Z. Y. 1997. Unique silane modified perfluorosulfonic acids as versatile reagents for new solid acid catalysts. Chem. Commun.:1803

Harmer, M. A., Farneth, W. E., and Sun, Q. 1996. High surface area nafion resin/silica nanocomposites: A new class of solid acid catalyst. Journal of the American Chemical Society. 118:7708

Harmer, M. A., Junk, C., Rostovtsev, V., Carcani, L. G., Vickery, J., and Schnepp, Z. 2007. Synthesis and applications of superacids. 1,1,2,2-tetrafluoroethanesulfonic acid, supported on silica. Green Chem. 9:30

Hayashi, . 2009. Chemoselective Synthesis of Folic Acid-Functionalized Magnetite Nanoparticles via Click Chemistry for Magnetic Hyperthermia. Chemistry of materials. 21:1318

Hendriks, A. T. W. M., and Zeeman, G. 2009. Pretreatments to enhance the digestibility of lignocellulosic biomass. Bioresour.Technol. 100:10-18

Herrera, A., Tellez-Luis, S. J., Gonzalez-Cabriales, J. J., Ramirez, J. A., and Vazquez, M. 2004. Effect of the hydrochloric acid concentration on the hydrolysis of sorghum straw at atmospheric pressure. J. Food Eng. 63:103

Hunter, M., Gordon, M., Barry, A., Hyde, J., and Heidenreich, R. 1947. Properties of Polyorganosiloxane Surfaces on Glass. Industrial engineering chemistry. 39:1389-1395

Iborra, S., Corma, A., and Huber, G. 2006. Synthesis of transportation fuels from biomass: Chemistry, catalysts, and engineering. Chem.Rev. 106:4044-4098

Ishida, H., and Koenig, J. 1978. Fourier-Transform Infrared Spectroscopic Study of Silane Coupling Agent-Porous Silica Interface. J.Colloid Interface Sci. 64:555-564

Jacobsen, S. E., and Wyman, C. E. 2002. Xylose monomer and oligomer yields for uncatalyzed hydrolysis of sugarcane bagasse hemicellulose at varying solids concentration. Industrial engineering chemistry research. 41:1454-1461

Kim, S. B., Lee, Y. Y., and Torget, R. 1987. Kinetics in acid-catalyzed hydrolysis of hardwood hemicellulose. Biotechnol. Bioeng. Symp. 17:71-84

Kim, T. H., Im, Y. H., and Hahn, Y. B. 2003. Plasma enhanced chemical vapor deposition of low dielectric constant SiCFO thin films. Chem. Phys. Lett. 368:36-40

Kim, S., Pham, T., Lee, J., and Roh, S. 2010. Releasing Properties of Proteins on SBA-15 Spherical Nanoparticles Functionalized with Aminosilanes. J. Nanosci. Nanotechnol. 10:3467-3472

Kitano, M., Yamaguchi, D., Suganuma, S., Nakajima, K., Kato, H., Hayashi, S., and Hara, M. 2009. Adsorption-enhanced hydrolysis of beta-1,4-glucan on graphene-based amorphous carbon bearing SO_3H, COOH, and OH groups. Langmuir. 25:5068-75

Klein Marcuschamer, D., Oleskowicz Popiel, P., Simmons, B., and Blanch, H. 2012. The challenge of enzyme cost in the production of lignocellulosic biofuels. Biotechnol.Bioeng. 109:1083-1087

Lai, D., Deng, L., Guo, Q., and Fu, Y. 2011a. Hydrolysis of biomass by magnetic solid acid. Energy environmental science. 4:3552-3557

Lai, D., Deng, L., Guo, Q., and Fu, Y. 2011b. Hydrolysis of biomass by magnetic solid acid. Energy environmental science. 4:3552-3557

Lee, Y., Lee, J., Park, J. G., Noh, H. J., Bae, C. J., and Hyeon, T. 2005. Large-Scale Synthesis of Uniform and Crystalline Magnetite Nanoparticles Using Reverse Micelles as Nanoreactors under Reflux Conditions. Advanced functional materials. 15:503-509

Lee, L. 1968. Wettability and conformation of reactive polysiloxanes. Journal of colloid and interface science. 27:751

Lee, Y., and Kim, S. 2002. Diffusion of sulfuric acid within lignocellulosic biomass particles and its impact on dilute-acid pretreatment. Bioresour.Technol. 83:165-171

Lien, H. L., and Zhang, W. X. 2007. Removal of methyl tert-butyl ether (MTBE) with Nafion. J. Hazard Mater. 144:194

Lim, M., Blanford, C., and Stein, A. 1998. Synthesis of ordered microporous silicates with organosulfur surface groups and their applications as solid acid catalysts. Chemistry of materials. 10:467

Liu, C. G., and Wyman, C. E. 2005. Partial flow of compressed-hot water through corn stover to enhance hemicellulose sugar recovery and enzymatic digestibility of cellulose. Bioresour. Technol. 96:1978

Liu, C., and Wyman, C. E. 2004. Effect of the flow rate of a very dilute sulfuric acid on xylan, lignin, and total mass removal from corn stover. Ind Eng Chem Res. 43:2781-2788

Lloyd, T., and Wyman, C. 2005. Combined sugar yields for dilute sulfuric acid pretreatment of corn stover followed by enzymatic hydrolysis of the remaining solids. Bioresour.Technol. 96:1967-1977

Macquarrie, D., Jackson, D., Mdoe, J., and Clark, J. 1999. Organomodified hexagonal mesoporous silicates. New journal of chemistry. 23:539-544

Marzialetti, T., Sievers, C., and Agrawal, P. 2008. Dilute acid hydrolysis of Loblolly pine: A comprehensive approach. Industrial engineering chemistry research. 47:7131-7140

Matsushika, A., Inoue, H., Murakami, K., Takimura, O., and Sawayama, S. 2009. Bioethanol production performance of five recombinant strains of laboratory and industrial xylose-fermenting Saccharomyces cerevisiae. Bioresour.Technol. 100:2392-2398

McMillan, J. D. 1994. Pretreatment of Lignocellulosic Biomass. Pages 292-294 in: Enzymatic Conversion of Biomass for Fuels Production. M. E. Himmel, J. O. Baker and R. P. Overend eds. American Chemical Society

Mealey, S. K., and Thomas, B. 2005. Past, present and future of organosilane treatments for fillers. Rubber world. 12:32-34

Melero, J. A., Stucky, G. D., van Grieken, R., and Morales, G. 2002. Direct syntheses of ordered SBA-15 mesoporous materials containing arenesulfonic acid groups. J. Mater. Chem. 12:1664

Melero, J., Fernando Bautista, L., Morales, G., Iglesias, J., and Sanchez Vazquez, R. 2010. Biodiesel production from crude palm oil using sulfonic acid-modified mesostructured catalysts. Chem.Eng.J. 161:323-331

Menon, V., Prakash, G., and Rao, M. 2010. Enzymatic hydrolysis and ethanol production using xyloglucanase and Debaromyces hansenii from tamarind kernel powder: Galactoxyloglucan predominant hemicellulose. J.Biotechnol. 148:233-239

Mooney, K., Nelson, J., and Wagner, M. 2004. Superparamagnetic Cobalt Ferrite Nanocrystals Synthesized by Alkalide Reduction. Chemistry of materials. 16:3155-3161

Morales, G., Athens, G., Chmelka, B., van Grieken, R., and Melero, J. 2008. Aqueous-sensitive reaction sites in sulfonic acid-functionalized mesoporous silicas. Journal of catalysis. 254:205-217

Moreau, C., Durand, R., Peyron, D., Duhamet,J., Rivalier, P.. 1998. Selective preparation of furfural from xylose over microporous solid acid catalysts. Industrial crops and products. 7:95-99

Mosier, N. S., Ladisch, C. M., and Ladisch, M. R. 2002. Characterization of acid catalytic domains for cellulose hydrolysis and glucose degradation. Biotechnol. Bioeng. 79:610-618

Mosier, N., Wyman, C., Dale, B., Elander, R., Lee, Y. Y., Holtzapple, M., and Ladisch, M. 2005. Features of promising technologies for pretreatment of lignocellulosic biomass. Bioresour.Technol. 96:673-686

Moumen, N., Bonville, P., and Pileni, M. 1996. Control of the size of cobalt ferrite magnetic fluids: Mossbauer spectroscopy. J.Phys.Chem. 100:14410-14416

Naseri, M., Saion, E., Ahangar, H., Shaari, A., and Hashim, M. 2010. Simple Synthesis and Characterization of Cobalt Ferrite Nanoparticles by a Thermal Treatment Method. Journal of Nanomaterials. 2010:1-8

Newell, R. 2010. Annual Energy Outlook 2011. DOE/EIA-0383(2011). U.S. Energy Information Administration

Nilsson, A., Gorwa-Grauslund, M. F., Hahn-Hagerdal, B., and Liden, G. 2005. Cofactor dependence in furan reduction by Saccharomyces cerevisiae in fermentation of acid-hydrolyzed lignocellulose. Apol. Environ. Microb. 71:7866

Nlebedim, I. C., Moses, A. J., Jiles, D.C. 2013. Non-stoichiometric cobalt ferrite, CoxFe3-xO4 (x=1.0 to 2.0): Structural, magnetic and magnetoelastic properties. J Magn Magn Mater. 343:49-54

Norton, F. J. 1944. Organo-silicon films. General Electric Review:6-16

Office of the Biomass Program. 2010. Biomass: Multi-year Program Plan, U.S. DOE

Okamura, K. 1991. Structure of Cellulose. Pages 89-111 in: Wood and Cellulosic Chemistry. D. N. -. Hon and N. Shiraishi eds. Marcel Dekker: New York

Olah, G., Mathew, T., Farnia, M., and Prakash, G. 1999. Nafion-H catalysed intramolecular Friedel-Crafts acylation: Formation of cyclic ketones and related heterocycles. Synlett. 1999:1067-1068

Olah, G., Shamma, T., and Prakash, G. 1997. Catalysis by solid superacids .31. Dehydration of alcohols to ethers over Nafion-H, a solid perfluoroalkanesulfonic acid resin catalyst. Catalysis letters. 46:1-4

Oliva, J. M., Negro, M. J., and Saez, F. 2006. Effects of acetic acid, furfural and catechol combinations on ethanol fermentation of Kluyveromyces marxianus. Process Biochem. 41:1223-1228

Olsson, L., Soerensen, H. R., Dam, B. P., Christensen, H., and Krogh, K. M. 2006. Separate and simultaneous enzymatic hydrolysis and fermentation of wheat hemicellulose with recombinant xylose utilizing Saccharomyces cerevisiae. Appl.Biochem.Biotechnol. 129:117-129

Onda, A., Ochi, T., and Yanagisawa, K. 2008. Selective hydrolysis of cellulose into glucose over solid acid catalysts. Green Chem. 10:1033-1037

Ordomsky, V., van der Schaaf, J., Schouten, J., Nijhuis,T. A. 2012. Fructose dehydration to 5-hydroxymethylfurfural over solid acid catalysts in a biphasic system. ChemSusChem. 5:1812-9

O'Sullivan, A. C. 1997. Cellulose: the structure slowly unravels. Cellulose. 4:173-207

Peña, L., Ikenberry, M., Hohn, K. L., and Wang, D. 2012. Acid-Functionalized Nanoparticles for Pretreatment of Wheat Straw. Journal of Biomaterials and Nanobiotechnology. 3:342-352

Peña, L., Ikenberry, M., Ware, B., Hohn, K. L., Boyle, D., and Wang, D. 2011. Cellobiose hydrolysis using acid-functionalized nanoparticles. Biotechnology and bioprocess engineering. 16:1214-1222

Phan, N. T. S., and Jones, C. W. 2006. Highly accessible catalytic sites on recyclable organosilane-functionalized magnetic nanoparticles: An alternative to functionalized porous silica catalysts. J. Mol. Catal. A-Chem. 253:123-131

Plueddemann, E. P. 1982. Silane Coupling Agents. Plenum Press: New York

Polshettiwar, V., and Varma, R. 2010. Green chemistry by nano-catalysis. Green Chem. 12:743-754

Prakash, G., Mathew, T., Krishnaraj, S., Marinez, E., and Olah, G. 1999. Nafion-H catalysed isomerization of epoxides to aldehydes and ketones. Applied catalysis.A, General. 181:283-288

Preston, R. D. 1986. Natural celluloses. Pages 3-3-27 in: Cellulose: Structure, Modification and Hydrolysis. R. A. Young and R. M. Rowell eds. Wiley and Sons: New York

Preston, R. 1951. Fibrillar Units in the Structure of Native Cellulose. Discuss.Faraday Soc. 11:165-170

Rac, B., Molnar, A., Forgo, P., Mohai, M., and Bertoti, I. 2006. A comparative study of solid sulfonic acid catalysts based on various ordered mesoporous silica materials. Journal of molecular catalysis. A, Chemical. 244:46

Raja, R., and Thomas, J. M. 2003. The expanding world of nanoparticle and nanoporous catalysts. Pages 329-357 in: The chemistry of nanostructured materials. P. Yang ed. World Scientific Publishing Co. Pte. Ltd.: Singapur

Renewable Fuels Association. 2010. 2010 ethanol industry outlook

Rodrussamee, N., Lertwattanasakul, N., Hirata, K., Limtong, S., and Kosaka, T. 2011. Growth and ethanol fermentation ability on hexose and pentose sugars and glucose effect under various conditions in thermotolerant yeast Kluyveromyces marxianus. Appl.Microbiol.Biotechnol. 90:1573-1586

Ronchin, L., Vavasori, A., and Toniolo, L. 2012. Acid catalyzed alkylation of phenols with cyclohexene: Comparison between homogeneous and heterogeneous catalysis, influence of cyclohexyl phenyl ether equilibrium and of the substituent on reaction rate and selectivity. Journal of molecular catalysis.A, Chemical. 355:134-141

Rondinone, A. J., Samia, A. C. S., and Zhang, Z. J. 1999. Superparamagnetic relaxation and magnetic anisotropy energy distribution in CoFe2O4 spinel ferrite nanocrystallites. J. Phys. Chem. B. 103:6876-6880

Saxena, I., and Brown, R. 2005. Cellulose biosynthesis: Current views and evolving concepts. Annals of botany. 96:9-21

Scaranto, J., Charmet, A. P., and Giorgianni, S. 2008. IR spectroscopy and quantum-mechanical studies of the adsorption of CH2CClF on TiO2. J. Phys. Chem. C. 112:9443-9447

Selig, M., Weiss, N., and Ji, Y. 2008. Enzymatic Saccharification of Lignocellulosic Biomass. NREL/TP-510-42629

Senapati, K., Borgohain, C., and Phukan, P. 2011. Synthesis of highly stable CoFe2O4 nanoparticles and their use as magnetically separable catalyst for Knoevenagel reaction in aqueous medium. Journal of molecular catalysis.A, Chemical. 339:24-31

Senate and House of Representatives of the United States of America in Congress. 2007. Energy Independence and Security Act

Shen, J., and Wyman, C. 2011. A novel mechanism and kinetic model to explain enhanced xylose yields from dilute sulfuric acid compared to hydrothermal pretreatment of corn stover. Bioresour.Technol. 102:9111-9120

Shen, X., Fang, X., Zhou, Y., and Liang, H. 2004. Synthesis and characterization of 3-aminopropyltriethoxysilane-modified superparamagnetic magnetite nanoparticles. Chem.Lett. 33:1468-1469

Shimizu, K., Furukawa, H., Kobayashi, N., Itaya, Y., and Satsuma, A. 2009. Effects of Bronsted and Lewis acidities on activity and selectivity of heteropolyacid-based catalysts for hydrolysis of cellobiose and cellulose. Green Chem. 11:1627-1632

Shylesh, S., Wagner, A., Seifert, A., Ernst, S., and Thiel, W. 2009. Cooperative Acid-Base Effects with Functionalized Mesoporous Silica Nanoparticles: Applications in Carbon-Carbon Bond-Formation Reactions. Chemistry : a European journal. 15:7052

Sievers, C., Marzialetti, T., Hoskins, T. J. C., Valenzuela Olarte, M. B., Agrawal, P., and Jones, C. 2009. Quantitative solid state NMR analysis of residues from acid hydrolysis of loblolly pine wood. Bioresour.Technol. 100:4758-4765

Silva, J., de Brito, W., and Mohallem, N. 2004. Influence of heat treatment on cobalt ferrite ceramic powders. Materials science engineering.B, Solid-state materials for advanced technology. 112:182-187

Siril, P. F., Davison, A. D., Randhawa, J. K., and Brown, D. R. 2007. Acid strengths and catalytic activities of sulfonic acid on polymeric and silica supports. Journal of molecular catalysis. A, Chemical. 267:72

Sluiter, A., Hames, B., Ruiz, R., Scarlata, C., Sluiter, J., and Templeton, D. 2008a. Determination of Sugars, Byproducts, and Degradation Products in Liquid Fraction Process Samples. NREL/TP-510-42623. National Renewable Energy Laboratory: Golden, CO

Sluiter, A., Hames, B., Ruiz, R., Scarlata, C., Sluiter, J., Templeton, D., and Crock, D. 2008b. Determination of Structural Carbohydrates and Lignin in Biomass. Laboratory Analytical Procedure TP-510-42618

Sluiter, A., Hyman, D., Payne, C., and Wolfe, J. 2008c. Determination of Insoluble Solids in Pretreated Biomass Material. NREL/TP-510-42627

Smith, A. L. 1960. Infrared spectra-structure correlations for organosilicon compounds. Spectrochimica acta. 16:87-105

Song, J., and Wei, D. 2010. Production and characterization of cellulases and xylanases of Cellulosimicrobium cellulans grown in pretreated and extracted bagasse and minimal nutrient medium M9. Biomass Bioenergy. 34:1930-1934

Sousa, L., Chundawat, S., Marshall, D., Sharma, L., Chambliss, C., and Balan, V. 2009. Enzymatic Digestibility and Pretreatment Degradation Products of AFEX-Treated Hardwoods (Populus nigra). Biotechnol.Prog. 25:365

Sterman, S., and Bradley, H.B. 1961. A New Interpretation Of The Glass-Coupling Agent Surface Through Use Of Electron Microscopy. SPE transactions. 1:224-233

Stevens, P. D., Fan, J., Gardimalla, H. M. R., Yen, M., and Gao, Y. 2005. Superparamagnetic Nanoparticle-Supported Catalysis of Suzuki Cross-Coupling Reactions. Org.Lett. 7:2085-2088

Stuhler, S. 2002. Effects of solids concentration, acetylation, and transient heat transfer on uncatalyzed batch pretreatment of corn stover. Dartmouth College: Hanover, NH

Suganuma, S., Nakajima, K., Kitano, M., Yamaguchi, D., Kato, H., Hayashi, S., and Hara, M. 2008. Hydrolysis of cellulose by amorphous carbon bearing SO3H, COOH, and OH groups. J. Am. Chem. Soc. 130:12787-12793

Teymouri, F., Gilbert, T., Dale, B., and Alizadeh, H. 2005. Pretreatment of switchgrass by ammonia fiber explosion (AFEX). Applied biochemistry and biotechnology. 121:1133

Teymouri, F., Laureano-Perez, L., Alizadeh, H., and Dale, B. 2004. Ammonia Fiber Explosion Treatment of Corn Stover. Appl.Biochem.Biotechnol. 115:951-963

Torget, R., and Hsu, T. 1994. Two-Temperature Dilute-Acid Prehydrolysis of Hardwood Xylan Using A Percolation Process. Appl. Biochem. Biotech. 45-6:5-21

Tripp, C., and Hair, M. 1995. Reaction of Methylsilanols with Hydrated Silica Surfaces - The Hydrolysis of Trichloromethylsilanes, Dichloromethylsilanes, and Monochloromethylsilanes and the Effects of Curing. Langmuir. 11:149-155

U.S. Department of Energy. 2012. Drought increases price of corn, reduces profits to ethanol producers. 2013

U.S. Department of Energy. 2006. Concentrated Acid Hydrolysis

U.S. Energy Information Administration. 2012. Monthly energy review

U.S. Energy Information Administration. . Annual Energy Review 2009. 2010

Ulman, A. 1996. Formation and structure of self-assembled monolayers. Chem.Rev. 96:1533-1554

Van Rhijn, W. M., De Vos, D. E., Sels, B. F., Bossaert, W. D., and Jacobs, P. A. 1998. Sulfonic acid functionalized ordered mesoporous materials as catalysts for condensation and esterification reactions. Chem.Commun. 1998:317-318

Varga, E., Reczey, K., and Zacchi, G. 2004. Optimization of Steam Pretreatment of Corn Stover to Enhance Enzymatic Digestibility. Appl.Biochem.Biotechnol. 114:509-509-523

Vigier, K. D. O., and Jerome, F. 2010. Heterogeneously-Catalyzed Conversion of Carbohydrates. Pages 63-92 in: Topics in Current Chemistry. A. P. Rauter, P. Vogel and Y. Queneau eds. Springer Berlin Heidelberg: Berlin

Vincken, J., York, W., Beldman, G., and Voragen, A. 1997. Two general branching patterns of xyloglucan, XXXG and XXGG. Plant Physiol. 114:9-13

Viola, E., Nanna, F., Larocca, E., Cardinale, M., Barisano, D., and Zimbardi, F. 2007. Acid impregnation and steam explosion of corn stover in batch processes. Ind. crop prod. 26:195

Wight, A. P., and Davis, M. E. 2002. Design and preparation of organic-inorganic hybrid catalysts. Chem.Rev. 102:3589-613

Wildschut, J., Smit, A., Reith, J., and Huijgen, W. J. J. 2013. Ethanol-based organosolv fractionation of wheat straw for the production of lignin and enzymatically digestible cellulose. Bioresour.Technol. 135:58-66

Wooley, R., Ruth, M., Glassner, D., and Sheehan, J. 1999. Process design and costing of bioethanol technology: A tool for determining the status and direction of research and development. Biotechnol.Prog. 15:794-803

Woolf, a. 1954. Fluorosulphonic acid .1. Some properties of the aqueous solution. Journal of the Chemical Society:2840-2843

Wyman, C. E., and Goodman, B. J. 1993. Biotechnology for production of fuels, chemicals, and materials from biomass. Appl.Biochem.Biotechnol. 39-40:41-59

Wyman, C. E., Dale, B. E., Elander, R. T., Holtzapple, M., Ladisch, M. R., and Lee, Y. Y. 2005. Coordinated development of leading biomass pretreatment technologies. Bioresour.Technol. 96:1959-1966

Xiang, Q., Lee, Y., and Torget, R. 2004. Kinetics of glucose decomposition during dilute-acid hydrolysis of lignocellulosic biomass. Appl. Biochem. Biotech. 113:1127

Xiros, C., Katapodis, P., and Christakopoulos, P. 2011. Factors affecting cellulose and hemicellulose hydrolysis of alkali treated brewers spent grain by Fusarium oxysporum enzyme extract. Bioresour.Technol. 102:1688

Yadav, G. D. 2005. Synergism of Clay and Heteropoly Acids as Nano-Catalysts for the Development of Green Processes with Potential Industrial Applications. Catal.Surv.Asia. 9:117-137

Yang, B., and Wyman, C. E. 2004. Effect of xylan and lignin removal by batch and flowthrough pretreatment on the enzymatic digestibility of corn stover cellulose. Biotechnol.Bioeng. 86:88-95

Yi, D. Y., Selvan, T., Lee, S. S., Papaefthymiou, G. C., Kundaliya, D., and Ying, J. Y. 2005. Silica-coated nanocomposites of magnetic nanoparticles and quantum dots. Journal of the American Chemical Society. 127:4990

Yoon, T., Lee, W., Oh, Y., and Lee, J. 2003. Magnetic nanoparticles as a catalyst vehicle for simple and easy recycling. New J. Chem. 27:227-229

Yurdakoc, M., Akcay, M., Tonbul, Y., and Yurdakoc, K. 1999. Acidity of silica-alumina catalysts by amine titration using Hammett indicators and FT-IR study of pyridine adsorption. Turk. J. Chem. 23:319-327

Zavadil, K., Armstrong, N., and Peden, C. 1989. Reactions at the interface between multi-component glasses and metallic lithium films. J.Mater.Res. 4:978-989

Zeng, M., Ximenes, E., Ladisch, M., Mosier, N., Vermerris, W., Huang, C., and Sherman, D. 2012. Tissue-specific biomass recalcitrance in corn stover pretreated with liquid hot-water: enzymatic hydrolysis (part 1). Biotechnol.Bioeng. 109:390-7

Zhang, M., Cushing, B. L., and O'Connor, C. J. 2008. Synthesis and characterization of monodisperse ultra-thin silica-coated magnetic nanoparticles. Nanotechnology. 19:1-5

Zhang, C. Q., Qi, W., Wang, F., Li, Q., and Su, R. X. 2011. Ethanol From Corn Stover Using SSF: An Economic Assessment. Energy sources.Part B, Economics, planning and policy. 6:136-144

Zhang, J., He, J., Liu, Z., Yu, Z., and Yu, J. 2009. Combinations of mild physical or chemical pretreatment with biological pretreatment for enzymatic hydrolysis of rice hull. Bioresour.Technol. 100:903

Zhao, X. S., Lu, G. Q., and Hu, X. 2000. Characterization of the structural and surface properties of chemically modified MCM-41 material. Micropor. Mesopor. Mater. 41:37-37-47